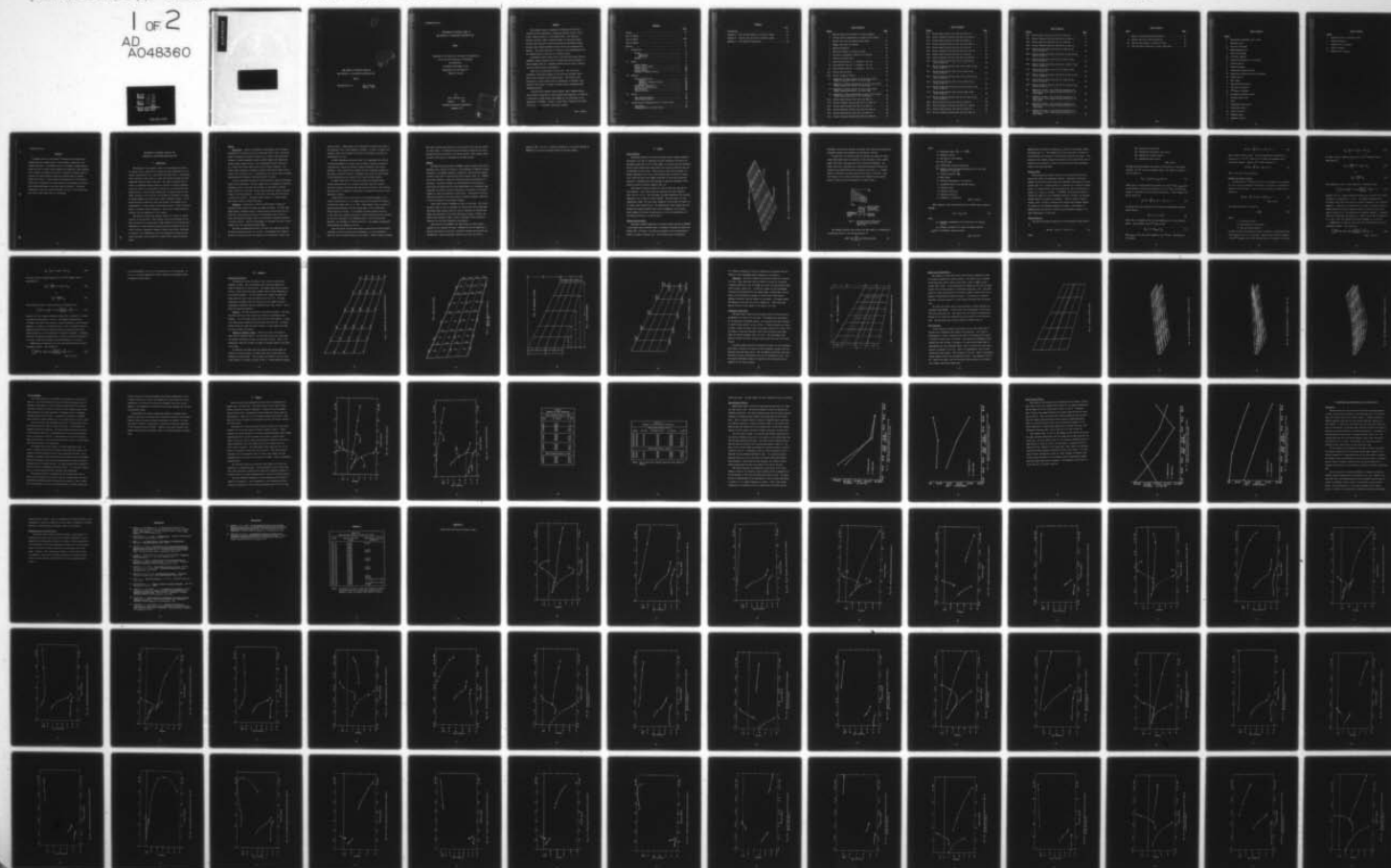


UNCLASSIFIED

AFIT/GAE/AA/77D-13

NL

1 OF 2
AD
A048360



1

DDC
JAN 16 1978
RECEIVED
F

THE EFFECTS OF EXTERNAL STORES ON
THE FLUTTER OF A NON-UNIFORM CANTILEVER WING

THESIS

AFIT/GAE/AA/77D-13

Van C. Sherrer
Captain USAF

AFIT/GAE/AA/77D-13

THE EFFECTS OF EXTERNAL STORES ON
THE FLUTTER OF A NON-UNIFORM CANTILEVER WING

THESIS

Presented to the Faculty of the School of Engineering
of the Air Force Institute of Technology
Air University
in Partial Fulfillment of the
Requirements for the Degree of
Master of Science

by
Van C. Sherrer, B.S.
Captain USAF
Graduate Aeronautical Engineering
December 1977

ACCESSION FOR	
NTIS	Value Section <input checked="" type="checkbox"/>
DDC	BLN Section <input type="checkbox"/>
UNANNOUNCED	<input type="checkbox"/>
IS I CATION	<input type="checkbox"/>
BY	
DISTRIBUTION/AVAILABILITY CODES	
DI	SP. CIAL
A	

Preface

This computer study is conducted to determine the effects of concentrated mass combinations, simulating external stores, on the flutter characteristics of a non-uniform wing. This approach, I believe, provides a rapid, versatile method of predicting flutter problems with aeroelastic structures during the preliminary design process, where flutter problems can most easily and economically be remedied. This study should be of interest to the aerodynamicist and the aeroelastician, as flutter is a concern of both.

An advanced version (Level 16.0) of the NASA Structural Analysis (NASTRAN) computer system is used to perform the flutter analysis. A finite element model of a strength optimized wing is used in conjunction with doublet-lattice aerodynamics.

There are two limitations of this study. One is that the aerodynamic interaction between the structure and attached stores has not been included in the computer model. The second is the availability of only doublet-lattice aerodynamics in NASTRAN, which restricts this method to subsonic lifting surfaces undergoing small sinusoidal motions.

I would like to thank my thesis advisor, Major Franklin Eastep, and my faculty committee for their guidance and assistance. In addition, I would like to thank Captain Gene Hemmig for his assistance in the application of NASTRAN. Finally, I would like to thank my wife Cheryl for her patience and support during this project.

Van C. Sherrer

Contents

	Page
Preface	ii
List of Figures	v
List of Tables	viii
List of Symbols	ix
Abstract	xi
I. Introduction	1
Flutter	2
Definitions	2
Background	2
NASTRAN	4
II. Theory	6
Finite Elements	6
Doublet Lattice Method	6
Surface Spline	10
Flutter Equation	10
k-Method of Flutter Solution	12
III. Analysis	15
Structure Description	15
Elements	15
Degrees of Freedom at Nodes	15
Wing Mass	20
Aerodynamic Description	20
Elastic Axis Determination	22
Free Vibration	22
Flutter Analysis	27
IV. Results	29
Mass Balancing Effects	29
Store Inertia Effects	34
V. Conclusions and Recommendations for Further Study	40
Conclusions	40
Recommendations for Further Study	41

Contents

	Page
Bibliography	42
Appendix A: Mass and Mass Moments of Inertia at Nodes	44
Appendix B: Flutter Speed and Flutter Frequency Graphs	45
Appendix C: Free Vibration Frequencies	84

List of Figures

<u>Figure</u>		<u>Page</u>
1	Wing Box Structure Represented by Finite Elements	7
2	Lifting Surface Idealization by Doublet-Lattice Method . .	8
3	Wing Box Top View with Numbered Node Points	16
4	Element Gage Sizes of Wing Box	17
5	Wing Box Dimensions	18
6	Additional Degrees of Freedom at Nodes	19
7	Top View of Aerodynamic Planform with Wing Box	21
8	Location of Elastic Axis	23
9	Free Vibration Mode No. 1, Frequency = 49.6 Hz	24
10	Free Vibration Mode No. 2, Frequency = 95.4 Hz	25
11	Free Vibration Mode No. 3, Frequency = 104.1 Hz	26
12-A	Flutter Speed Solution	30
12-B	Flutter Frequency Solution	31
13	Comparison of Flutter Speeds of 100 lb Store Versus Single Concentrated Mass at 3/4 Chord Nodes	35
14	Comparison of Flutter Frequencies of 100 lb Store Versus Single Concentrated Mass at 3/4 Chord Nodes	36
15	Comparison of Flutter Speeds of 200 lb Store Versus Single Concentrated Mass at 3/4 Chord Nodes	38
16	Comparison of Flutter Frequencies of 200 lb Store Versus Single Concentrated Mass at 3/4 Chord Nodes	39
17-A	Flutter Speed Solution with 100 lb at Node 40	46
17-B	Flutter Frequency Solution with 100 lb at Node 40	47
18-A	Flutter Speed Solution with 100 lb at Node 46	48
18-B	Flutter Frequency Solution with 100 lb at Node 46	49
19-A	Flutter Speed Solution with 100 lb at Node 48	50
19-B	Flutter Frequency Solution with 100 lb at Node 48	51

List of Figures

<u>Figure</u>		<u>Page</u>
20-A	Flutter Speed Solution with 100 lb at Node 50	52
20-B	Flutter Frequency Solution with 100 lb at Node 50	53
21-A	Flutter Speed Solution with 100 lb at Node 56	54
21-B	Flutter Frequency Solution with 100 lb at Node 56	55
22-A	Flutter Speed Solution with 100 lb at Node 58	56
22-B	Flutter Frequency Solution with 100 lb at Node 58	57
23-A	Flutter Speed Solution with 100 lb at Node 60	58
23-B	Flutter Frequency Solution with 100 lb at Node 60	59
24-A	Flutter Speed Solution with 50 lb at Node 36 and 50 lb at Node 40	60
24-B	Flutter Frequency Solution with 50 lb at Node 36 and 50 lb at Node 40	61
25-A	Flutter Speed Solution with 50 lb at Node 46 and 50 lb at Node 50	62
25-B	Flutter Frequency Solution with 50 lb at Node 46 and 50 lb at Node 50	63
26-A	Flutter Speed Solution with 50 lb at Node 54 and 50 lb at Node 58	64
26-B	Flutter Frequency Solution with 50 lb at Node 54 and 50 lb at Node 58	65
27-A	Flutter Speed Solution with 50 lb at Node 56 and 50 lb at Node 60	66
27-B	Flutter Frequency Solution with 50 lb at Node 56 and 50 lb at Node 60	67
28-A	Flutter Speed Solution with 200 lb at Node 28	68
28-B	Flutter Frequency Solution with 200 lb at Node 28	69
29-A	Flutter Speed Solution with 200 lb at Node 38	70
29-B	Flutter Frequency Solution with 200 lb at Node 38	71

List of Figures

<u>Figure</u>		<u>Page</u>
30-A	Flutter Speed Solution with 200 lb at Node 48	72
30-B	Flutter Frequency Solution with 200 lb at Node 48	73
31-A	Flutter Speed Solution with 200 lb at Node 58	74
31-B	Flutter Frequency Solution with 200 lb at Node 58	75
32-A	Flutter Speed Solution with 100 lb at Node 26 and 100 lb at Node 30	76
32-B	Flutter Frequency Solution with 100 lb at Node 26 and 100 lb at Node 30	77
33-A	Flutter Speed Solution with 100 lb at Node 36 and 100 lb at Node 40	78
33-B	Flutter Frequency Solution with 100 lb at Node 36 and 100 lb at Node 40	79
34-A	Flutter Speed Solution with 100 lb at Node 46 and 100 lb at Node 50	80
34-B	Flutter Frequency Solution with 100 lb at Node 46 and 100 lb at Node 50	81
35-A	Flutter Speed Solution with 100 lb at Node 56 and 100 lb at Node 60	82
35-B	Flutter Frequency Solution with 100 lb at Node 56 and 100 lb at Node 60	83
36	Comparison of Mode 1 Free Vibration Frequencies of 100 lb Store Versus Single Concentrated Mass at 3/4 Chord Nodes	85
37	Comparison of Mode 2 Free Vibration Frequencies of 100 lb Store Versus Single Concentrated Mass at 3/4 Chord Nodes	86
38	Comparison of Mode 1 Free Vibration Frequencies of 200 lb Store Versus Single Concentrated Mass at 3/4 Chord Nodes	87
39	Comparison of Mode 2 Free Vibration Frequencies of 200 lb Store Versus Single Concentrated Mass at 3/4 Chord Nodes	88

List of Tables

<u>Table</u>		<u>Page</u>
I	Results from Mass Balancing Experiment	32
II	Results From Store Inertia Simulation	33
III	Mass and Mass Moments of Inertia at Nodes	44
IV	Free Vibration Frequencies of First Three Modes	84

List of Symbols

Symbol

A	Generalized aerodynamic force matrix
c	Reference chord
C_p	Pressure coefficient
G	Modal damping matrix
g	Artificial damping
g_s	Structural damping
h	Vertical displacement of the surface
I	Identity matrix
k	Reduced frequency
K	Generalized stiffness matrix
\bar{K}	Generalized stiffness matrix with damping
KF	Kernel function
m	Mach number
M	Generalized mass matrix
P	Any point on planform
P_j	j^{th} point on planform
Q	Aerodynamic influence matrix
S	Lifting surface area
t	Time
u	Generalized modal vector
U	Freestream velocity
U_f	Flutter velocity
w	Downwash angle
\bar{w}	Downwash velocity

List of Symbols

Symbol

α	Streamwise slope of deformed surface
ρ	Freestream density
ω	Undamped cyclic frequency
ω_f	Flutter frequency
Ω	Damped cyclic frequency

Abstract

A computer study of the effects of external stores simulated by lumped masses was conducted with a finite element, cantilever, non-uniform wing model. The NASTRAN (Level 16.0) computer program flutter format was used to obtain flutter speeds and frequencies. Mass balancing with a single concentrated mass caused a reduction in flutter speed as the mass was moved chordwise toward the trailing edge and spanwise toward the wing tip. Flutter speeds and frequencies of a 100 lb and a 200 lb store, simulated by two equal masses, were compared to an equivalent concentrated mass at the store center of gravity. The stores consistently raised the flutter frequency over that of the single mass, but flutter speed results were not conclusive.

THE EFFECTS OF EXTERNAL STORES ON THE FLUTTER OF A NON-UNIFORM CANTILEVER WING

I. Introduction

The purpose of this computer study is to investigate the effects of external stores, simulated by concentrated mass combinations, on the flutter characteristics of a non-uniform cantilever wing. A non-uniform wing is defined in this study as a wing with varying stiffness and mass properties along the span of the wing. This type of analysis will be useful in preliminary design studies as a method of rapidly estimating the flutter speed of an aeroelastic structure as it evolves during the design process. Flutter speed determination is required when the mass and/or stiffness of the structure is increased or decreased as a result of design changes, and during stores flutter clearance studies. If the predicted flutter speeds are lower than desired, then changes can be incorporated at an early stage of the design process to raise the flutter speed or eliminate flutter altogether. The earlier a design problem is detected, the less expensive it is to remedy.

The flutter of wings with external stores is a subject of current interest in the Air Force. Each aircraft that carries external stores must be cleared for its particular flight envelope for each unique store combination, or else operating restrictions must be imposed on the aircraft in order to guarantee a margin of safety from flutter. The number of external store combinations can reach astronomical proportions with certain aircraft, thus the need for a rapid flutter prediction method exists.

Flutter

Definitions. Flutter is described by Bisplinghoff as the "dynamic instability of an elastic body in an airstream" (Ref. 2:527). The flutter speed is defined as the lowest airspeed, U_f , at which a given structure flying at a given atmospheric density and Mach number will exhibit sustained, simple harmonic motion. The corresponding circular frequency, ω_f , at which the flutter speed occurs is the flutter frequency. The flutter speed represents a boundary condition below which stable oscillations of the structure occur. At speeds above the flutter speed, divergent oscillations with resultant structural failure can occur.

A static instability problem of lifting surfaces, known as divergence, should also be mentioned. The most common case of divergence is torsional divergence, which occurs when the increment in aerodynamic torsional moment caused by an increase in twist angle exceeds the elastic restoring torque of the wing structure. At that point, the wing structure suffers a catastrophic failure. Divergence speed, however, is usually higher than flutter speed for swept back wings.

Background. Historically, flutter problems began to appear as airplanes became capable of higher and higher airspeeds. To reach these higher speeds, designers began to abandon biplane construction with its relatively high torsional stiffness and aerodynamic drag in favor of lower drag monoplane designs, which had insufficient torsional stiffness to prevent flutter. During the development of monoplane aircraft, serious research into the aeroelastic problem began.

The basic two-dimensional theory of flutter was originally devised by Theodore Theodorsen (Ref. 12) in 1934. He recognized that classical flutter is characterized by the interaction of aerodynamic, elastic, and

inertial forces. Additionally, this interaction is usually the result of the coupling of two or more degrees of freedom. In order to prevent this coupling, either the stiffness of the wing is increased or the mass is redistributed, or both.

In 1940, Theodorsen and Garrick (Ref. 13) investigated the effects of various parameters on flutter, such as center of gravity location of a wing section, structural friction, radius of gyration, and flutter frequency. They concluded that normally the most important parameter is the center of gravity location. In general, the further aft the location of the chordwise center of gravity, the lower the flutter speed.

In 1945, Goland (Ref. 5) was able to solve the bending-torsion flutter problem exactly for a uniform cantilever wing with constant chord and uniformly distributed mass and elastic properties. This solution was then used as a standard of comparison to estimate the accuracy of more approximate methods.

A wind tunnel study of the effects of concentrated weights on the flutter characteristics of a straight cantilever wing model was conducted by Runyan and Sewall (Ref. 11) in 1948. Their general result was that as mass was moved chordwise from the leading edge to the trailing edge, flutter speed was reduced. As the weight was moved spanwise from root to tip, there was a general reduction of flutter speed and then an increase at the tip as compared to the unweighted wing. The flutter mode was generally first bending for inboard positions of the weights and generally second bending for weights at the tip.

Since the advent of high speed computer technology and finite element techniques for both structures and aerodynamics, it is now possible to solve the flutter problem rapidly and accurately. Several computer programs

have been developed specifically for the solution of the flutter problem in recent years. An existing structural analysis program has now incorporated the flutter solution in its latest version. This program, which is used in this study, is described in the next section.

NASTRAN

The NASA Structural Analysis (NASTRAN) computer system (Level 16.0), developed under contract for NASA by a team composed of Computer Sciences Corporation, the MacNeal-Schwendler Corporation, and the Martin Company, is used in this study to perform the flutter analysis (Ref. 8). NASTRAN uses finite elements to model the distributed physical properties of a structure. The finite elements are interconnected at grid points to which loads are applied and for which displacements are calculated. Mass properties are either calculated internally as properties of structural elements or input as properties of grid points. Constraints of various kinds may be applied to the grid points to simulate boundary conditions or tie the movements of grid points together.

Three rigid formats of NASTRAN are used in this study. The Static Analysis format is used to determine the elastic axis of the wing model. The Normal Modes Analysis format is used to determine the natural mode shapes and frequencies of the wing vibrating in vacuum. Finally, the Modal Flutter Analysis format is used to determine flutter speed and frequency for each mass combination investigated.

With Level 16.0 of NASTRAN, the rigid format for modal flutter analysis by the k-method was added. NASTRAN now has the capability to generate aerodynamic grid points, interpolate between the structure and aerodynamics, compute aerodynamic matrices, and solve the flutter

equations (Ref. 7:17.1-1). A general discussion of the theory employed by NASTRAN for the flutter analysis follows in the next chapter.

II. Theory

Finite Elements

The matrix methods of structural analysis used by digital computers are based on the idea of replacing an actual continuous structure by an equivalent model made up of a finite number of discrete structure elements. Each of these elements has known elastic and inertial properties that can be expressed in matrix form. These matrices, when joined together in a manner consistent with a set of rules derived from the theory of elasticity, yield the static and dynamic properties of the actual continuous structure. Przemieniecki's book provides an extensive treatment of the theory of matrix structural analysis (Ref. 10).

Three types of finite elements are used to model the wing used in this analysis: rods, shear panels and quadrilateral plate elements (Ref. 8:1.3-4, 1.3-5). The rod element includes extensional and torsional properties, but it does not resist bending. The shear panel is a two-dimensional element that can resist tangential forces along its edges, but it cannot resist normal forces. The quadrilateral plate element has both inplane and bending stiffness with a solid homogeneous cross section. These elements are joined at node points to form the representation of the wing box structure, as seen in Fig. 1.

Doublet Lattice Method

The basic technique employed to represent lifting surfaces in NASTRAN is the Doublet-Lattice Method (DLM) as originally described by Albano and Rodden (Ref. 1:279-285). The DLM is an extension of the Vortex-Lattice Method to subsonic unsteady flow. The lifting surface is modeled by

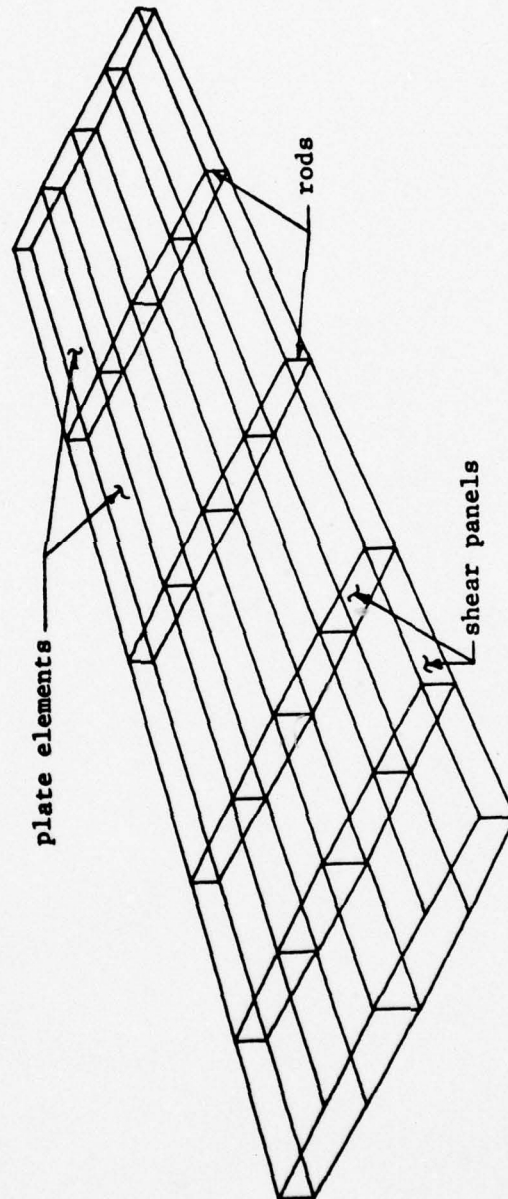


Fig. 1. Wing Box Structure Represented by Finite Elements

horseshoe vortices that represent the steady flow effects and acceleration potential doublets that represent the oscillatory effects.

To apply DLM, the lifting surface is divided into arrays of trapezoidal boxes whose sides lie parallel to the freestream so that surface edges, fold lines, and hinge lines fall on the box boundaries. The bound vortex and a distribution of acceleration potential doublets are placed on the quarter-chord line of each box, as in Fig. 2. A control point is centered on the three-quarter chord point of each box. Then the effects of all vortices and doublets are summed for each control point to obtain the total normalwash at a control point.

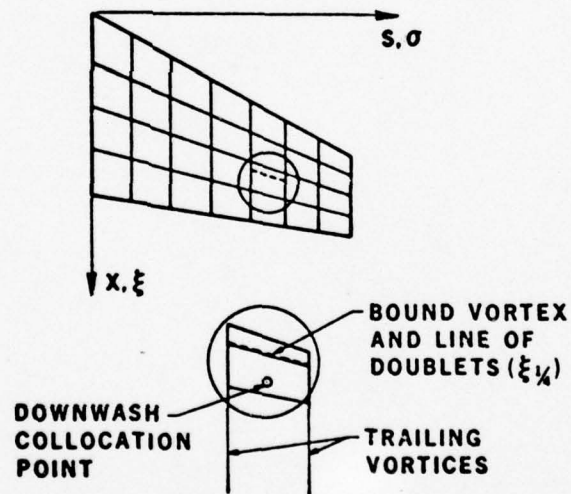


Fig. 2. Lifting Surface Idealization by Doublet-Lattice Method (Ref. 4:14)

The integral equation that relates the wash normal to a harmonically oscillating surface to the lifting pressure is

$$w(P_j) = \frac{1}{8\pi} \iint_S C_P(P) K_F(P_j, P, k, m) dS \quad (1)$$

where

w = normalwash angle = $\frac{\bar{w}}{U} = \alpha + i \left(\frac{2k}{c}\right)h$

\bar{w} = downwash velocity

P = any point on the planform

P_j = the j^{th} point

C_p = differential pressure coefficient

KF = kernel function relating normalwash at P_j to the unit pressure at P (Ref. 14)

k = reduced frequency = $\frac{c\omega}{2U}$

m = Mach number

h = vertical displacement of the surface

α = streamwise slope of the deformed surface

c = reference chord

S = lifting surface area

U = freestream velocity

ω = frequency of oscillation

(Ref. 12:78-79)

This integral is then discretized and put in matrix form as used in NASTRAN:

$$\{w_j\} = [A_{jj}] \{P_j\} \quad (2)$$

where

w_j = downwash (normalwash) at 3/4 chord point for doublet lattice

P_j = pressure (acting at 1/4 chord for doublet lattice)

$A_{jj}(k,m)$ = aerodynamic influence matrix.

(Ref. 6:17.5-1)

NASTRAN takes all codes for computing A_{jj} directly from Giesing, Kalman, and Rodden (Ref. 4). The downwash at the 3/4 chord point is related to the deflection and rotation of the box control point at the center. After solving for the unknown pressure distribution of the wing from Eq. (2), a spline fitting technique is used to relate the set of point aerodynamic loads to the structural grid.

Surface Spline

The structural grid points usually do not coincide with the grid points that define the aerodynamic elements. Equations of restraint between the two sets of grid points are supplied by the theory of surface splines (Ref. 6). A surface spline is a solution for an infinite uniform plate, or a function $h(x,y)$ for all points (x,y) , when a discrete set of points, $h_i = h(x_i, y_i)$, is known. In NASTRAN, the structural degrees of freedom are taken to be the independent degrees of freedom, and the aerodynamic degrees of freedom are dependent. From the theory of surface splines, then, a matrix is obtained which relates the dependent degrees of freedom to the independent degrees of freedom. This feature of NASTRAN allows the choice of structural and aerodynamic elements to be made independently of each other.

Flutter Equation

The basic differential equation for an oscillating lifting surface is

$$[M] \{\ddot{u}\} - [A] \{\dot{u}\} + [K] \{u\} = 0 \quad (3)$$

where

[M] = generalized mass matrix

[A] = generalized aerodynamic force matrix

[K] = generalized stiffness matrix

{u} = generalized modal vector.

(Ref. 15:92)

The generalized aerodynamic force matrix is the product of the dynamic pressure, $1/2 \rho U^2$, and the aerodynamic matrix, [Q], where an element of [Q] is defined as

$$Q_{rs} = \iint_S Q_r(x,y) C_{p(s)}(x,y) dS \quad (4)$$

where $Q_r(x,y)$ is the deflection distribution of the r^{th} mode, $C_{p(s)}(x,y)$ is the pressure coefficient distribution in the s^{th} mode, and the integration is performed over the lifting surface area S. Then, Equation (3) may be written as

$$[M] \{\ddot{u}\} - \frac{\rho U^2}{2} [Q] \{u\} + [K] \{u\} = 0 \quad (5)$$

To include structural damping in the system, the generalized stiffness matrix becomes

$$[\bar{K}] = [I + i G] [K] \quad (6)$$

where [G] is a diagonal matrix of modal damping and [I] is an identity matrix. The stiffness in the j^{th} mode is then

$$\bar{K}_{jj} = (1 + i g_{s(j)}) K_{jj} \quad (7)$$

where $g_{s(j)}$ is the structural damping in the j^{th} mode. Then Equation (5) becomes

$$[M] \{\ddot{u}\} - \frac{\rho U^2}{2} [Q] \{u\} + [\bar{K}] \{u\} = 0 \quad (8)$$

Assume simple harmonic motion. Then the generalized coordinates are written as $\{u\} = \{\bar{u}\} e^{\Omega t}$, where \bar{u} is no longer time dependent and Ω may contain damping. Equation (8) is then rewritten as

$$[\Omega^2 [M] - \frac{\rho U^2}{2} [Q] + [\bar{K}]] \{\bar{u}\} = 0 \quad (9)$$

This is the basic flutter equation.

K-Method of Flutter Solution

In the k-method of flutter solution, Ω is considered to be undamped ($\Omega = i\omega$), and the aerodynamic force matrix is a function of reduced frequency k and Mach number m . Then, the basic equation for modal flutter analysis is

$$\left[-\omega^2 [M] - \frac{\rho U^2}{2} [Q(k, m)] + [\bar{K}] \right] \{\bar{u}\} = 0 \quad (10)$$

(Ref. 15:93)

The reduced frequency is defined as

$$k = \frac{c\omega}{2U} \quad (11)$$

where

c = a reference length

ω = the frequency of oscillation

U = the free stream velocity.

In order to bring the system into neutral stability, an artificial structural damping term, g , is introduced. Applying this artificial damping to the j^{th} diagonal term of the stiffness matrix of Equation (10) yields

$$\bar{K}_{jj} = \frac{1}{\omega^2} (1 + i g_s(j) + i g) K_{jj} \quad (12)$$

For small values of damping ($g \cdot g_s(j) \ll 1$), the j^{th} diagonal term is approximated by

$$\bar{K}_{jj} \doteq \left(\frac{1+ig}{\omega^2}\right) (1 + i g_s(j)) K_{jj} \quad (13)$$

or

$$\bar{K}_{jj} \doteq \left(\frac{1+ig}{\omega^2}\right) \bar{K}_{jj} \quad (14)$$

The aerodynamic terms are then converted to aerodynamic mass:

$$\left[- \left[[M] + \frac{\rho}{2} \left(\frac{c}{2k}\right)^2 [Q(k,m)] \right] \left[\frac{\omega^2}{1+ig} \right] + [\bar{K}] \right] \{\bar{u}\} = 0 \quad (15)$$

Equation (15) is a complex eigenvalue problem that is solved for a series of values for parameters k , m , and ρ . The complex eigenvalues are $\omega^2/(1+ig)$, which yield real values of circular frequency ω and structural damping, g . Velocity U is obtained from $U = c\omega/2k$. A positive value of damping requires structural damping be added to bring the system into neutral stability, or, the system may be considered unstable. A negative value has the opposite interpretation. Flutter occurs when the values of k , m , and ρ force the artificial structural damping, g , to be zero.

NASTRAN uses a variation of Eq. (15) that allows solution of static divergence problems. The equation is

$$\left[\left[\left(\frac{2k}{c}\right)^2 [M] + \left(\frac{\rho}{2}\right) [Q(k,m)] \right] \left[\frac{-U^2}{1+ig} \right] + [\bar{K}] \right] \{\bar{u}\} = 0 \quad (16)$$

(Ref. 7:17.6-1)

$$\bar{K}_{jj} = \frac{1}{\omega^2} (1 + ig_s(j) + ig) K_{jj} \quad (12)$$

For small values of damping ($g \cdot g_s(j) \ll 1$), the j^{th} diagonal term is approximated by

$$\bar{K}_{jj} \doteq \left(\frac{1+ig}{\omega^2}\right) (1 + ig_s(j)) K_{jj} \quad (13)$$

or

$$\bar{K}_{jj} \doteq \left(\frac{1+ig}{\omega^2}\right) \bar{K}_{jj} \quad (14)$$

The aerodynamic terms are then converted to aerodynamic mass:

$$\left[- \left[[M] + \frac{\rho}{2} \left(\frac{c}{2k}\right)^2 [Q(k,m)] \right] \left[\frac{\omega^2}{1+ig} \right] + [\bar{K}] \right] \{\bar{u}\} = 0 \quad (15)$$

Equation (15) is a complex eigenvalue problem that is solved for a series of values for parameters k , m , and ρ . The complex eigenvalues are $\omega^2/(1+ig)$, which yield real values of circular frequency ω and structural damping, g . Velocity U is obtained from $U = c\omega/2k$. A positive value of damping requires structural damping be added to bring the system into neutral stability, or, the system may be considered unstable. A negative value has the opposite interpretation. Flutter occurs when the values of k , m , and ρ force the artificial structural damping, g , to be zero.

NASTRAN uses a variation of Eq. (15) that allows solution of static divergence problems. The equation is

$$\left[\left[\left(\frac{2k}{c}\right)^2 [M] + \left(\frac{\rho}{2}\right) [Q(k,m)] \right] \left[\frac{-U^2}{1+ig} \right] + [\bar{K}] \right] \{\bar{u}\} = 0 \quad (16)$$

(Ref. 7:17.6-1)

It is then possible to let $k = 0$, as division by k is not required. At $k = 0$, $\omega = 0$, which indicates the static condition of divergence exists if damping becomes positive.

III. Analysis

Structure Description

The wing box top view is shown in Fig. 3 with its node points numbered as shown. The corresponding lower node point numbers are found by adding one to the top node. The element gage sizes are shown in Fig. 4, where the bottom plate elements have the same dimensions as the top plate elements. The rod elements that connect the upper and lower nodes all have a cross sectional area of 0.10 in^2 . The wing dimensions and element sizes are the same as the strength optimized intermediate complexity wing from AFFDL-TR-75-137 (Ref. 15:167). Fig. 5 gives the wing box dimensions.

Elements. The wing box consists of 100 finite elements. The upper and lower surfaces of the wing box are covered by trapezoidal plate elements - 20 on the upper surface and 20 on the lower surface. A total of 35 shear panels represent the three spars and five ribs. To inhibit motion between the upper and lower surfaces, 25 rods connect the upper and lower surface node points.

Degrees of Freedom at Nodes. There are a total of 60 nodes at which the 100 elements connect. The ten nodes in the root chord plane are rigidly constrained in order to cantilever the wing. Each of the remaining 50 nodes are allowed one degree of freedom normal to the plane of the wing.

In addition, the nodes along the leading and trailing edges are allowed a rotational degree of freedom about axes running along the leading and trailing edge. The tip nodes are allowed to have two rotational degrees of freedom, as shown in Fig. 6. These additional degrees

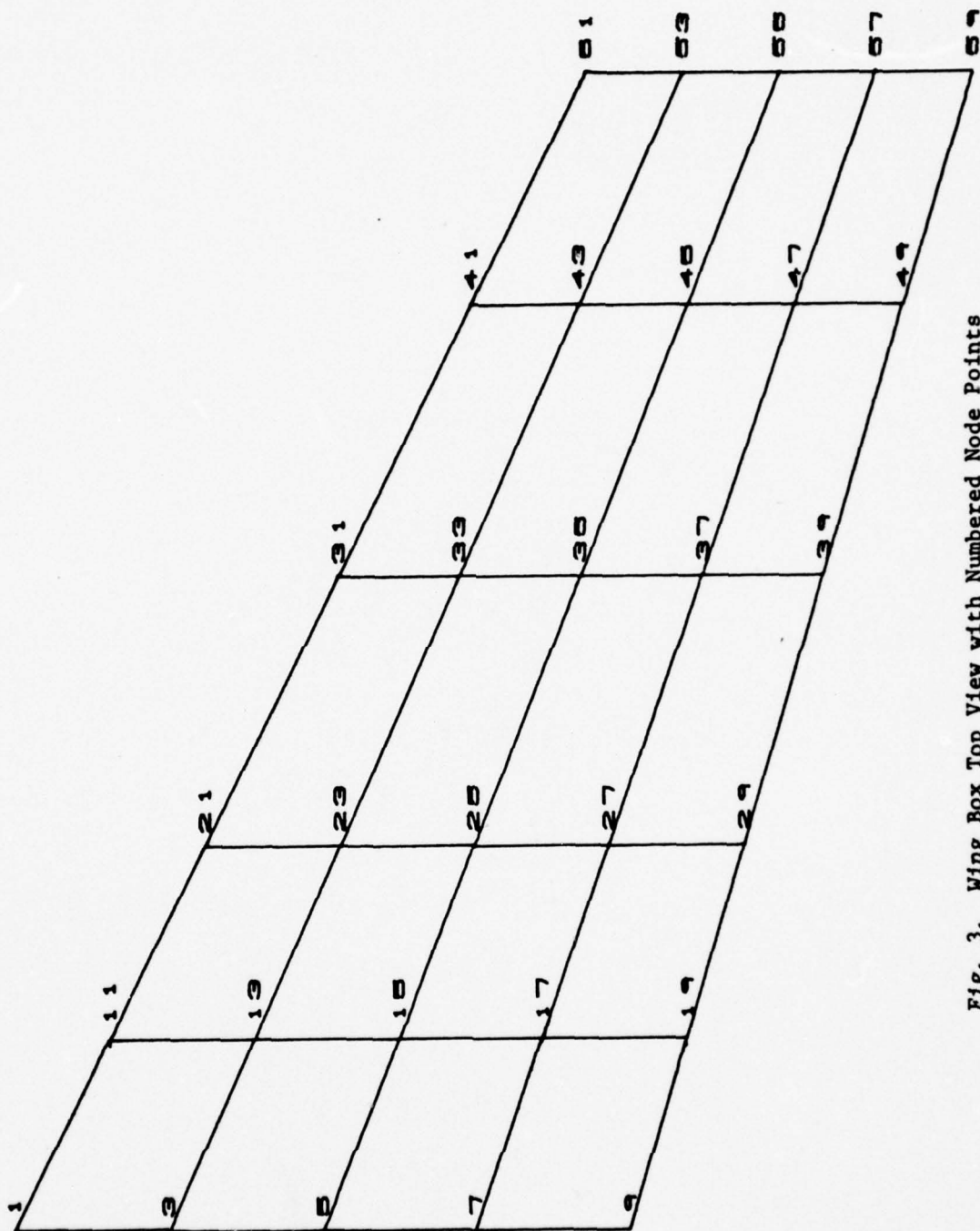


Fig. 3. Wing Box Top View with Numbered Node Points

Note: Gage Sizes in Inches

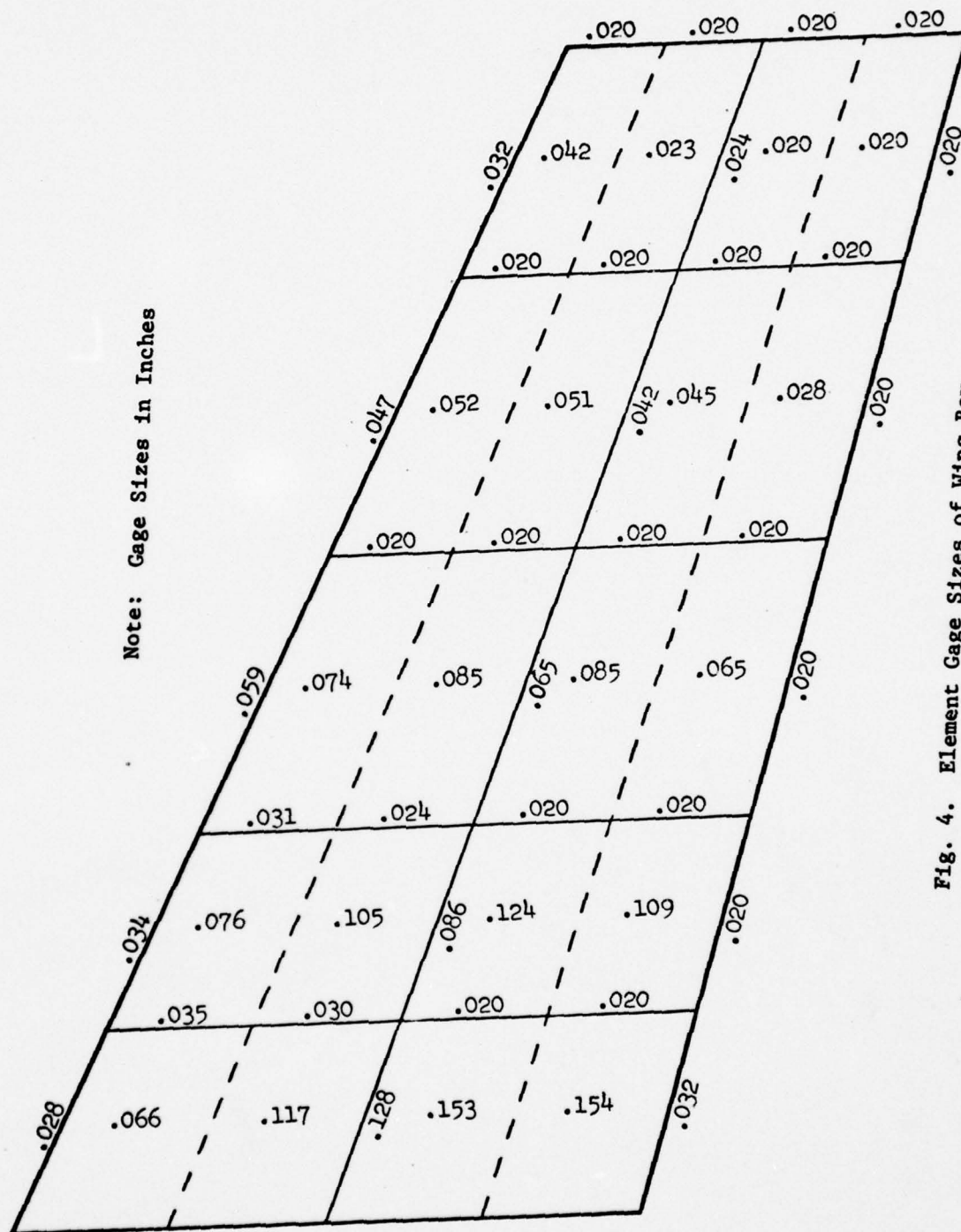


Fig. 4. Element Gage Sizes of Wing Box
(Ref. 15 :167)

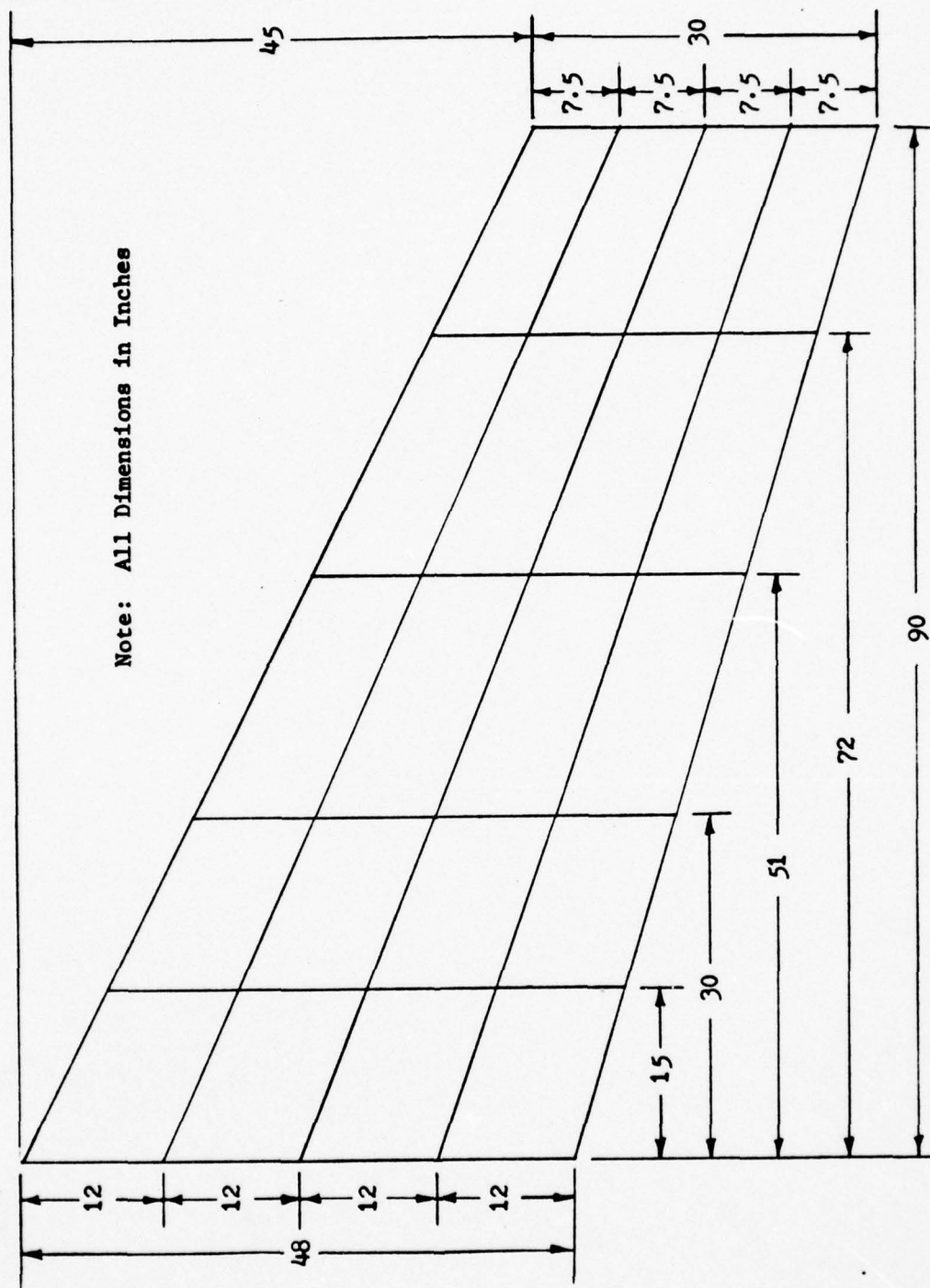


Fig. 5. Wing Box Dimensions

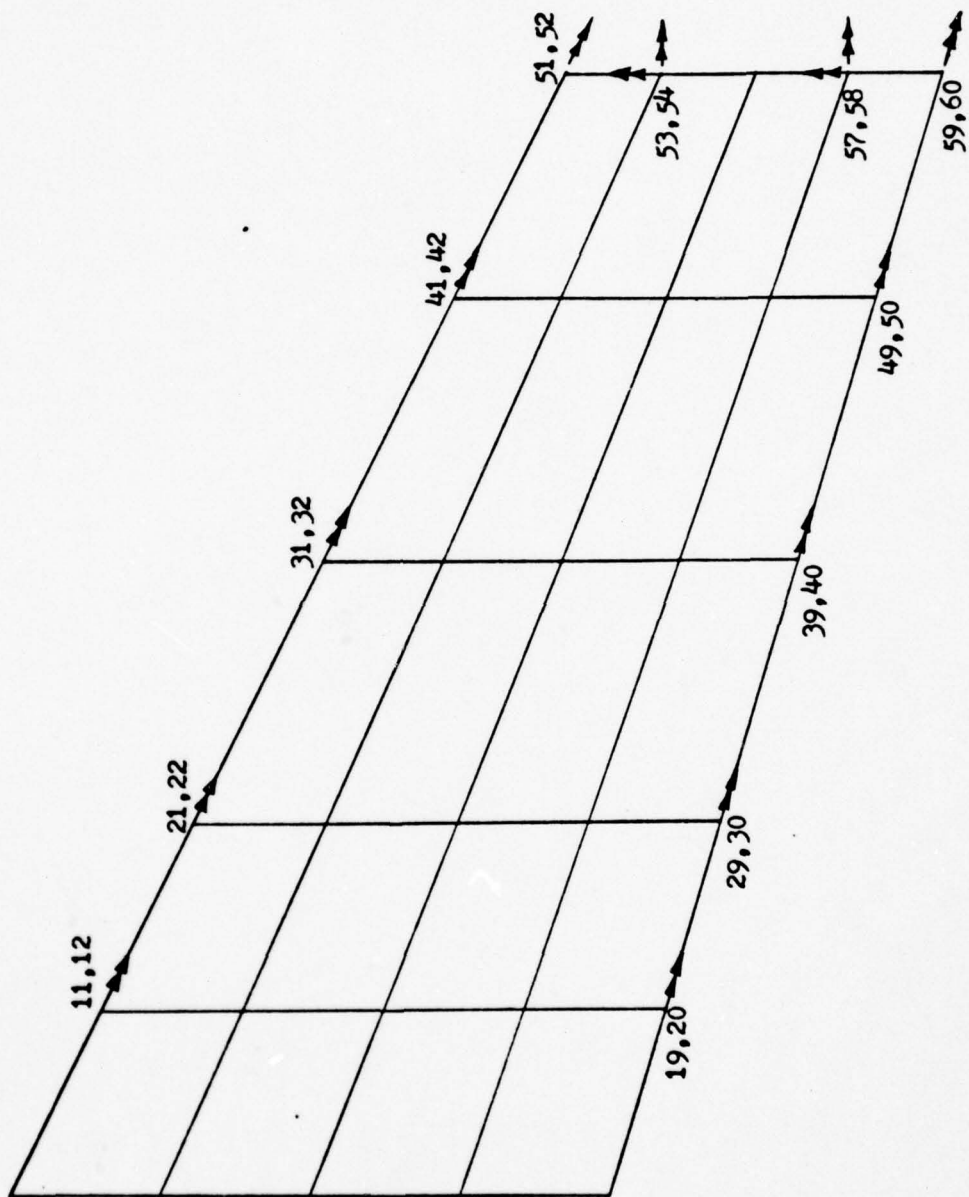


Fig. 6. Additional Degrees of Freedom at Nodes

of freedom are necessary in order to simulate the rotational inertial effects of the overhanging panels connected to the wing box.

Wing Mass. The fully stressed wing structure weight was initially 61.1 lbs. Then, additional mass was added to account for structural connection materials, such as flanges and rivets, and nonstructural mass such as pumps, tubing, etc. In addition, weight for the overhanging structure was incorporated at the leading edge, trailing edge, and tip nodes, with representative moments of inertia about these nodes to simulate rotational inertial effects of the panels. The lumped masses and moments at each node are found in Appendix A. These additional masses raised the total weight of the wing to 374.6 lbs.

Aerodynamic Description

The wing flutter analysis was performed using the doublet-lattice aerodynamics for Mach 0.9 at sea level. The planform was represented by 32 trapezoidal aerodynamic panels, four chordwise and eight spanwise at equal division points, as seen in Fig. 7. These divisions were chosen in order to make the aspect ratio of the boxes roughly one or less. Also, the number of boxes per reference chord should be greater than eight times the reduced frequency (Ref. 8:1.11-1). The aerodynamic model does not include the effect external stores would have upon the lifting surface.

A surface spline was used to interpolate between all the aerodynamic grid points, located at the center of each aerodynamic element, and the selected structural grid points. The odd numbered structural nodes were selected for spline interpolation with all the aerodynamic nodes. Only the normal displacement degree of freedom for each structural node is required for the surface spline.

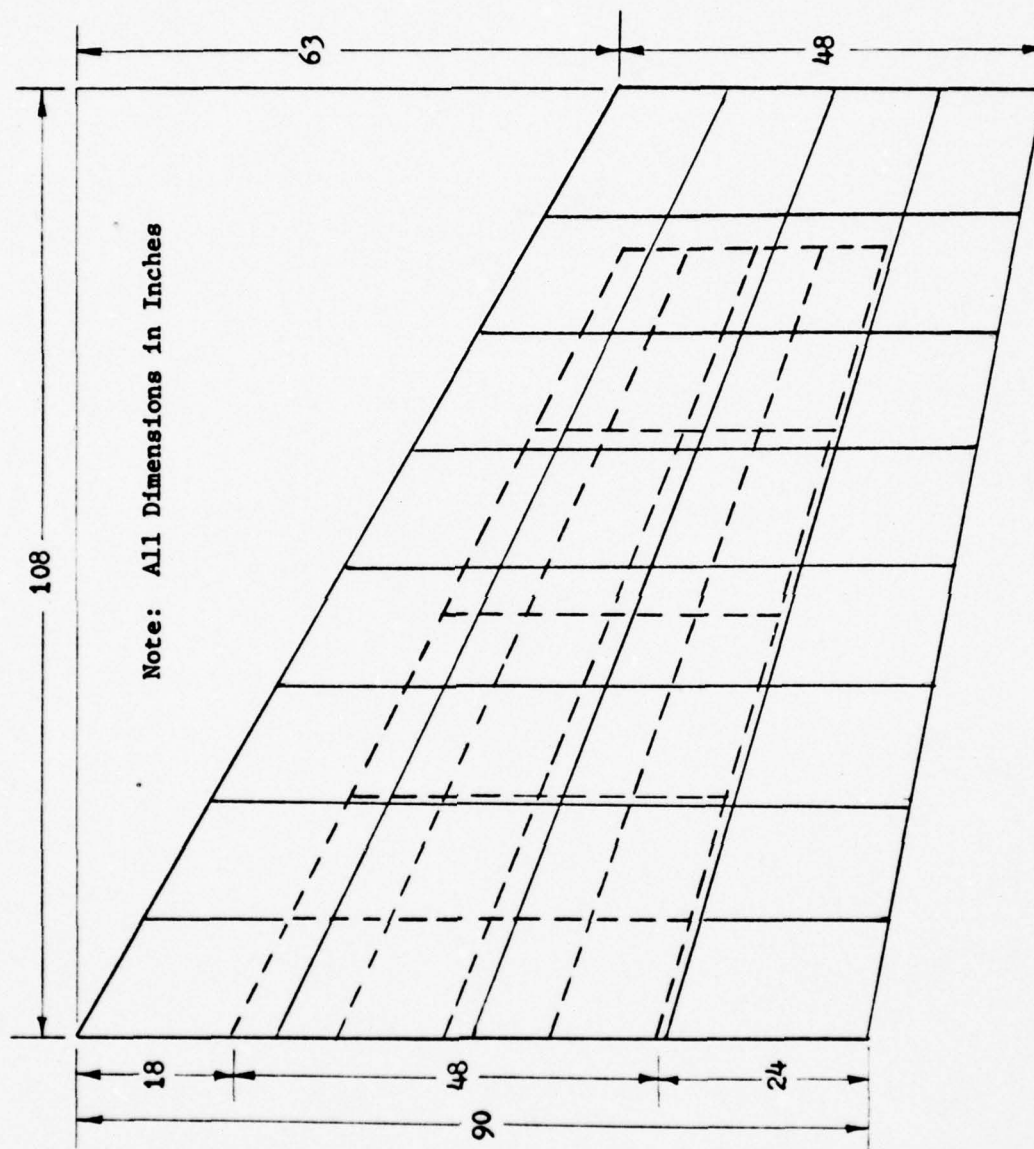


Fig. 7. Top View of Aerodynamic Planform with Wing Box

Elastic Axis Determination

The location of the elastic axis of the wing was essential in order to correctly interpret the flutter results. The elastic axis is defined as the axis about which rotation occurs when a wing is loaded in pure torsion (Ref. 9:448). It may alternately be defined as the locus of shear centers of the cross sections of a cantilever wing (Ref. 3:17). The shear center of a wing cross section is the point at which a shear force acts to produce a wing deflection without rotation. If the wing is an elastic structure, the shear center of a cross section coincides with the elastic axis.

To locate the elastic axis on the wing model, a static analysis was performed using NASTRAN. A static shear force was applied to each lower node point along each rib. The elastic axis was located by interpolation between the two nodes that produced the least rotation of the cross section. The resulting locus of shear centers is shown in Fig. 8.

Free Vibration

A free vibration analysis was performed on the basic wing model to determine the fundamental mode shapes and frequencies. Only vertical displacement of nodes 11 through 60 were used in the analysis with nodes 1 through 10 being totally restrained. The first three fundamental modes obtained are seen in Figs. 9 through 11, in which the deformed shape is superimposed over the undeformed shape. Mode 1 is seen to be first bending with a frequency of 49.6 Hz. Mode 2 is predominantly first torsion coupled with some bending. This frequency is 95.4 Hz. Mode 3 is primarily second bending coupled with considerable torsion. This frequency is 104.1 Hz. These three modes, used for the modal flutter analysis, are typical for a simple cantilevered swept wing.

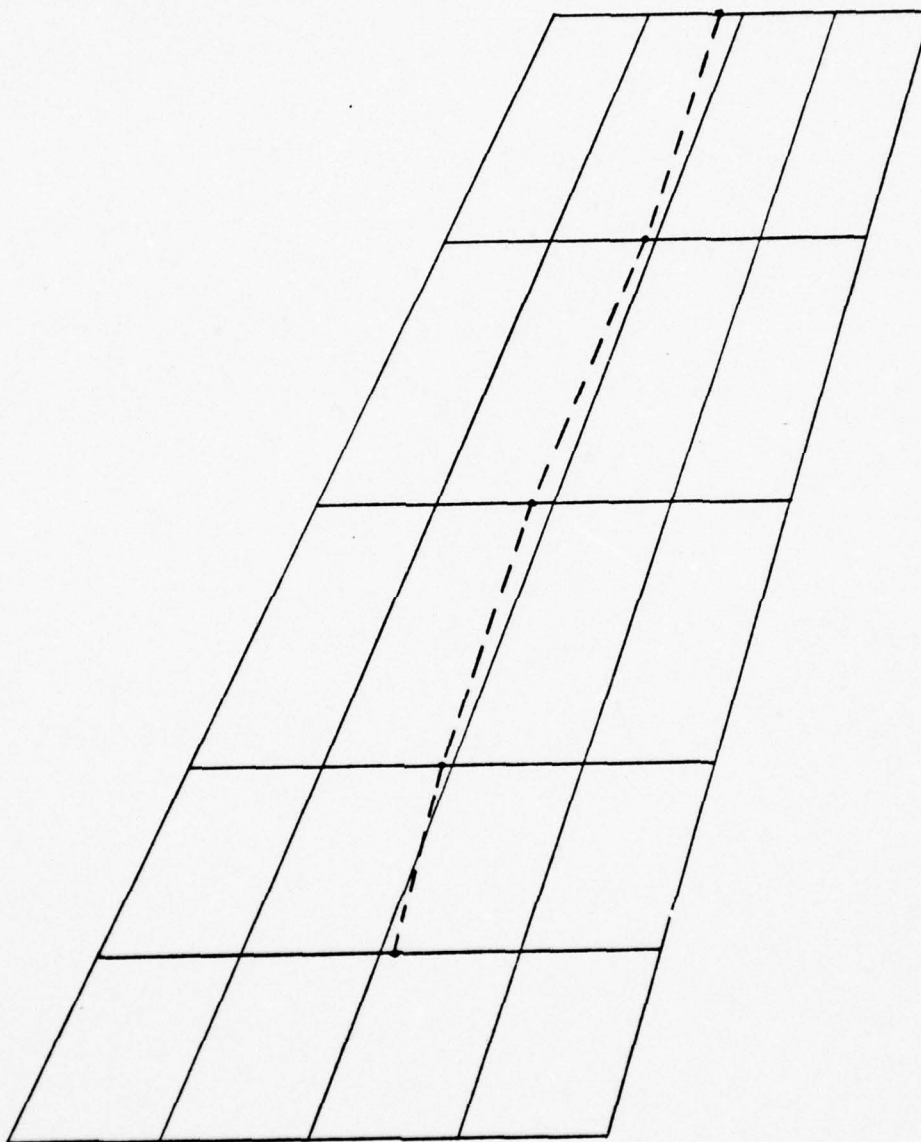


Fig. 8. Location of Elastic Axis

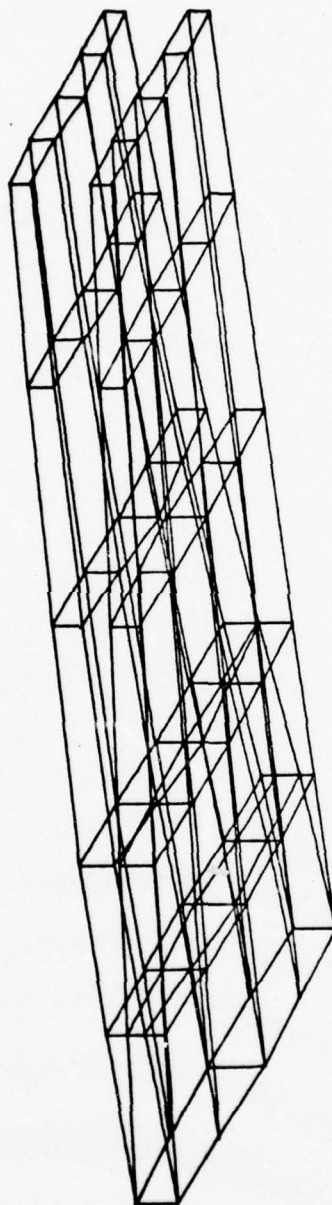


Fig. 9. Free Vibration Mode No. 1, Frequency = 49.6 Hz

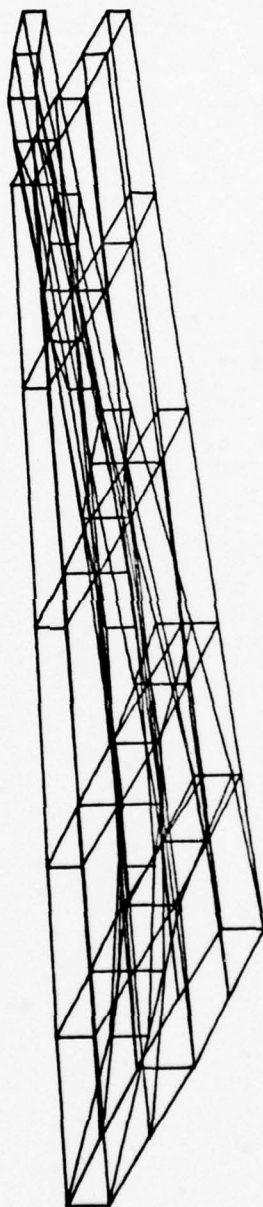


Fig. 10. Free Vibration Mode No. 2, Frequency = 95.4 Hz

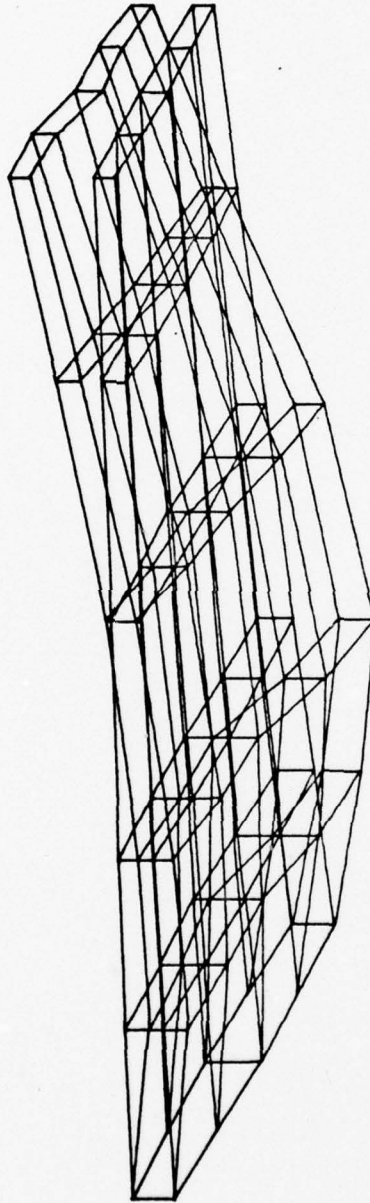


Fig. 11. Free Vibration Mode No. 3, Frequency = 104.1 Hz

Flutter Analysis

All flutter analysis is performed for conditions at sea level and Mach 0.9. The first flutter test was for the basic wing model with no external stores added. A reduced frequency range from $k=0.75$ to $k=0.0$ was used to check for flutter. At $k=0.0$, flutter frequency goes to zero, which indicates the static condition of divergence occurs if damping becomes positive at that point. As mentioned in Chapter II, NASTRAN uses a modified flutter equation, Eq. (16), which allows k to go to zero.

The next flutter test determined the effect of concentrated masses placed along ribs and spars at nodes of the wing. This procedure is commonly called mass balancing. Two mass values were used for the test. A 3.10 slug mass (100 lb), or approximately 27% of the total wing mass, and a 6.21 slug mass (200 lb), or approximately 53% of the total wing mass, were selected. For each node that received a mass, a flutter speed and flutter frequency were determined.

To simulate store pitch inertia, two equal masses were used. In order to compare results with the single concentrated mass results, the centers of gravity and mass value for both cases were the same. As an example, to simulate a 100 lb store with pitch inertia, two 50 lb weights were placed along the rib on the two nodes adjacent to where the single concentrated 100 lb weight had been. The same procedure was followed for the 200 lb store to simulate store pitch inertia. For each mass combination, a flutter speed and flutter frequency were determined.

The normal procedure to determine flutter characteristics was to first use a wide range of k values to find two k values where the value of artificial damping changed from negative to positive. Then, a range of k values between the two k values was selected to closely bracket the

flutter velocity and flutter frequency values where damping goes to zero. A linear variation of velocity and frequency was then assumed for the interpolation to the values of velocity and frequency that occur at zero damping. This assumption is accurate if the flutter frequency and velocity are bracketed closely.

For problems that require considerable amounts of computer time, a saving in time could be realized when refining the location of the flutter speed by using the restart procedure incorporated in NASTRAN. By using the restart procedure, recomputation of the natural modes and frequencies of the structure would be avoided. Likewise, only newly requested aerodynamic matrices would be computed, which is a sizeable saving in computer time.

IV. Results

The two flutter plots generated for each case are represented by example Figs. 12-A and 12-B. The flutter plots for each case in which flutter occurred are found in Appendix B. Figure 12-A is the damping versus velocity plot, from which the flutter speed and flutter mode may be determined. Figure 12-B is the frequency versus velocity plot, from which the flutter frequency is determined by knowing the flutter velocity and flutter mode.

The values for flutter speed and frequency obtained by linear interpolation for the various cases are listed in Tables I and II. Table I contains the values obtained for the mass balancing experiment where single concentrated 100 lb and 200 lb weights were placed at various nodes. Table II lists the flutter speeds and frequencies obtained for the store inertia simulation, plus the computed store pitch inertia about the store center of gravity. The investigative Mach number was 0.9, or 577 knots for conditions at sea level, for all cases. The flutter speeds obtained were all much greater than 577 knots, which means that this wing model will not flutter at sea level at 0.9 Mach. This is a desirable characteristic.

For the basic wing with no external stores added, no flutter was detected up to divergence speed. The wing diverged in the torsion mode. This result indicates a wing that has sufficient torsional stiffness to prevent flutter up to wing divergence when it carries no external stores.

The free vibration frequencies for each loading case are given in Table IV of Appendix C. Also in Appendix C, plots comparing the free vibration frequencies of store versus concentrated mass at the 3/4 node

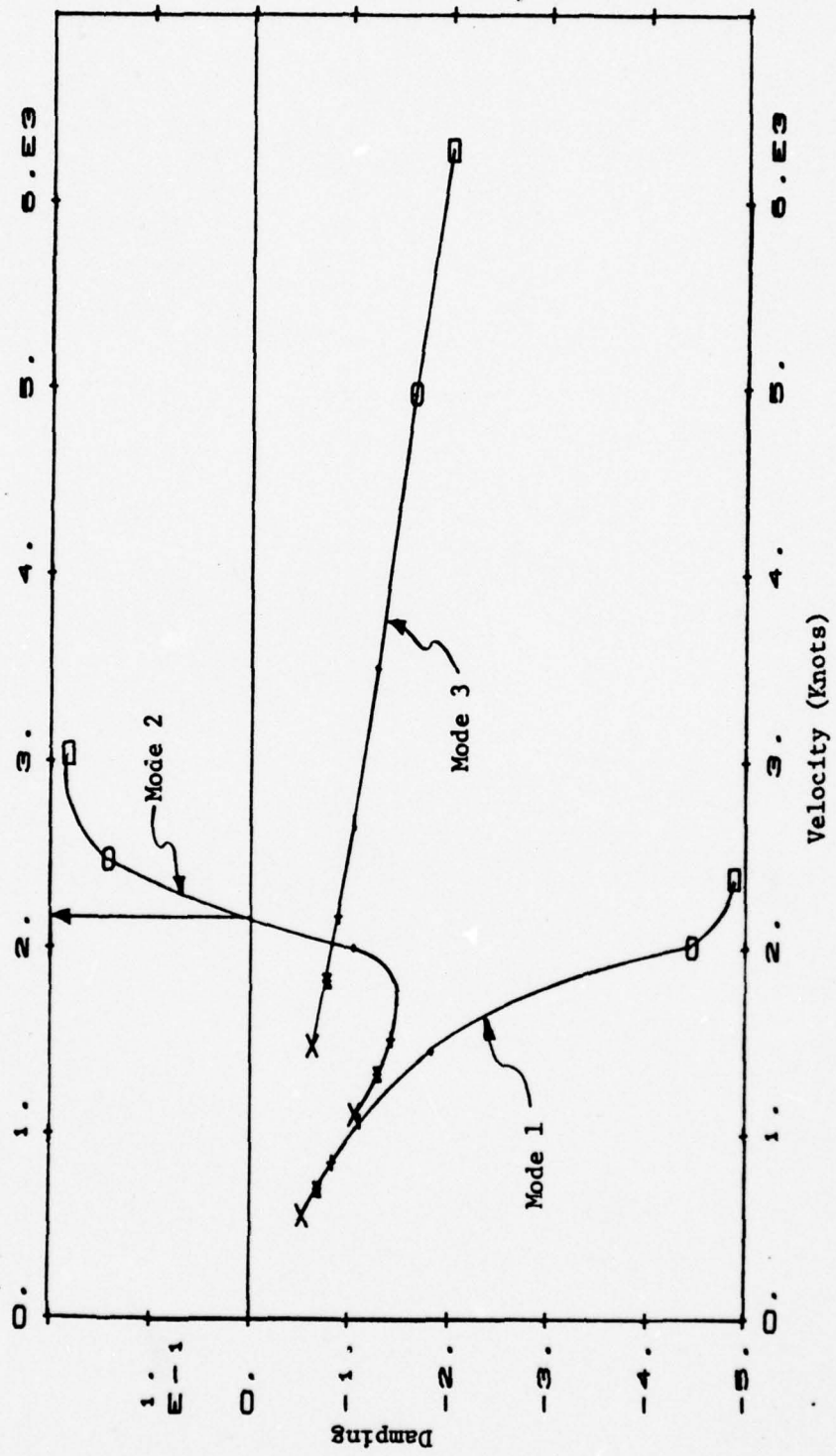


Fig. 12-A. Flutter Speed Solution

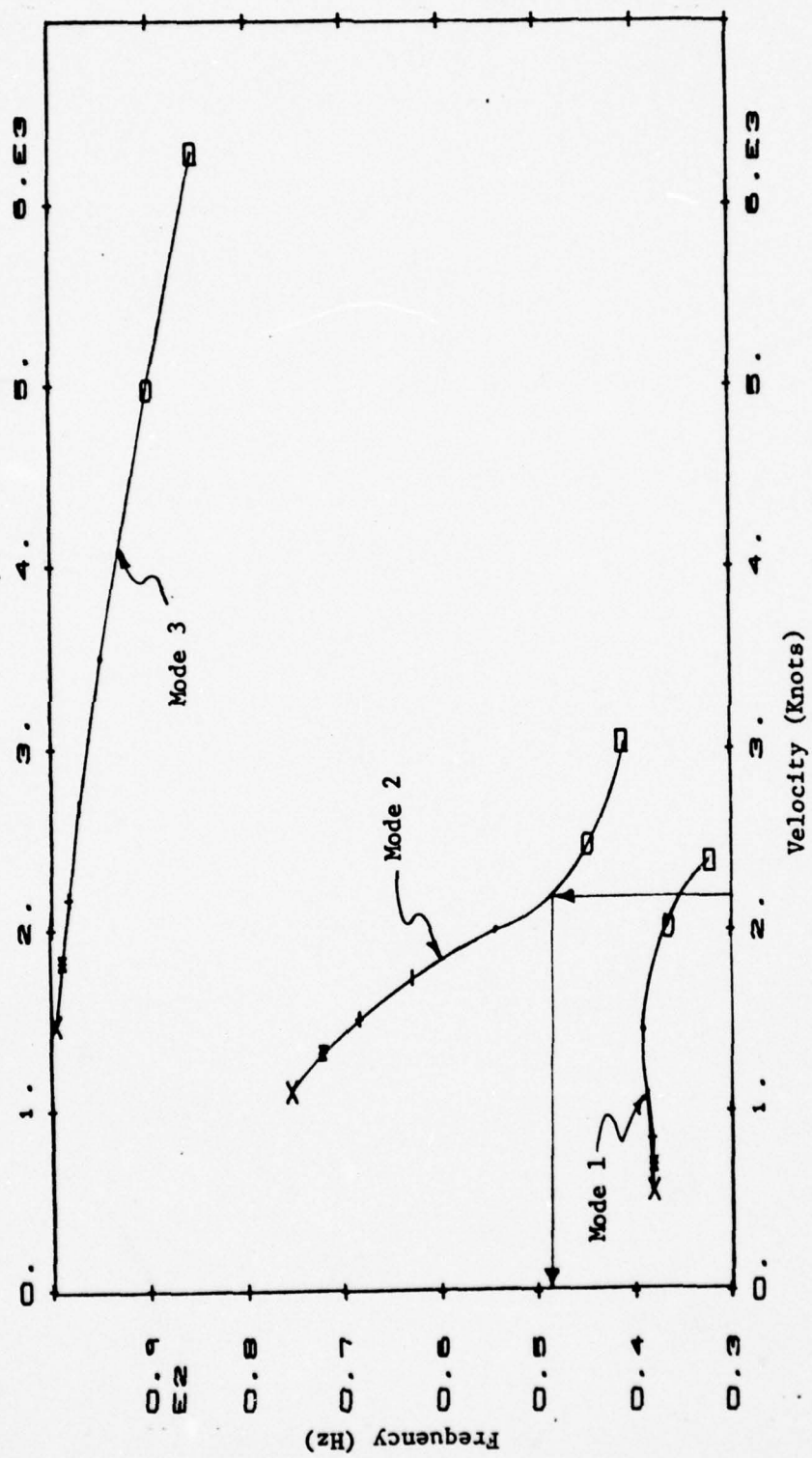


Fig. 12-B. Flutter Frequency Solution

Table I Results for Mass Balancing		
100 lb Concentrated at a Node		
Node	U_f (knots)	ω_f (Hz)
28	none	---
30	none	---
36	none	---
38	2357	45.6
40	2096	49.4
44	none	---
46	2226	44.1
48	2169	41.6
50	1961	48.0
54	none	---
56	2133	39.8
58	2136	36.7
60	1937	42.2
200 lb Concentrated at a Node		
28	2262	42.5
38	2387	38.1
48	2243	33.5
58	2182	28.8

Table II Results for Store Inertia Simulation				
100 lb Store (Two x 50 lb)				
Nodes	CG Node	*Icg(lb-ft-sec ²)	U _f (knots)	ω _f (Hz)
26, 30	28	342	none	---
34, 38	36	277	none	---
36, 40	38	277	2414	49.5
44, 48	46	219	none	---
46, 50	48	219	2153	48.9
54, 58	56	175	2618	36.7
56, 60	58	175	2139	50.7
200 lb Store (Two x 100 lb)				
26, 30	28	685	2435	49.8
36, 40	38	555	2263	48.4
46, 50	48	438	2130	44.5
56, 60	58	350	2270	40.4

*Note: Icg is store pitch inertia about the store center of gravity

points are given. The mode shapes for each loading case were not obtained.

Mass Balancing Effects

Masses were added to the basic wing using one mass value at a node for each flutter test. The mass was shifted in both the spanwise and chordwise directions. The first observation was that no flutter could be produced by placing the mass between the leading edge and the elastic axis. This is a normal result as flutter is damped in most cases where the center of gravity of a wing is shifted forward of the elastic axis. When the mass was shifted aft of the elastic axis, flutter was produced except for those cases of the 100 lb weight placed near the wing root.

As can be seen in Table I, as the mass was shifted chordwise from the nodes at midchord along a rib to the nodes at the trailing edge, the flutter speed generally decreased. The lowest flutter speeds occurred when the mass was placed on the trailing edge nodes of each rib. The most critical flutter speed was produced by placing the mass at node 60 located at the tip. No definite trend for flutter frequency could be detected for the chordwise movement of mass. As the mass was moved spanwise toward the tip of the wing, the flutter speed and frequency both decreased. When moving the mass spanwise, the critical flutter speed occurred when the mass was located at the tip of the wing.

The flutter mode was the fundamental torsion mode in all cases. Evident on most of the frequency versus velocity plots in Appendix B is the interaction of the first two modes when flutter occurs. The interaction is characterized by the frequencies of the two modes converging, or nearly so, to a single frequency at flutter. This is the classic coalescence of frequencies that is a characteristic of modal flutter.

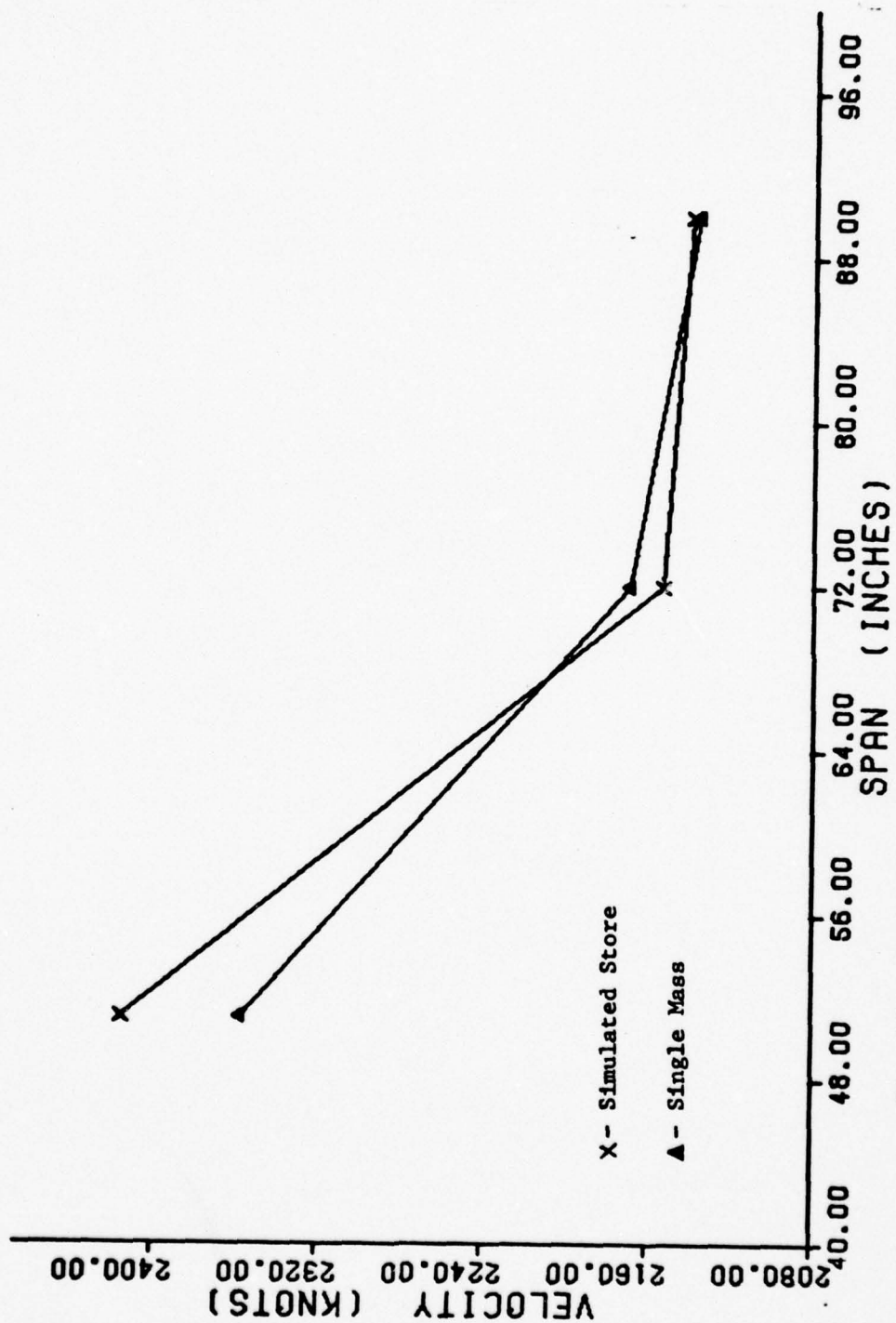


Fig. 13. Comparison of Flutter Speeds of 100 lb Store Versus Single Concentrated Mass at 3/4 Chord Nodes

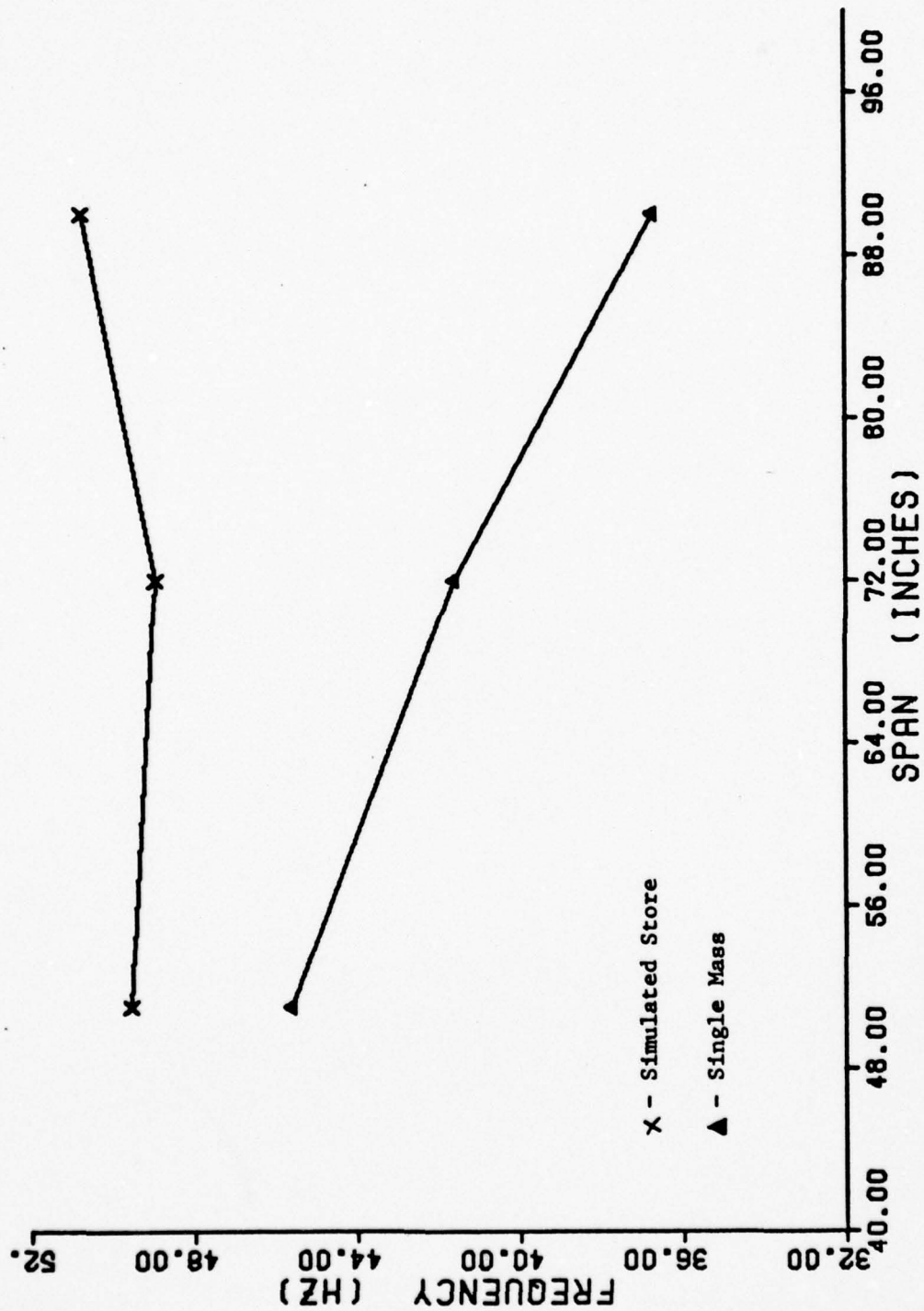


Fig. 14. Comparison of Flutter Frequencies of 100 lb Store Versus Single Concentrated Mass at 3/4 Chord Nodes

Store Inertia Effects

The results of the flutter test involving two 50 lb weights, simulating a 100 lb store, are compared with results for the single concentrated 100 lb weight at the $3/4$ chord nodes in Figs. 13 and 14. Looking at Fig. 13 first, the largest difference in flutter speed for the two cases was at node 38. Here, the store pitch inertia raised the flutter speed over the single concentrated mass flutter speed by fifty-seven knots. There is a definite trend in Fig. 14, as the flutter frequency of the store simulation is consistently higher than the single mass case. The difference increases from 3.9 Hz at node 38 to 14.0 Hz at node 58.

Now consider Figs. 15 and 16, and compare flutter results of the 200 lb store (two-mass combination) with the single 200 lb mass along the $3/4$ chord line. As can be seen in Fig. 15, the two-mass combination tends to damp flutter at nodes 38 and 48, and conversely, to promote flutter at nodes 28 and 58, relative to the single mass. Thus, there is no definite trend with flutter speeds as affected by store pitch inertia. But looking at flutter frequencies in Fig. 16, there is again a definite trend as the flutter frequency of the simulated store is consistently higher than the single mass flutter frequency. The difference varied from 7.3 Hz at node 28 to 11.6 Hz at node 58.

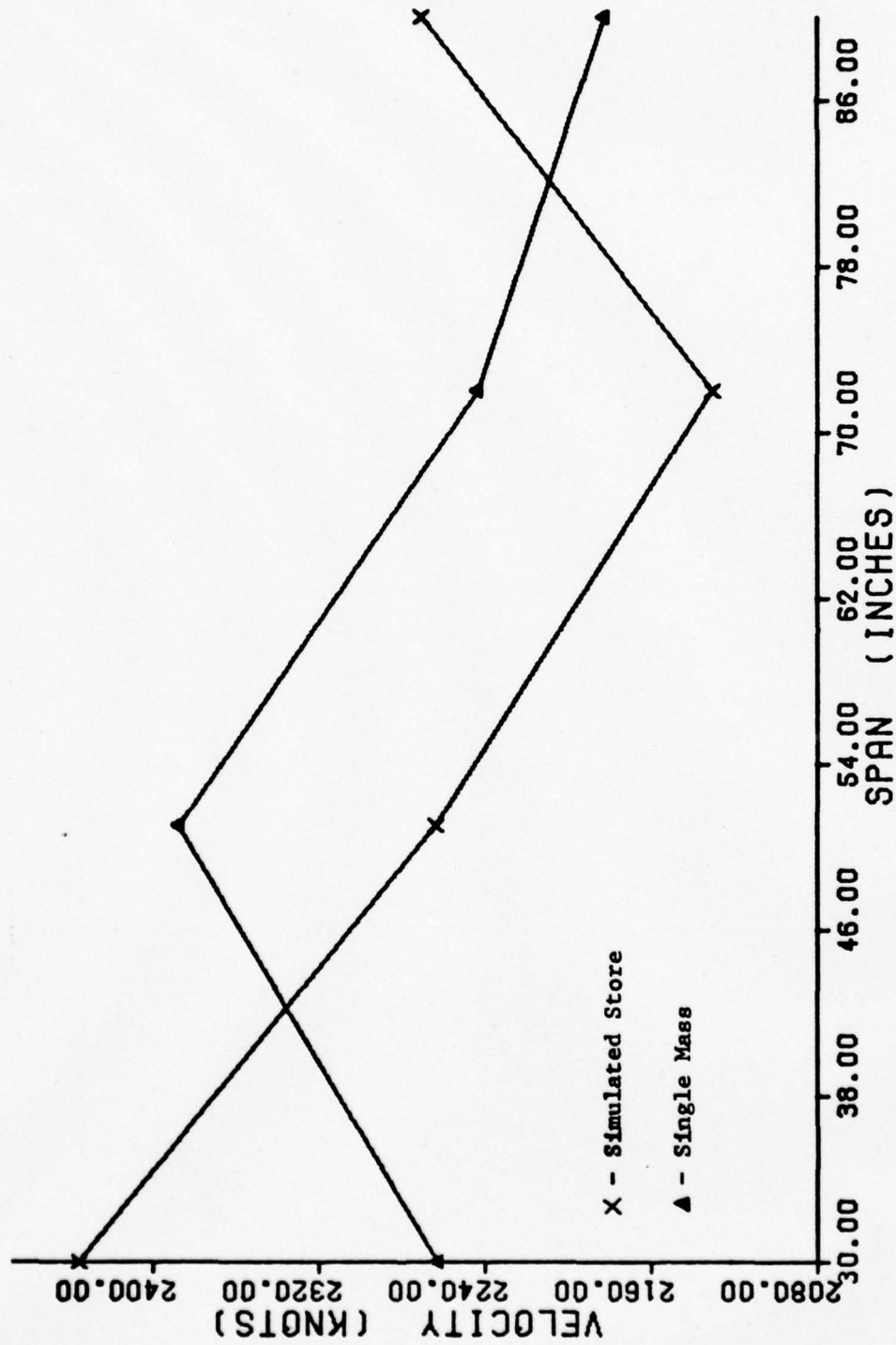


Fig. 15. Comparison of Flutter Speeds of 200 lb Store Versus Single Concentrated Mass at 3/4 Chord Nodes

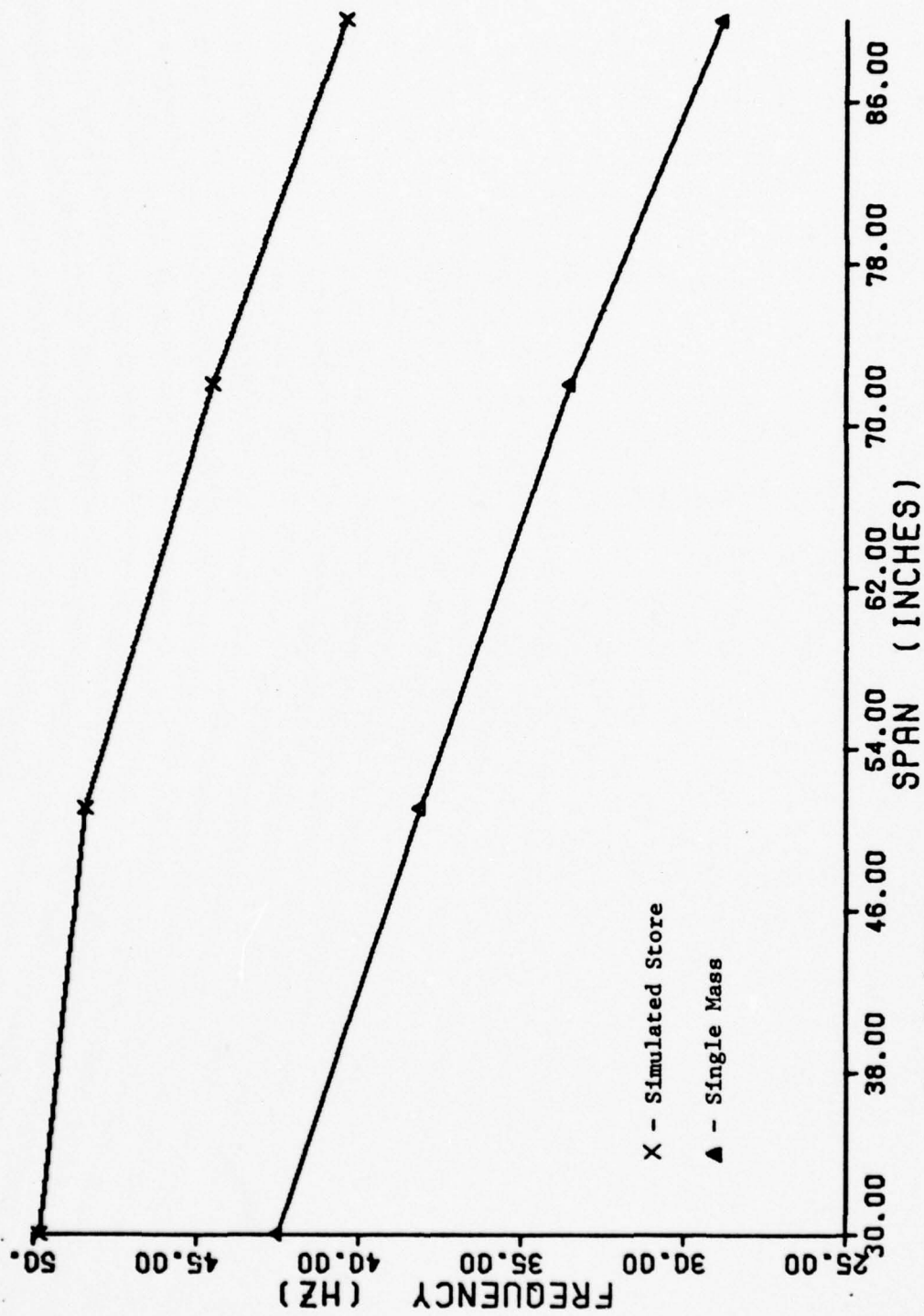


Fig. 16. Comparison of Flutter Frequencies of 200 lb Store Versus Single Concentrated Mass at 3/4 Chord Nodes

V. Conclusions and Recommendations for Further Study

Conclusions

The conclusion that can be drawn from the mass balancing analysis is that, as the center of gravity of the wing moves aft of the elastic axis, the flutter speed of the wing is reduced. Likewise, as mass is shifted spanwise toward the tip, the flutter speed and frequency are both reduced. It should not be inferred that all swept back wings will react in this manner, as the mode shape interactions differ from wing to wing due to mass distribution and stiffness variations. For example, in the experimental flutter tests of Runyan and Sewall (Ref. 11:6), the flutter modes were first and second bending, versus first torsion for the wing used in this study. Nevertheless, mass balancing produced definite flutter speed trends for this particular wing.

In the external store simulation, there was a definite increase in the flutter frequency due to store pitch inertia when compared to the flutter frequency of a concentrated mass at the store center of gravity. No definite trend was established for flutter speed, however. The upward shift in flutter frequency indicated that the torsional mode had a stronger participation in the simulation than with the single concentrated mass.

As for the method of analysis, NASTRAN is a versatile structural analysis computer program and is relatively easy to use. However, the user must have a good understanding of finite elements, and now must be versed in aerodynamic theory as well to successfully use the flutter format. To add versatility to the flutter package, the p-k method needs to be added, as it gives better subcritical frequency and damping

trends than the k method. Also, to supplement the subsonic doublet-lattice aerodynamics, supersonic capability should be added to NASTRAN by including Mach Box or Kernel Function aerodynamic theory in the program.

Recommendations for Further Study

For further stores flutter clearance studies, a wing model of an operational aircraft, such as the F-16, should be considered so that a comparison with experimental results is possible. Another possibility is the modeling of store-wing aerodynamic interaction to see what effect there is on flutter, versus a model with no interaction, as in this study. Finally, a more accurate mass model of a store could be used. For example, a store that is flexibly connected to the wing structure would be a more realistic representation of store-wing dynamic interaction.

Bibliography

1. Albano, E., and Rodden, W. P., "A Doublet-Lattice Method for Calculating Lift Distributions on Oscillating Surfaces in Subsonic Flows", AIAA Journal, 7: 279-285 (February 1969); errata, AIAA Journal, 7: 2192 (November 1969).
2. Bisplinghoff, R. L. et al. Aeroelasticity. Reading, Massachusetts; Addison-Wesley Publishing Co., 1955.
3. Fung, Y. C. An Introduction to the Theory of Aeroelasticity. New York: John Wiley and Sons, Inc., 1955.
4. Giesing, J. P. et al. Application of the Doublet-Lattice Method and the Method of Images to the Lifting-Surface/Body Interference. AFFDL-TR-71-5, Part II, Vol. I. Wright-Patterson Air Force Base, Ohio: Air Force Flight Dynamics Laboratory, April 1972.
5. Goland, M. "The Flutter of a Uniform Cantilever Wing", Journal of Applied Mechanics, 12: A197-A207 (December 1945).
6. Harder, R. L. et al. A Design Study for the Incorporation of Aeroelastic Capability into NASTRAN. NASA-CR-111918. Washington: National Aeronautics and Space Administration, 1971.
7. MacNeal, R. H., editor. The NASTRAN Theoretical Manual, NASA-SP-221 (Level 16.0). Washington: National Aeronautics and Space Administration, March 1976.
8. NASA-SP-222 (Level 16.0), The NASTRAN Users Manual. Washington: National Aeronautics and Space Administration, March 1976.
9. Peery, D. J. Aircraft Structures. New York: McGraw-Hill Book Co., Inc., 1950.
10. Przemieniecki, J. S. Theory of Matrix Structural Analysis. New York: MacGraw-Hill Book Co., 1968.
11. Runyan, H. L. and Sewall, J. L. Experimental Investigation of the Effects of Concentrated Weights on Flutter Characteristics of a Straight Cantilever Wing. NACA-TN-1594. Washington: National Advisory Committee for Aeronautics, June 1948.
12. Theodorsen, T. General Theory of Aerodynamic Instability and the Mechanism of Flutter. NACA Technical Report 496. Washington: National Advisory Committee for Aeronautics, 1935.
13. Theodorsen, T., and Garrick, I. E. Mechanism of Flutter, A Theoretical and Experimental Investigation of the Flutter Problem. NACA Technical Report 685. Washington: National Advisory Committee for Aeronautics, 1940.

Bibliography

14. Watkins, C. E. et al. On the Kernel Function of the Integral Equation Relating the Lift and Downwash Distributions of Oscillating Finite Wings in Subsonic Flow. NACA Technical Report 1234. Washington: National Advisory Committee for Aeronautics, 1957.
15. Wilkinson, K. et al. An Automated Procedure for Flutter and Strength Analysis and Optimization of Aerospace Vehicles. AFFDL-TR-75-137. Wright-Patterson Air Force Base, Ohio: Air Force Flight Dynamics Laboratory, December 1975.

Appendix A

Table III Mass and Mass Moments of Inertia at Nodes		
Nodes	Mass at Each Node (slugs)	Mass Moment of Inertia (slug-ft ²)
11, 12	0.6525	0.0324
13, 14	0.1798	
15, 16	0.2919	
17, 18	0.2869	
19, 20	0.4438	0.0259
21, 22	0.4177	0.0125
23, 24	0.1873	
25, 26	0.2633	
27, 28	0.2345	
29, 30	0.3444	0.01725
31, 32	0.4000	0.0097
33, 34	0.1627	
35, 36	0.2093	
37, 38	0.1696	
39, 40	0.3028	0.0140
41, 42	0.2484	0.0054
43, 44	0.0928	
45, 46	0.1106	
47, 48	0.0792	
49, 50	0.2174	0.0151
51, 52	0.1437	0.0058
*53, 54	0.0838	(1) 0.0058; (2) 0.0049
55, 56	0.0937	
*57, 58	0.0758	(1) 0.0051; (2) 0.0051
59, 60	0.1242	0.0086

*Note: All moments are about a local axis parallel to edge of structure except at wing tip where second value of inertia is about the normal axis depicted in Fig. 6.

22

Appendix B

Flutter Speed and Flutter Frequency Graphs

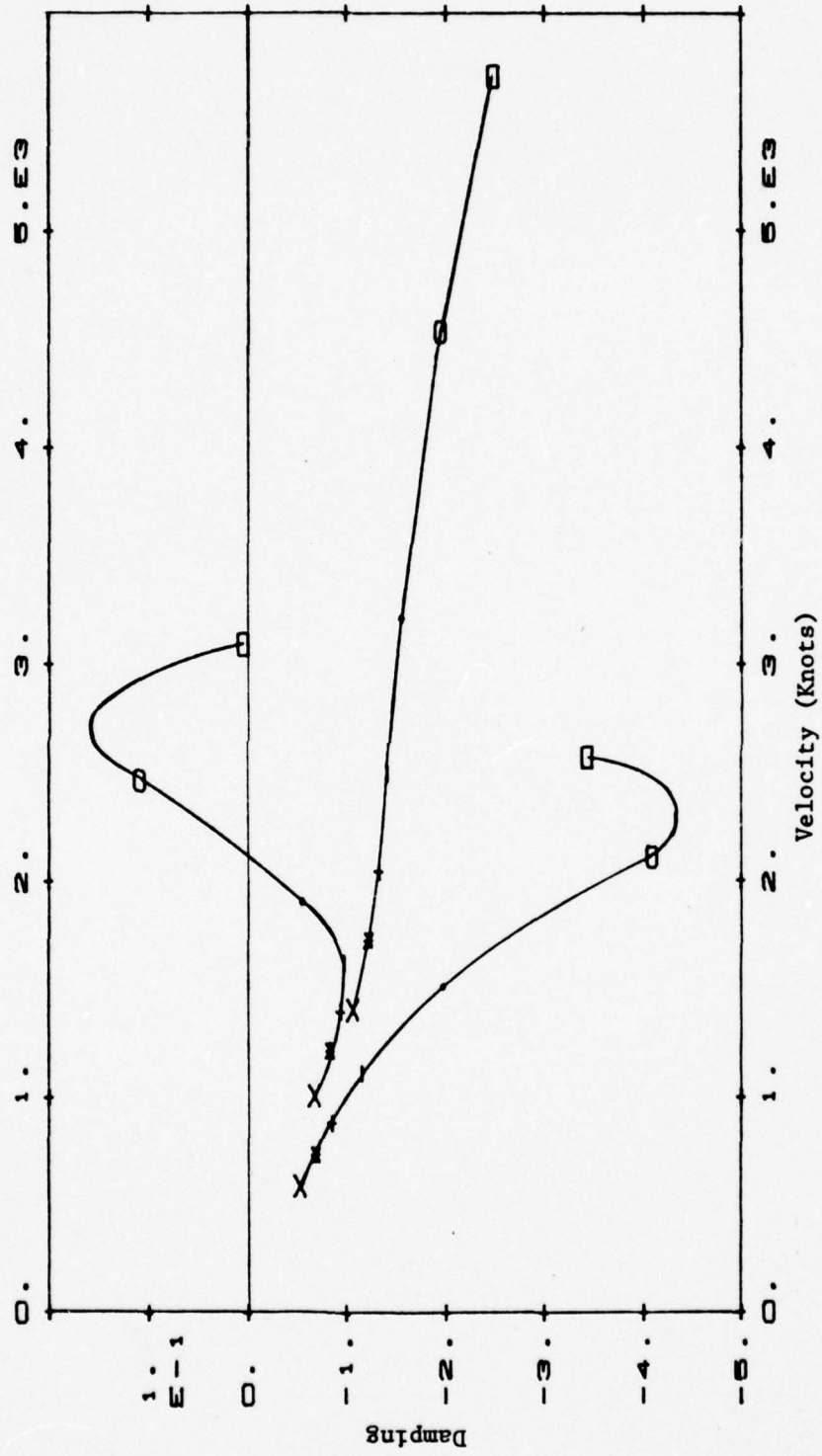


Fig. 17-A. Flutter Speed Solution with 100 lb at Node 40

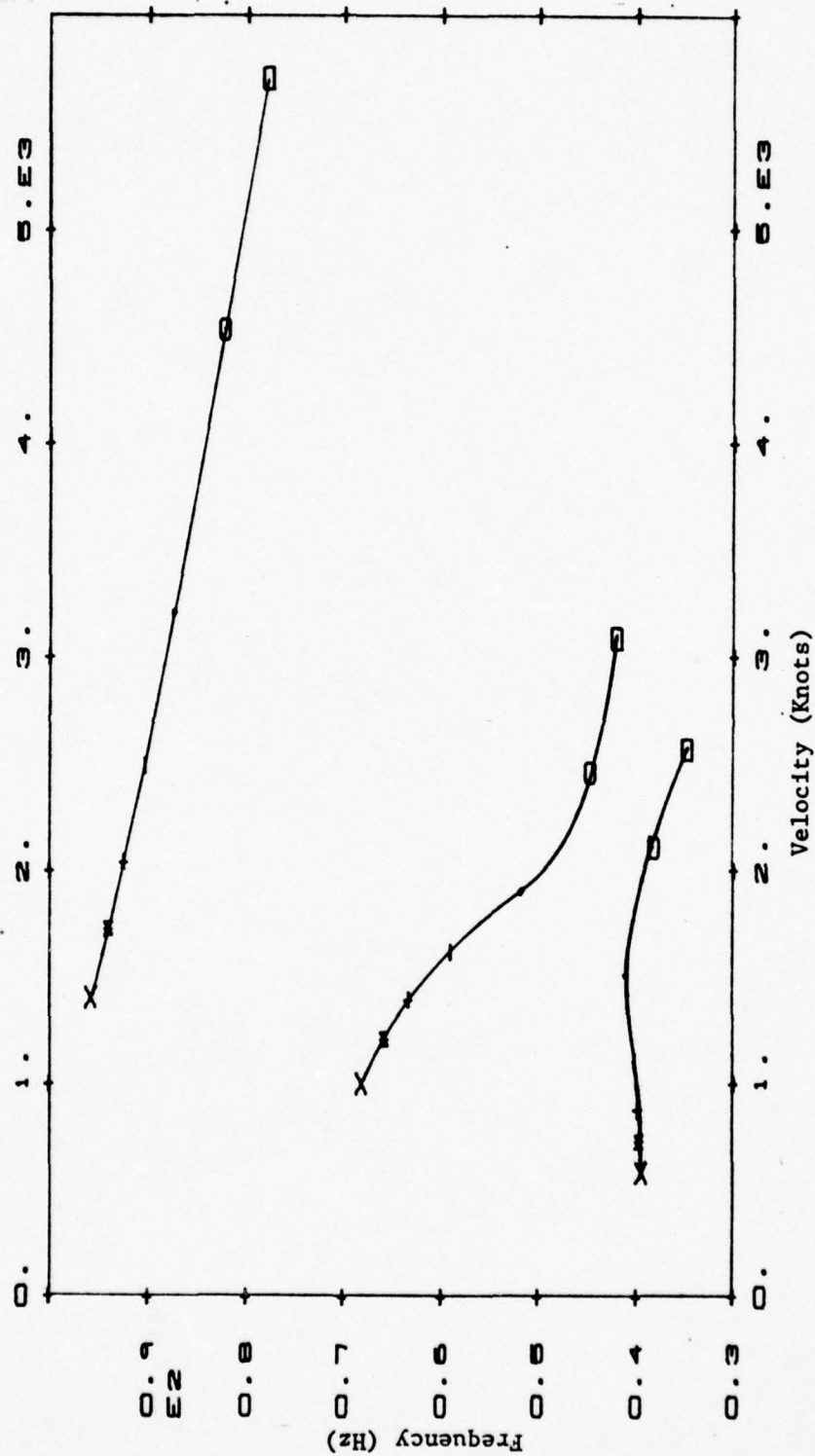


Fig. 17-B. Flutter Frequency Solution with 100 lb at Node 40

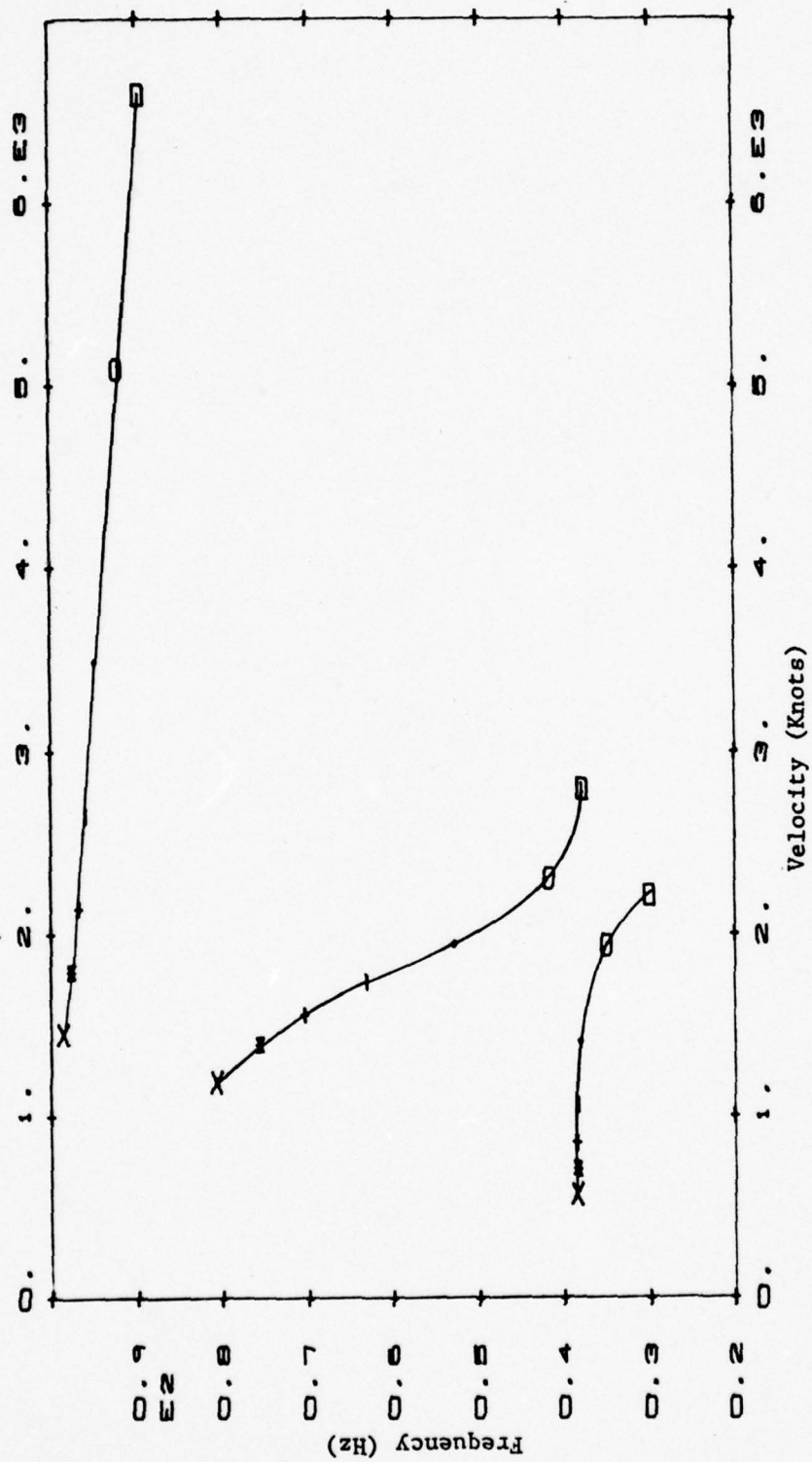


Fig. 18-B. Flutter Frequency Solution with 100 lb at Node 46

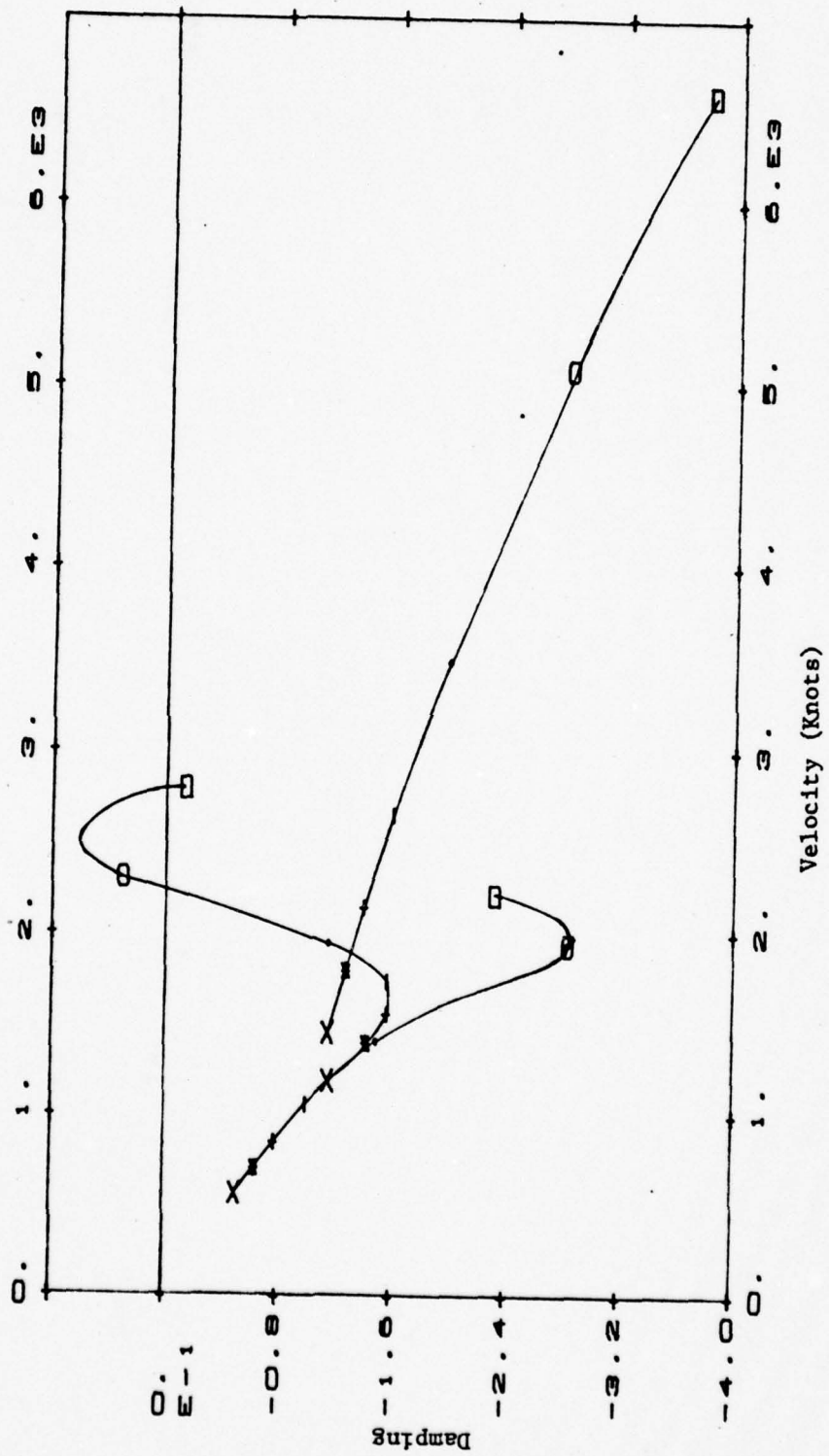


Fig. 18-A. Flutter Speed Solution with 100 lb at Node 46

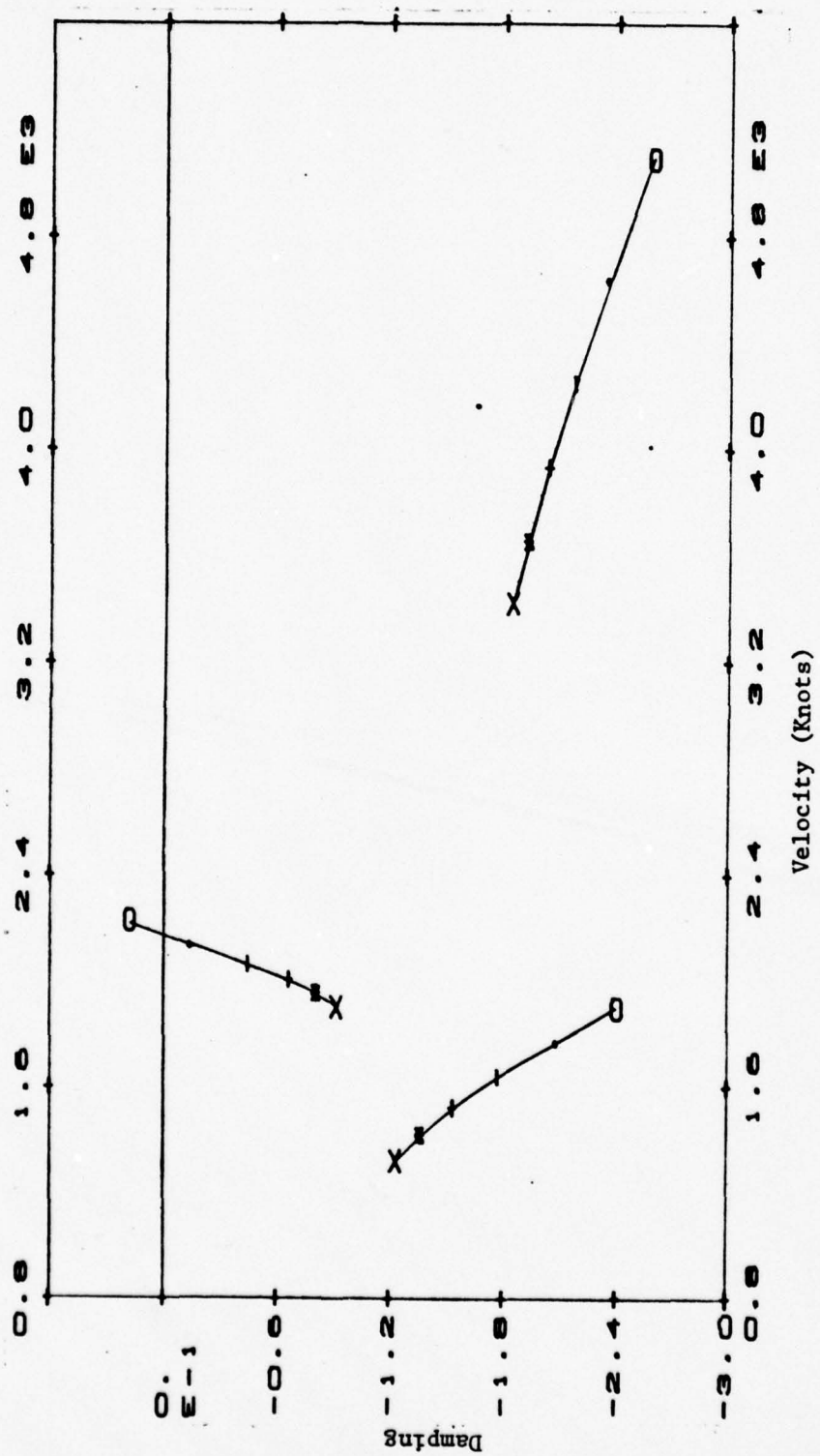


Fig. 19-A. Flutter Speed Solution with 100 lb at Node 48

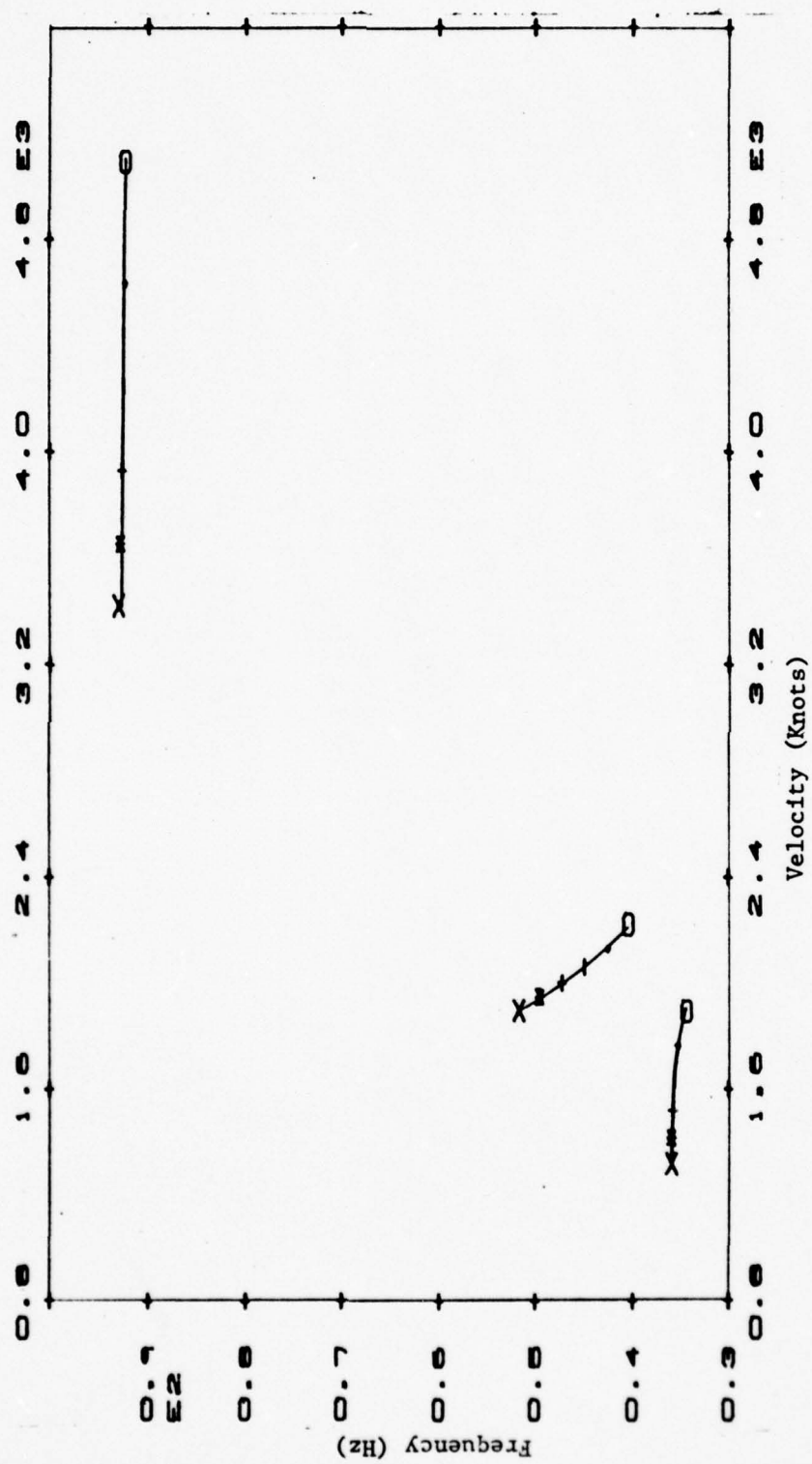


Fig. 19-B. Flutter Frequency Solution with 100 lb at Node 48

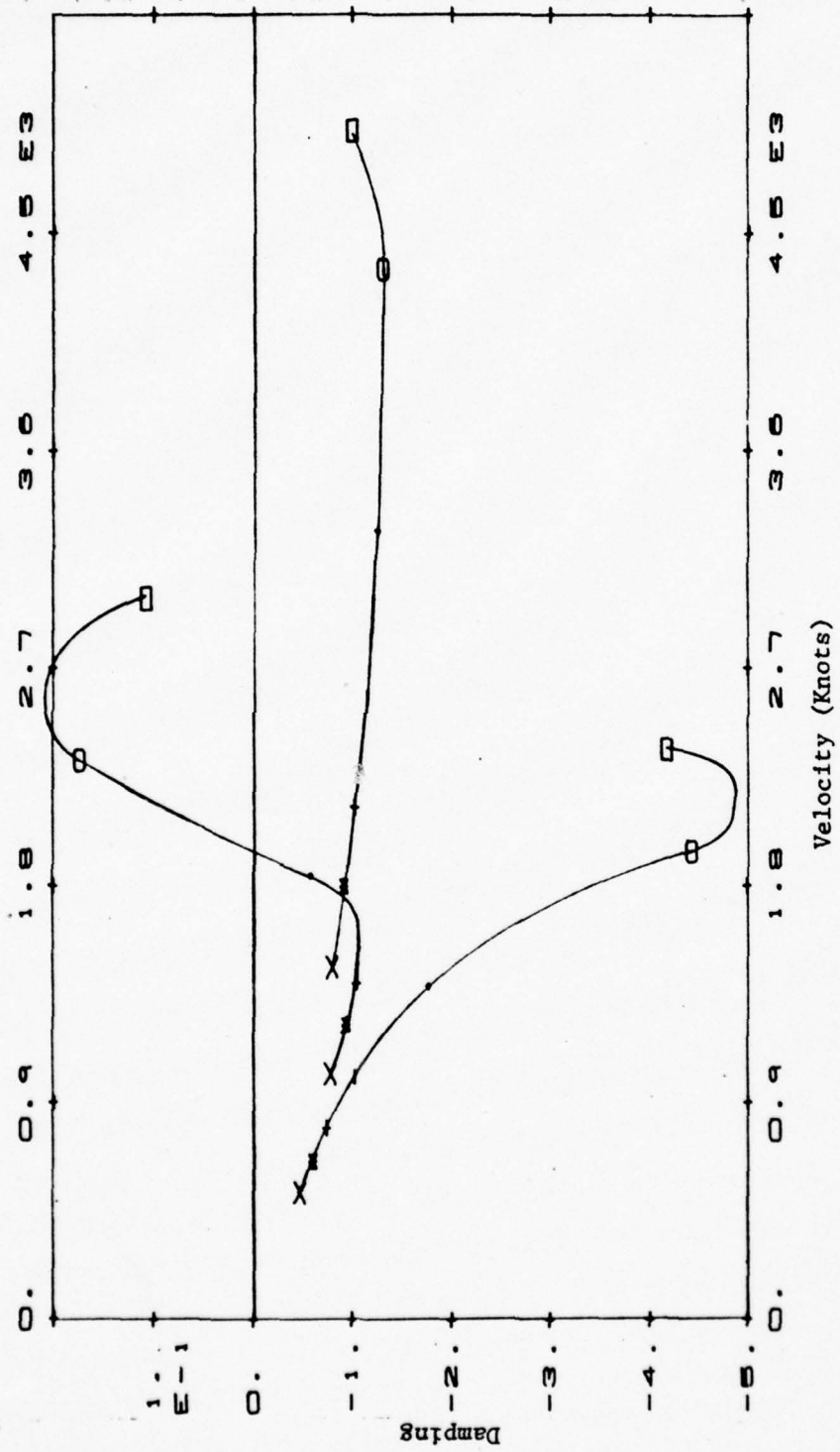


Fig. 20-A. Flutter Speed Solution with 100 lb at Node 50

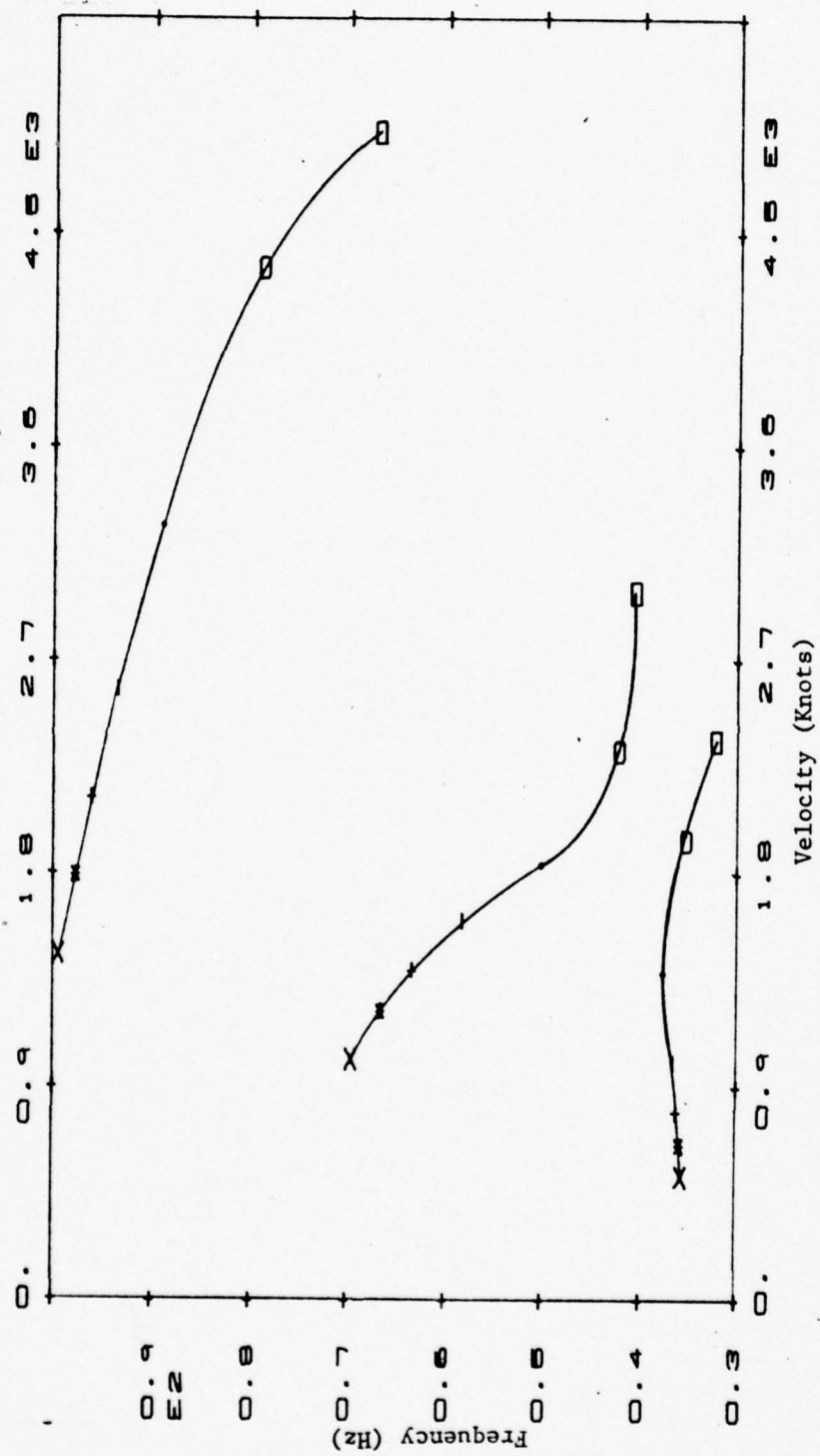


Fig. 20-B. Flutter Frequency Solution with 100 lb at Node 50

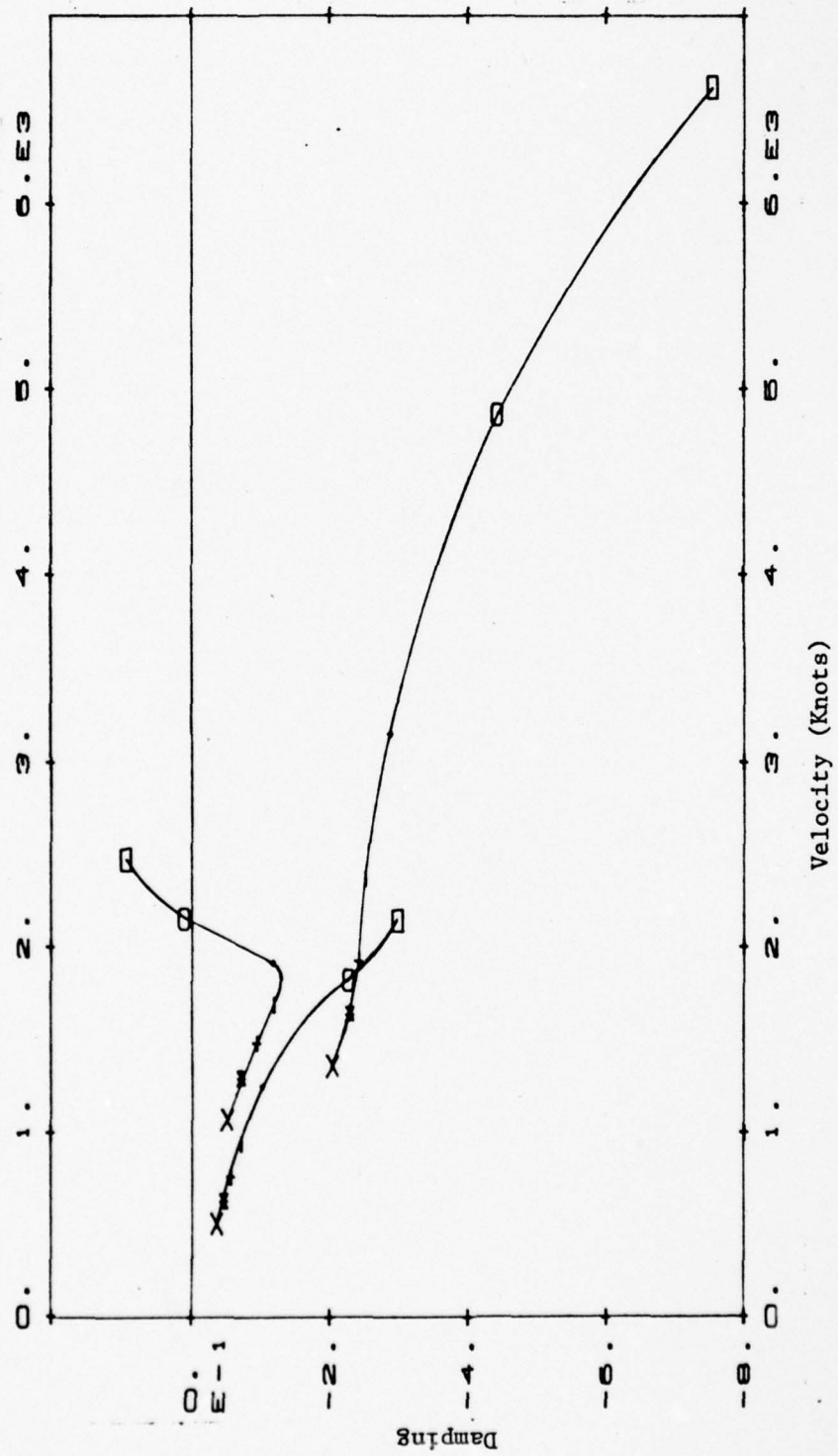


Fig. 21-A. Flutter Speed Solution with 100 lb at Node 56

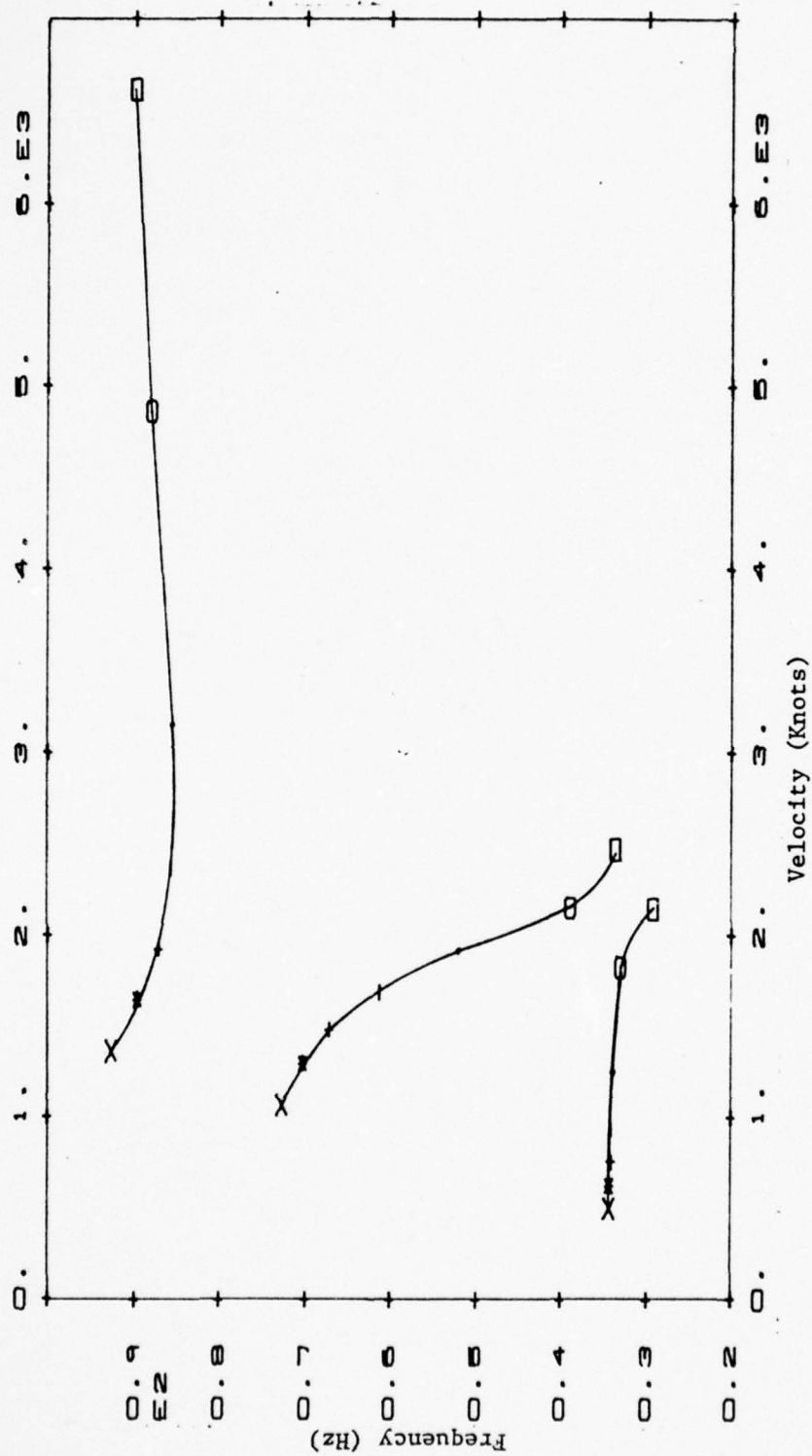


Fig. 21-B. Flutter Frequency Solution with 100 lb at Node 56

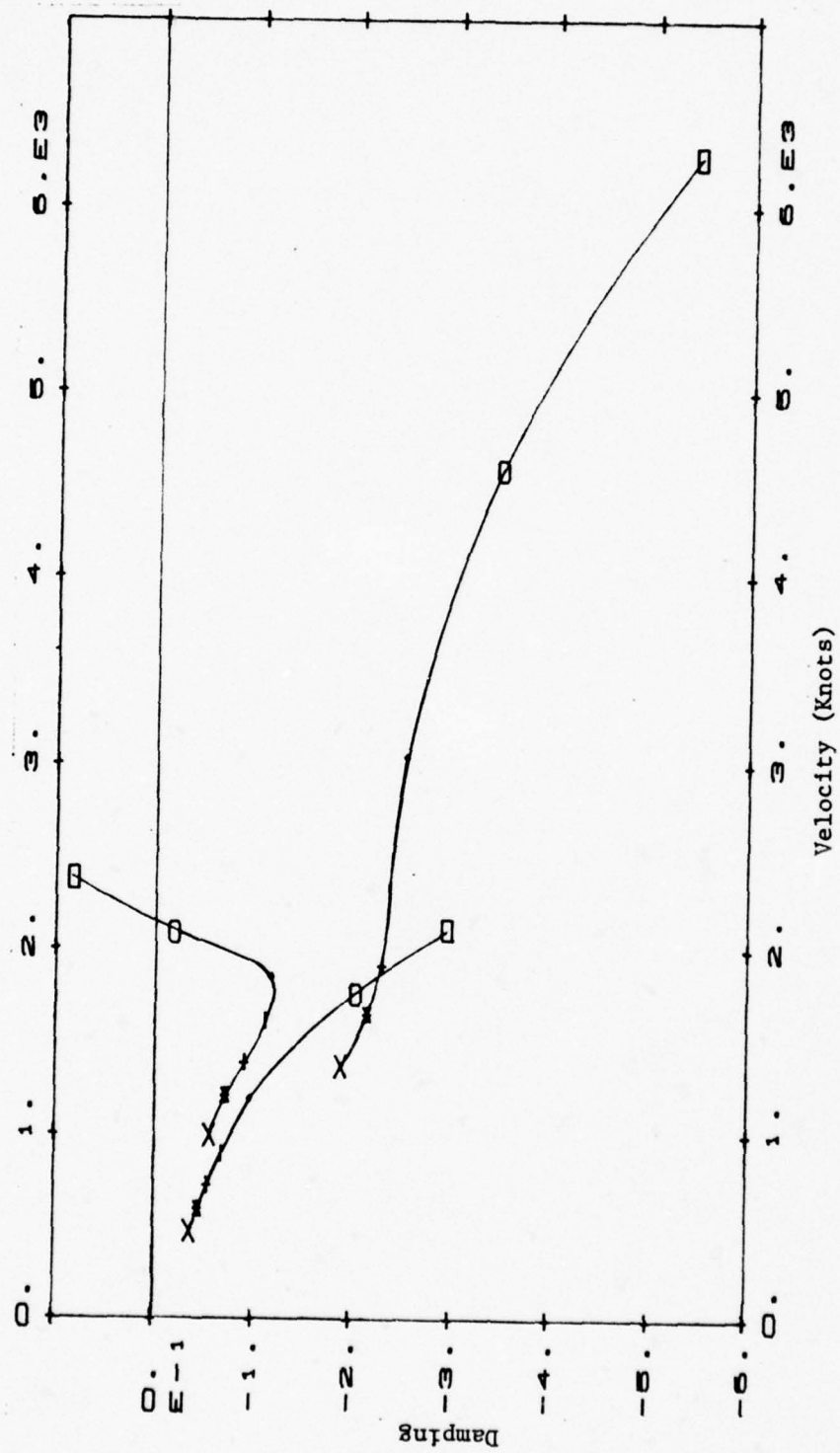


Fig. 22-A. Flutter Speed Solution with 100 lb at Node 58

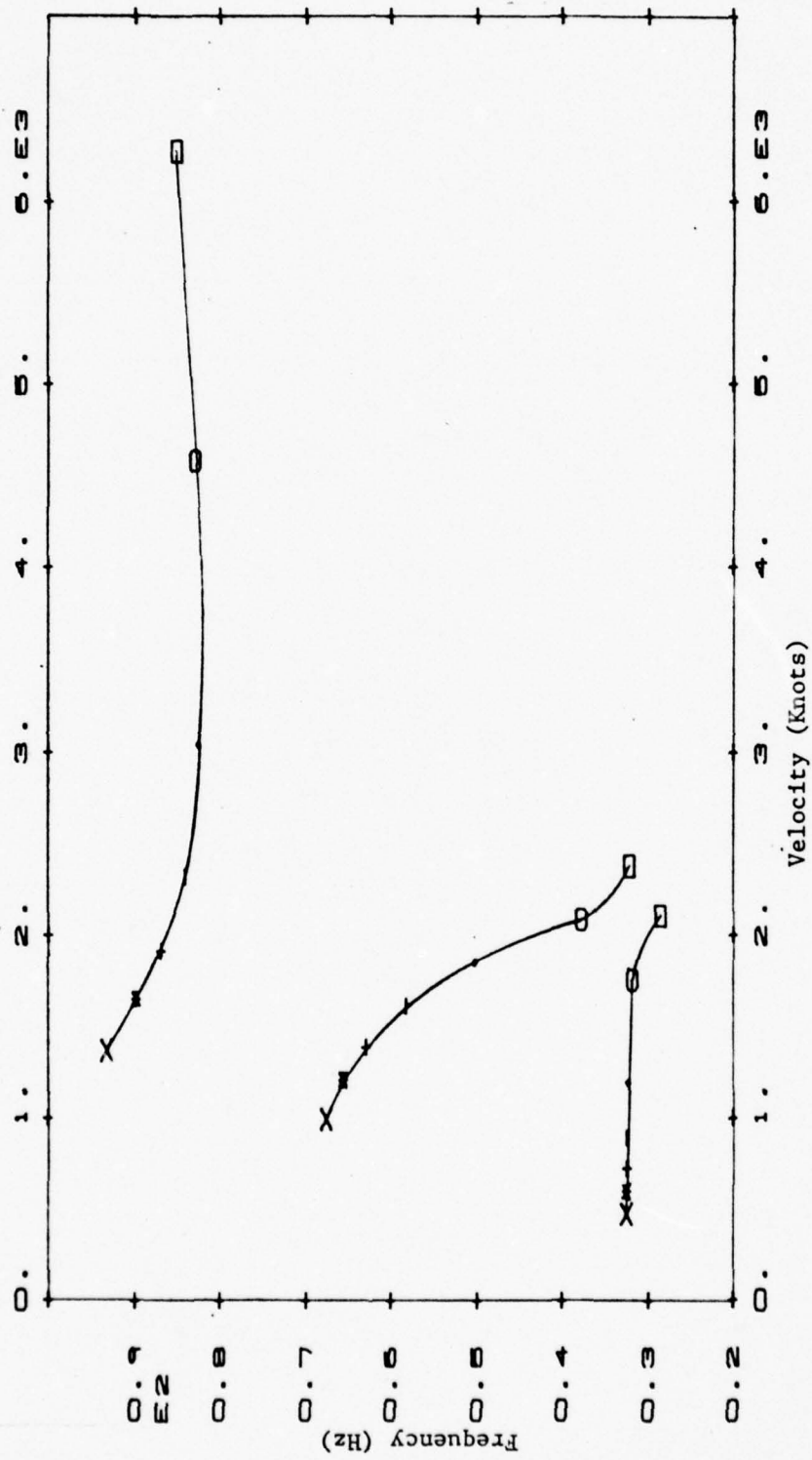


Fig. 22-B. Flutter Frequency Solution with 100 lb at Node 58

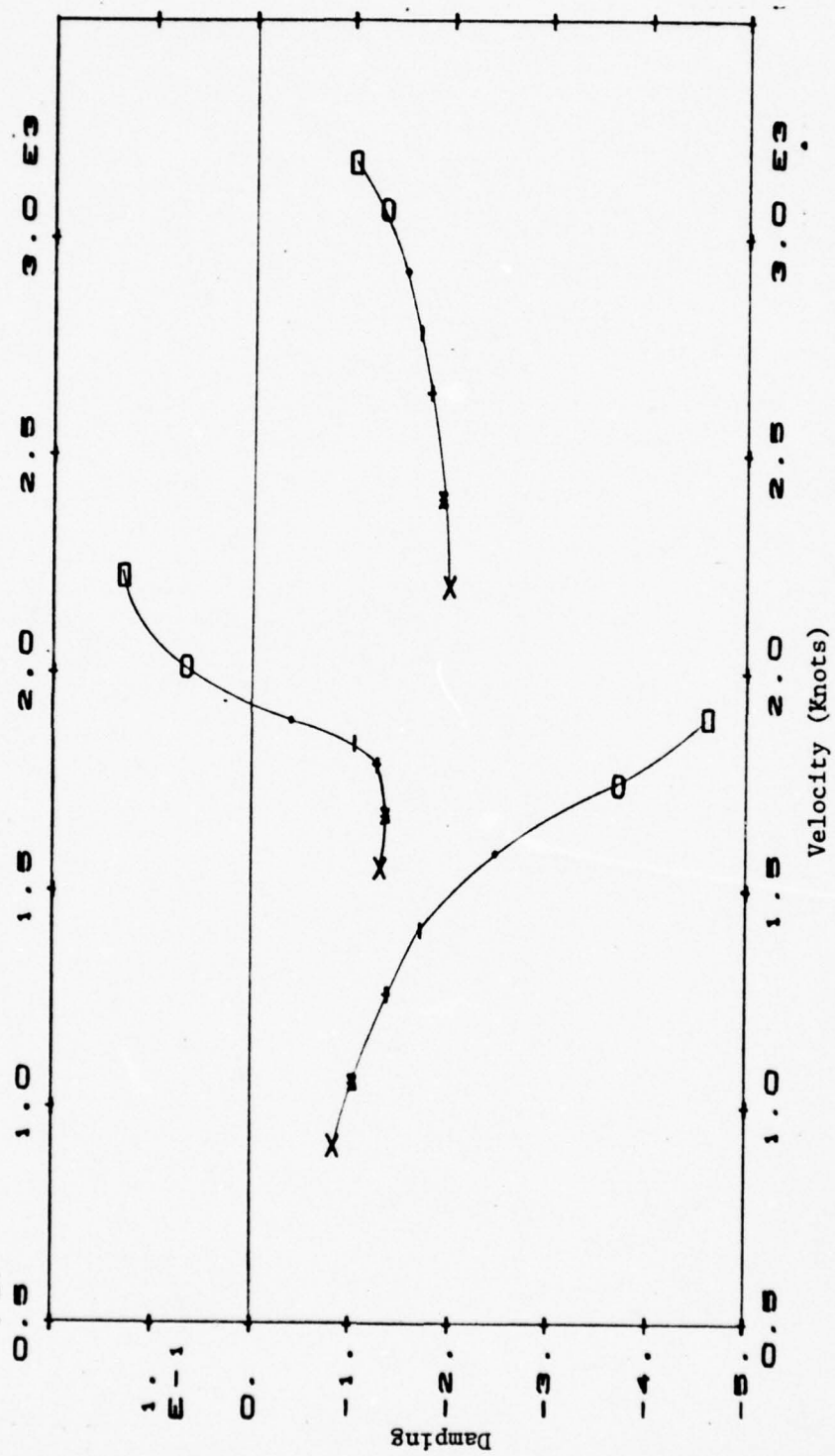


Fig. 23-A. Flutter Speed Solution with 100 lb at Node 60

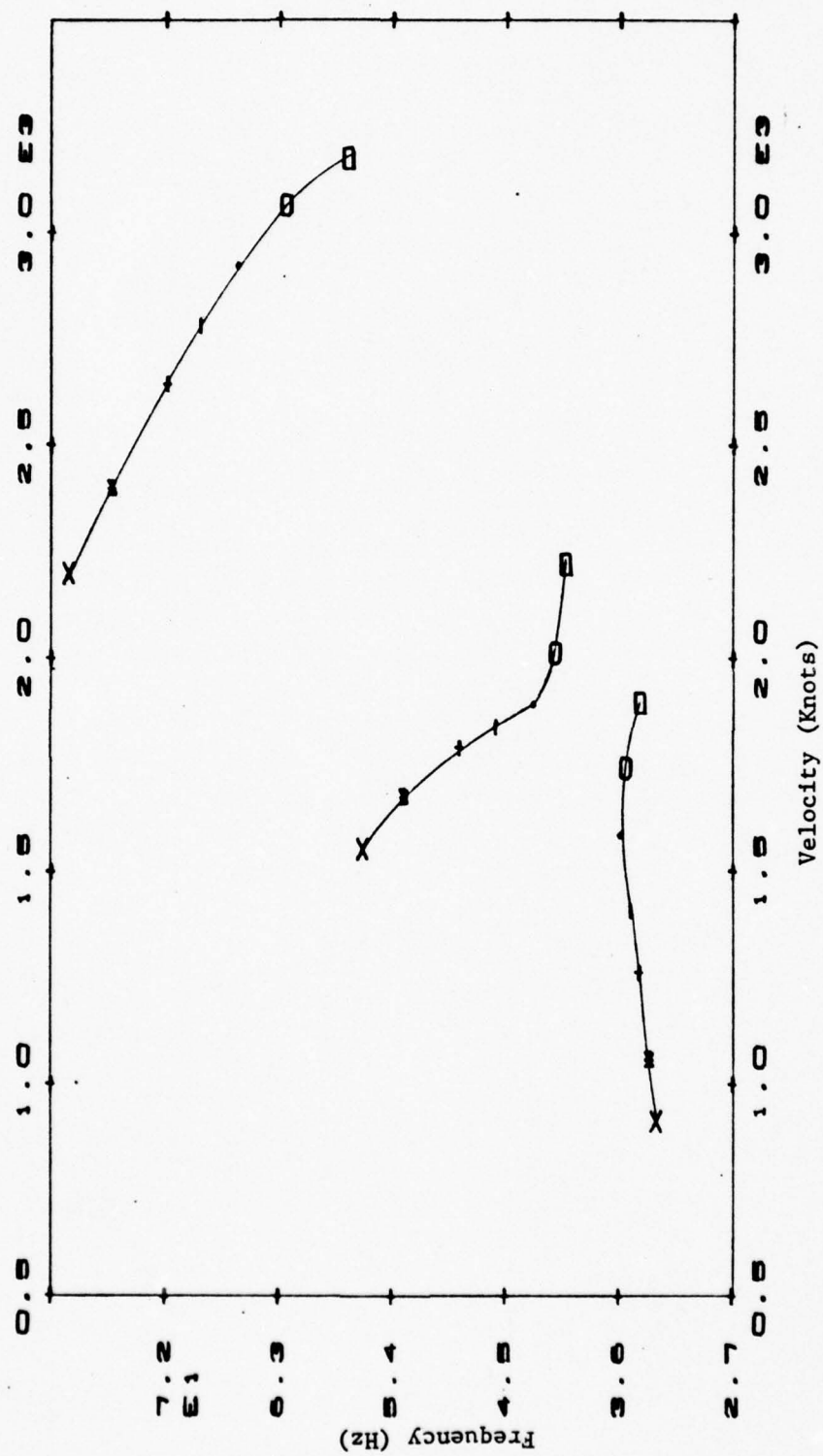


Fig. 23-B. Flutter Frequency Solution with 100 lb at Node 60

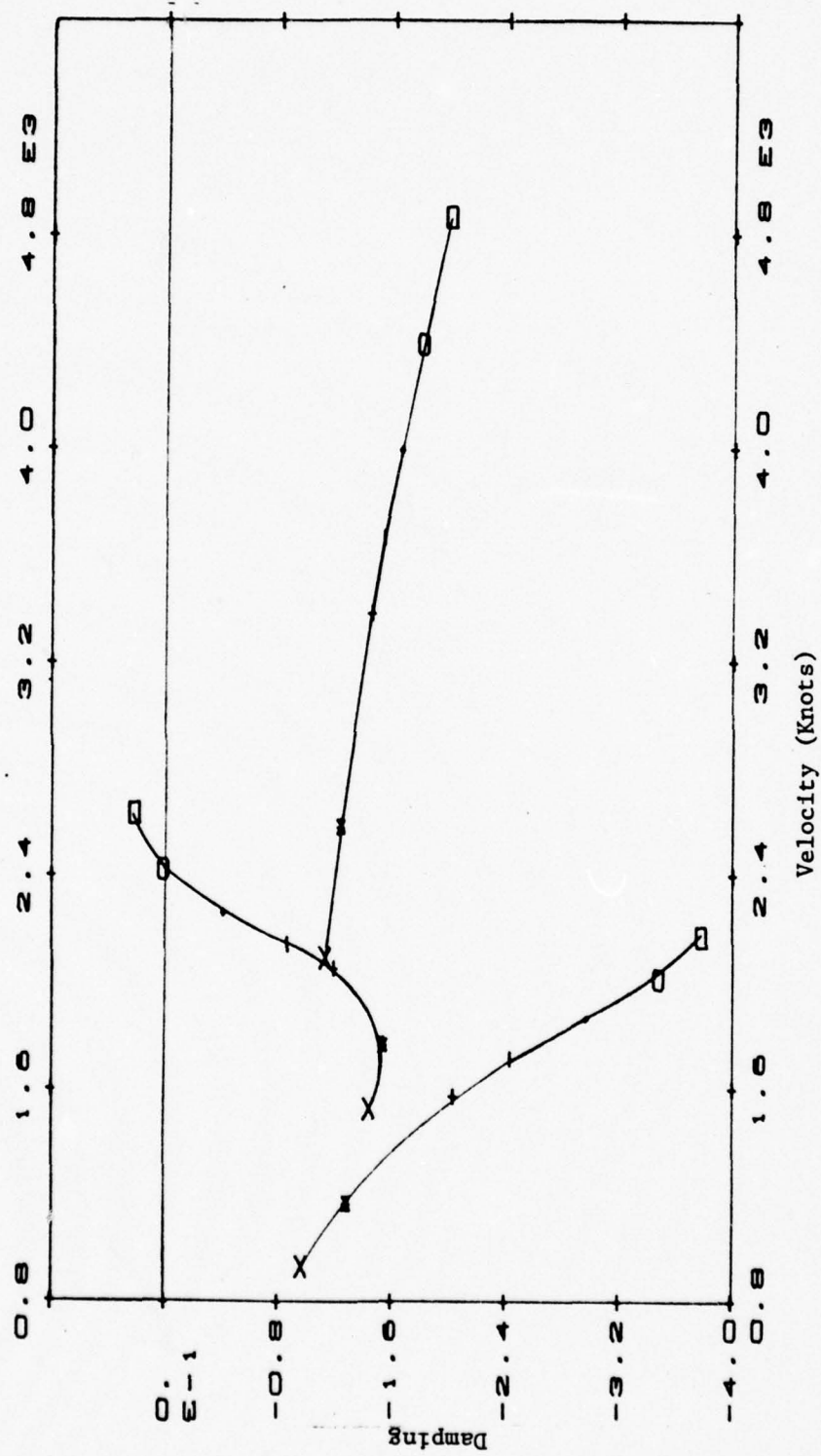


Fig. 24-A. Flutter Speed Solution with 50 lb at Node 36 and 50 lb at Node 40

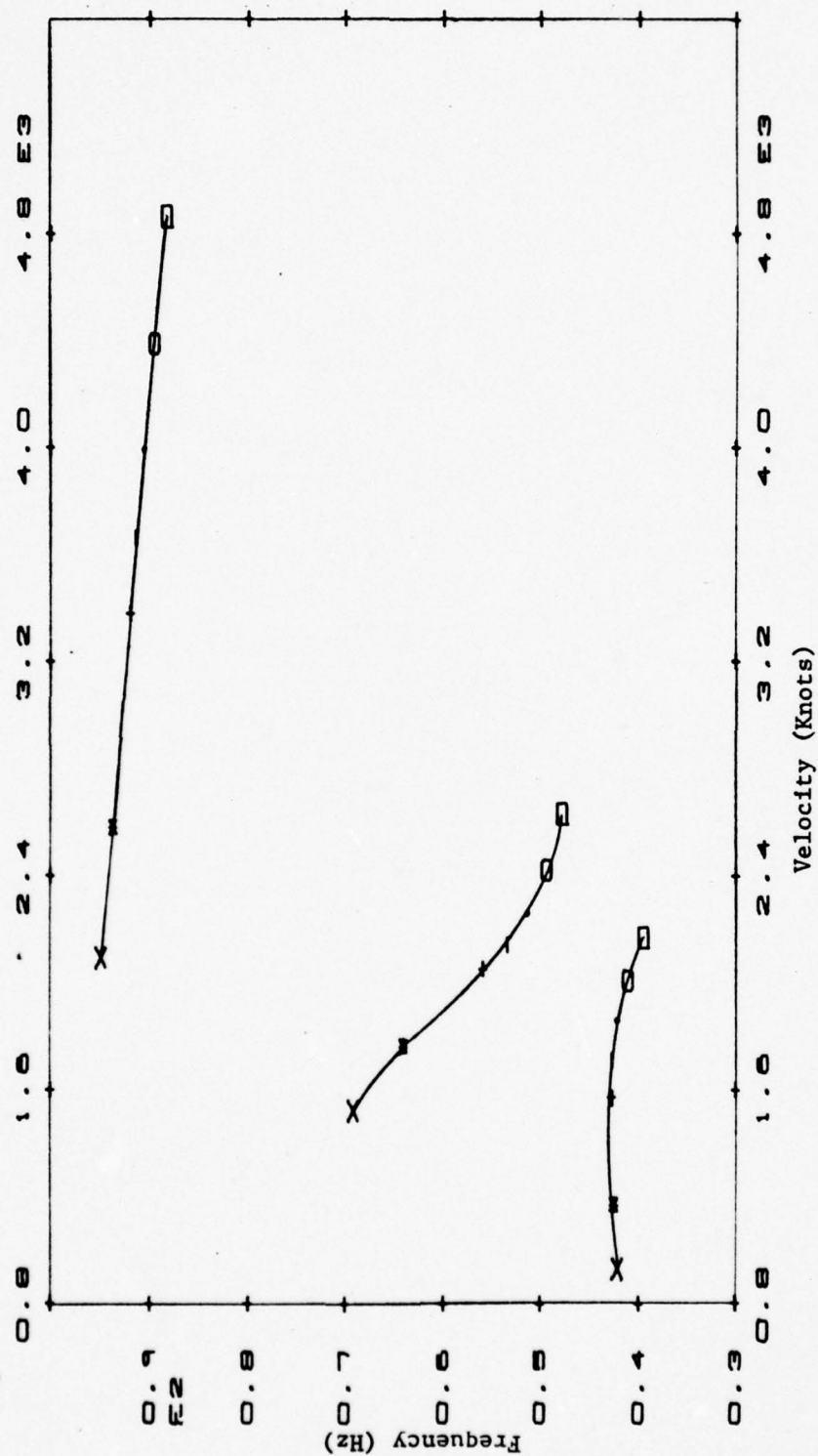


Fig. 24-B. Flutter Frequency Solution with 50 lb at Node 36 and 50 lb at Node 40

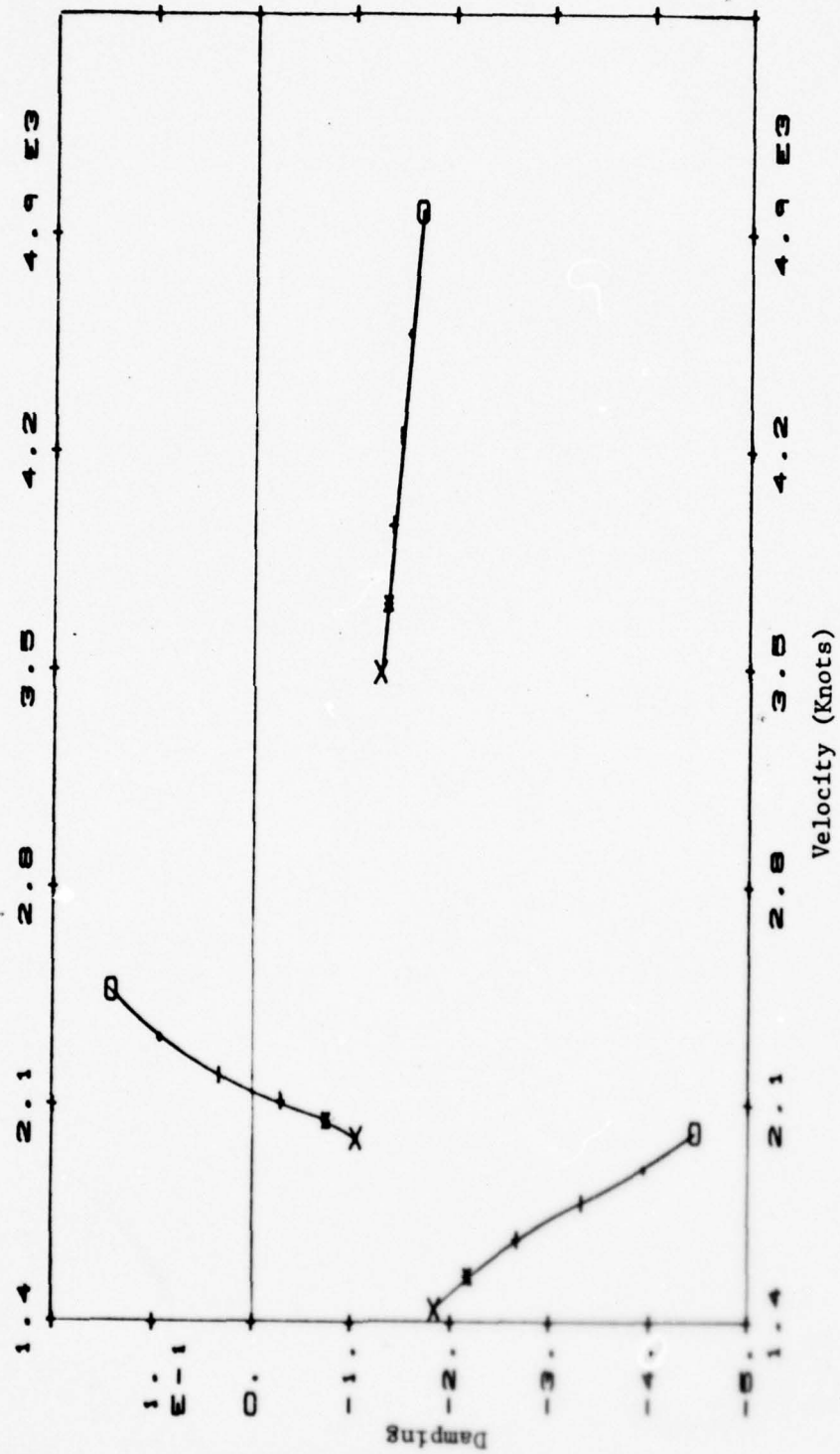


Fig. 25-A. Flutter Speed Solution with 50 lb at Node 46 and 50 lb at Node 50

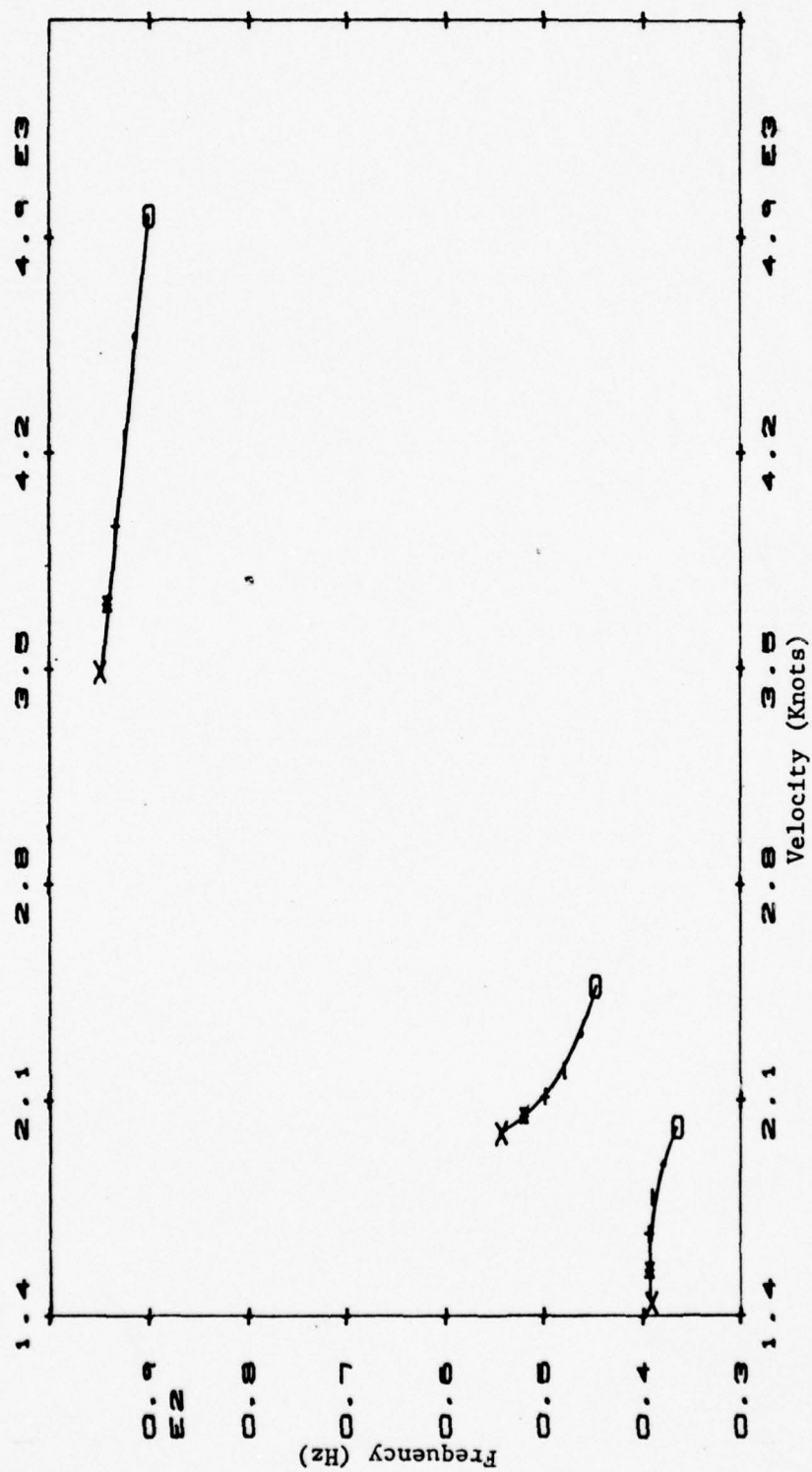


Fig. 25-B. Flutter Frequency Solution with 50 lb at Node 46
and 50 lb at Node 50

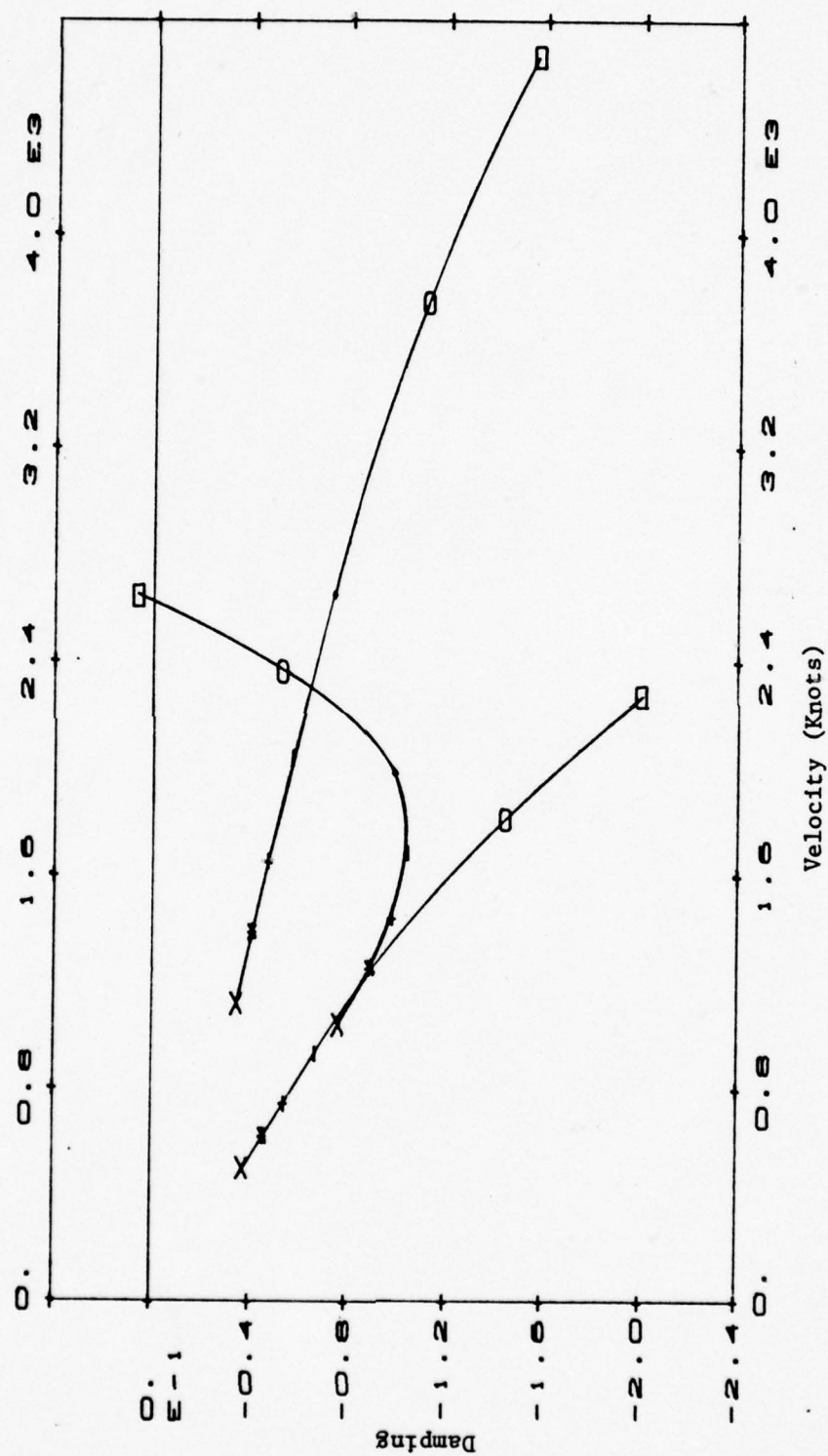


Fig. 26-A. Flutter Speed Solution with 50 lb at Node 54 and 50 lb at Node 58

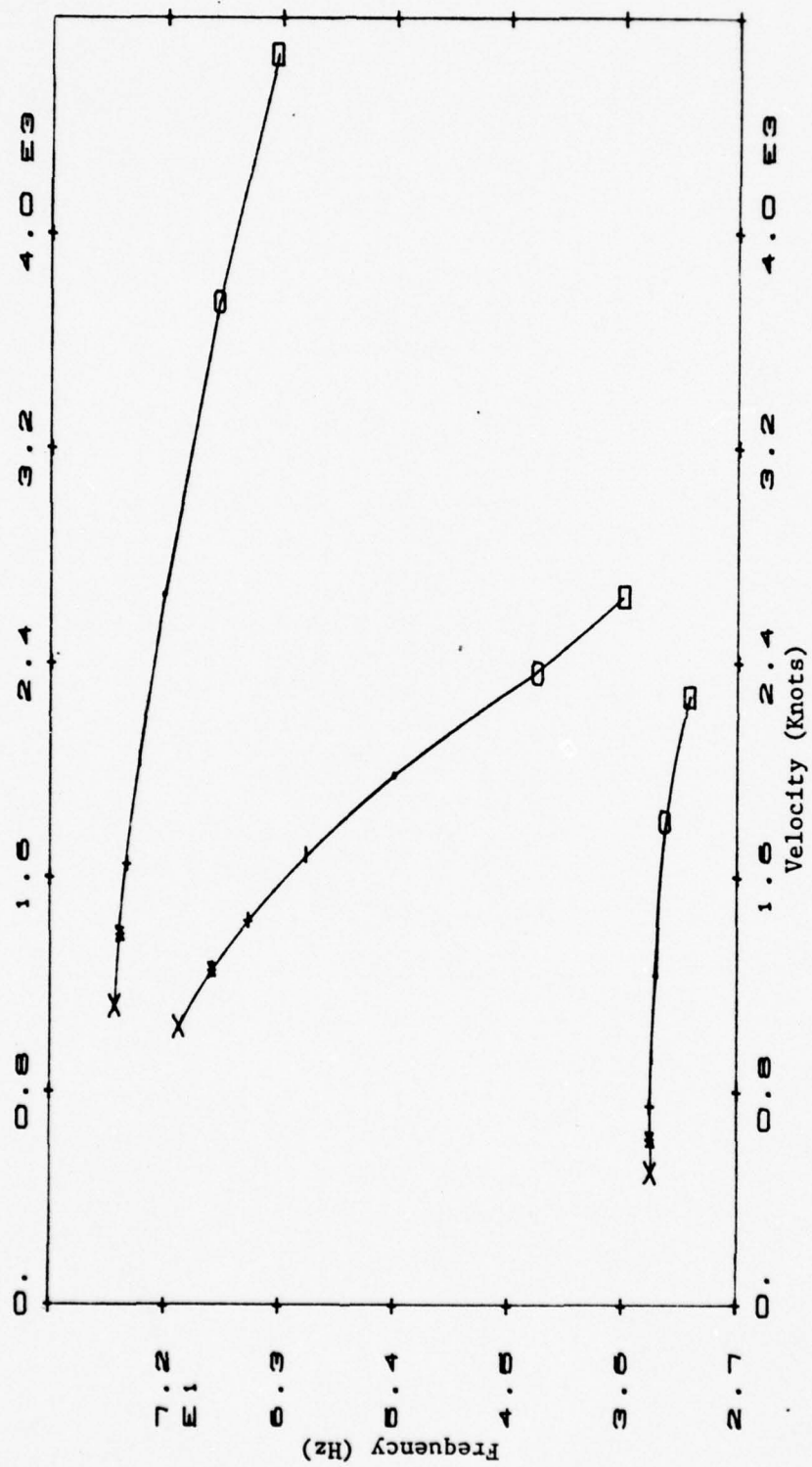


Fig. 26-B. Flutter Frequency Solution with 50 lb at Node 54 and 50 lb at Node 58

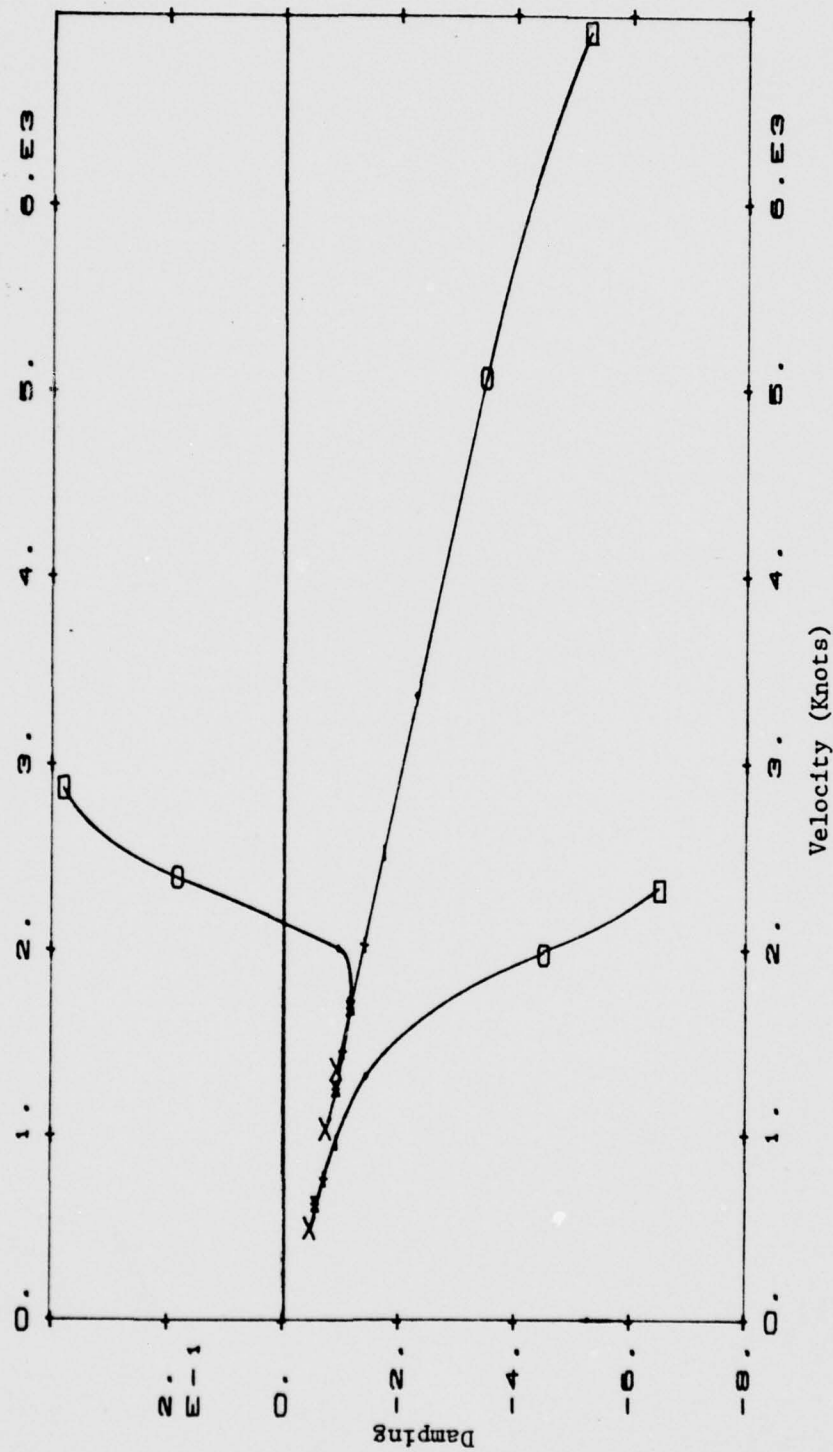


Fig. 27-A. Flutter Speed Solution with 50 lb at Node 56 and 50 lb at Node 60

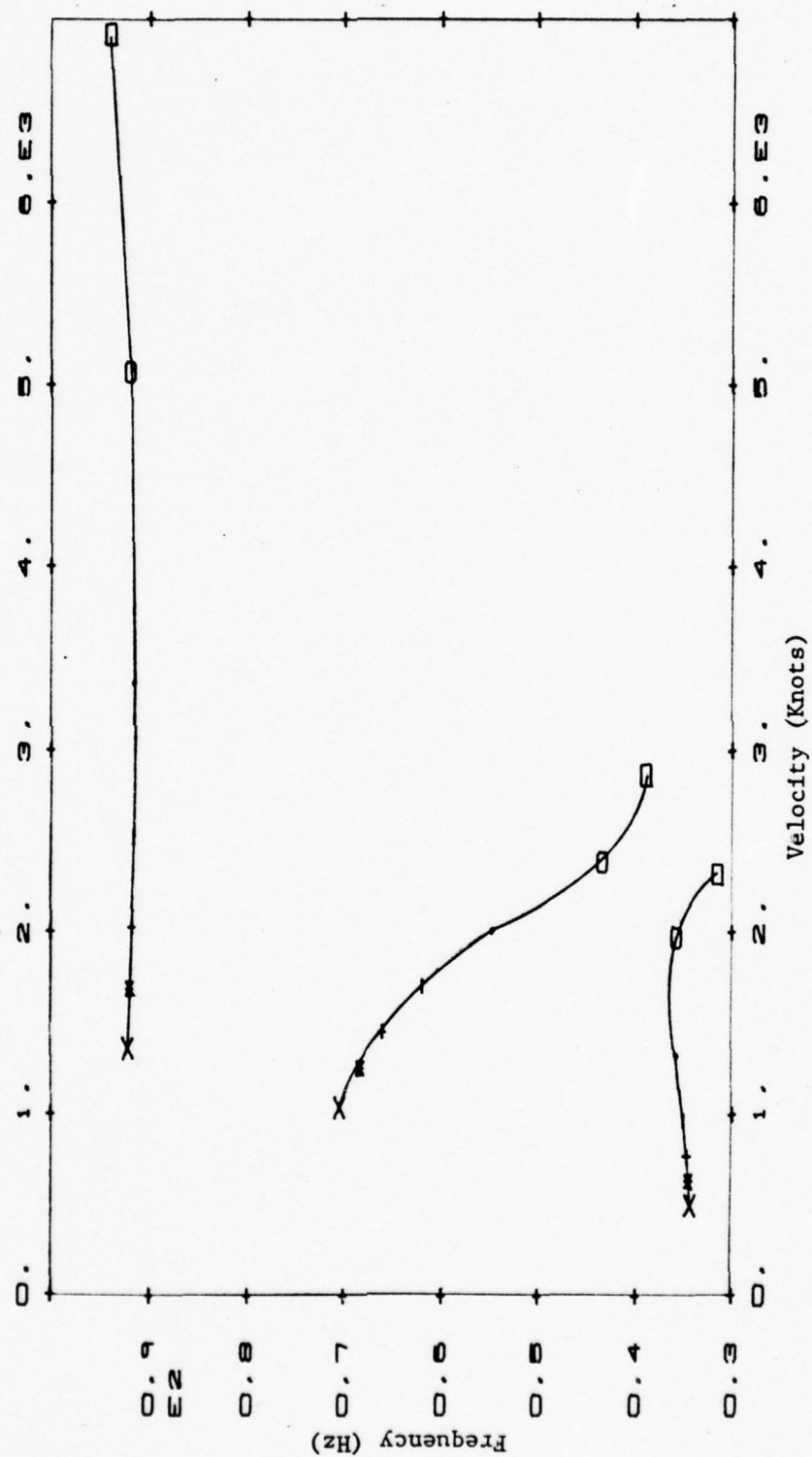


Fig. 27-B. Flutter Frequency Solution with 50 lb at Node 56 and 50 lb at Node 60

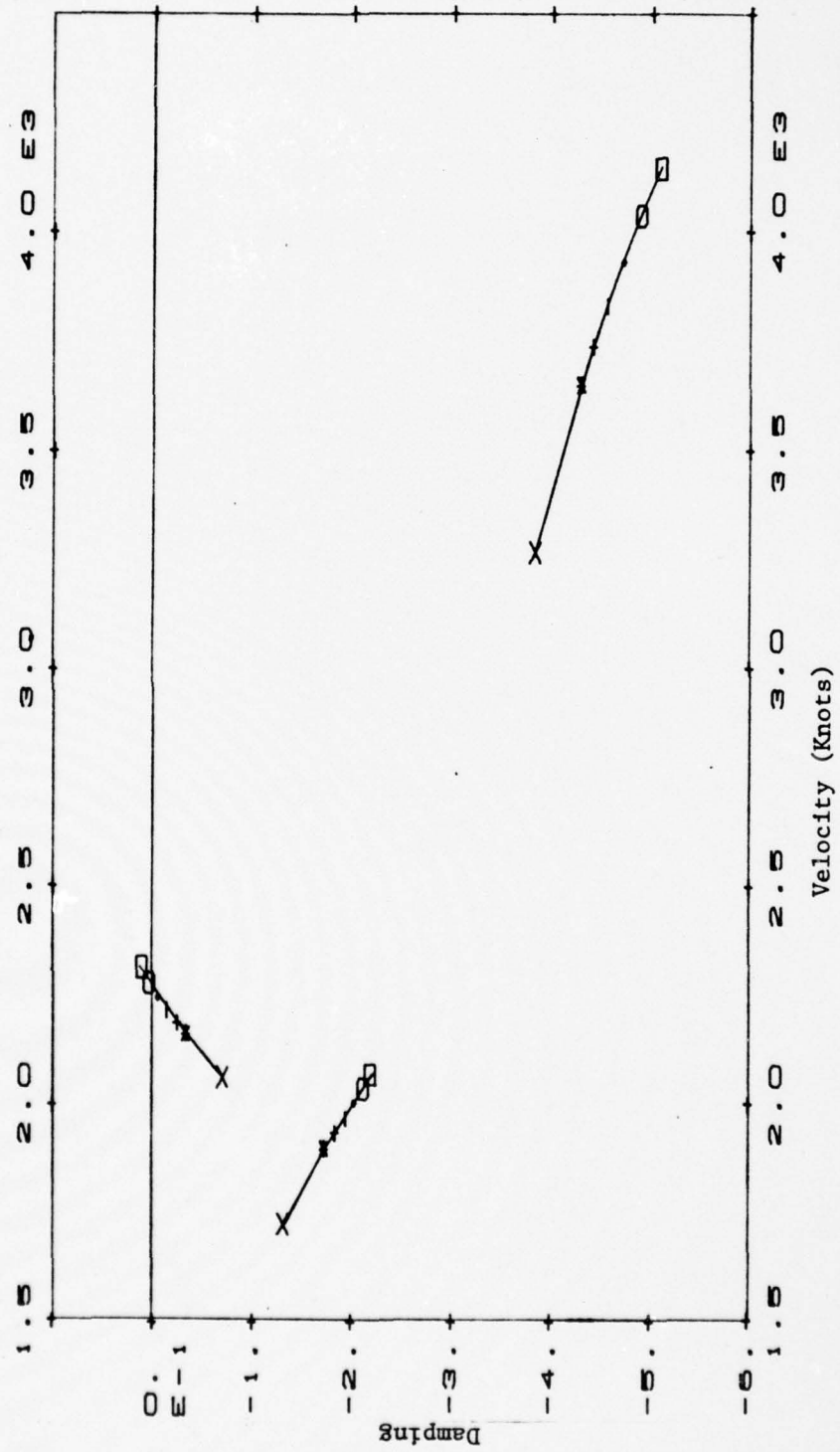


Fig. 28-A. Flutter Speed Solution with 200 lb at Node 28

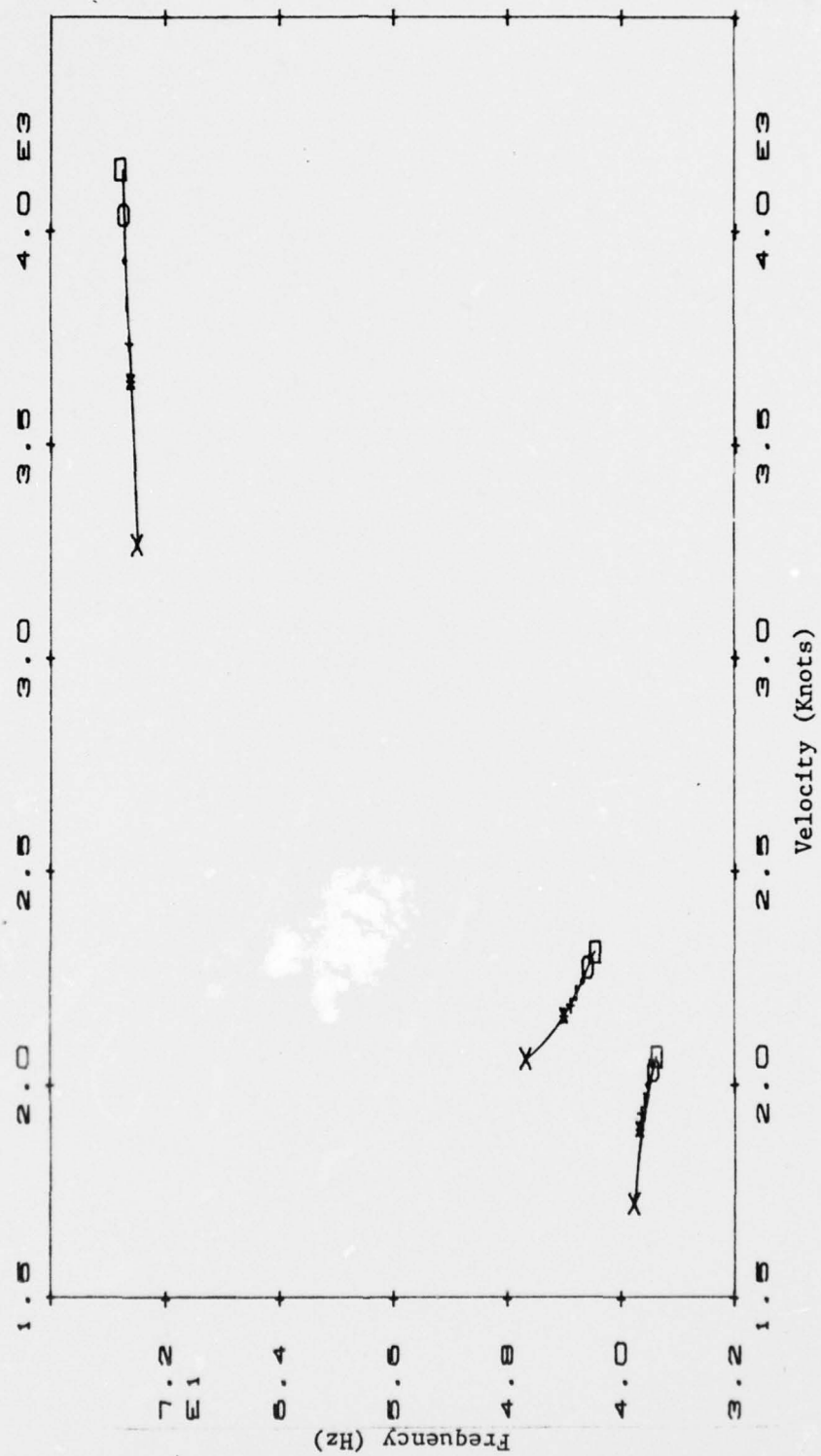


Fig. 28-B. Flutter Frequency Solution with 200 lb at Node 28

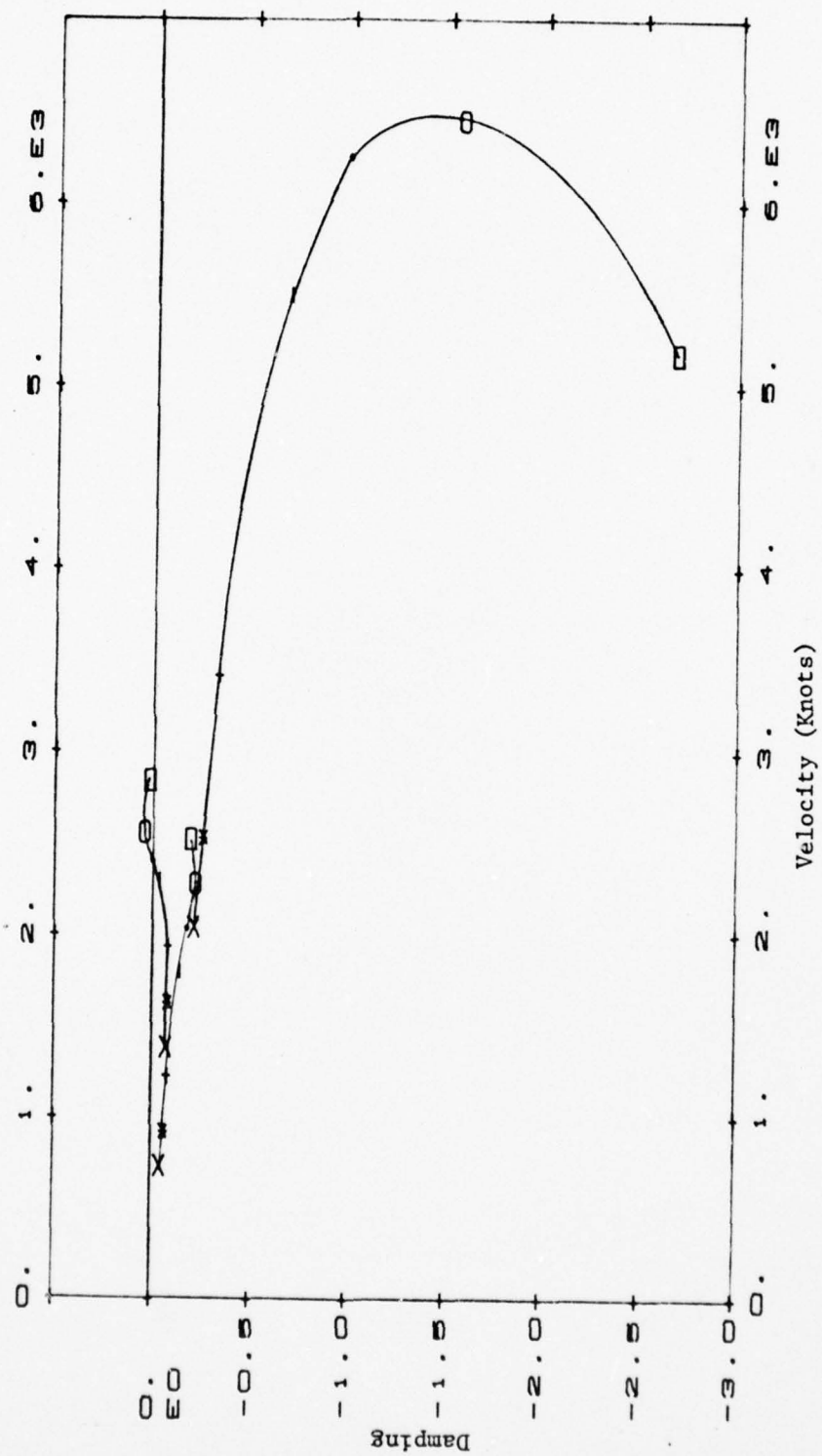


Fig. 29-A. Flutter Speed Solution with 200 lb at Node 38

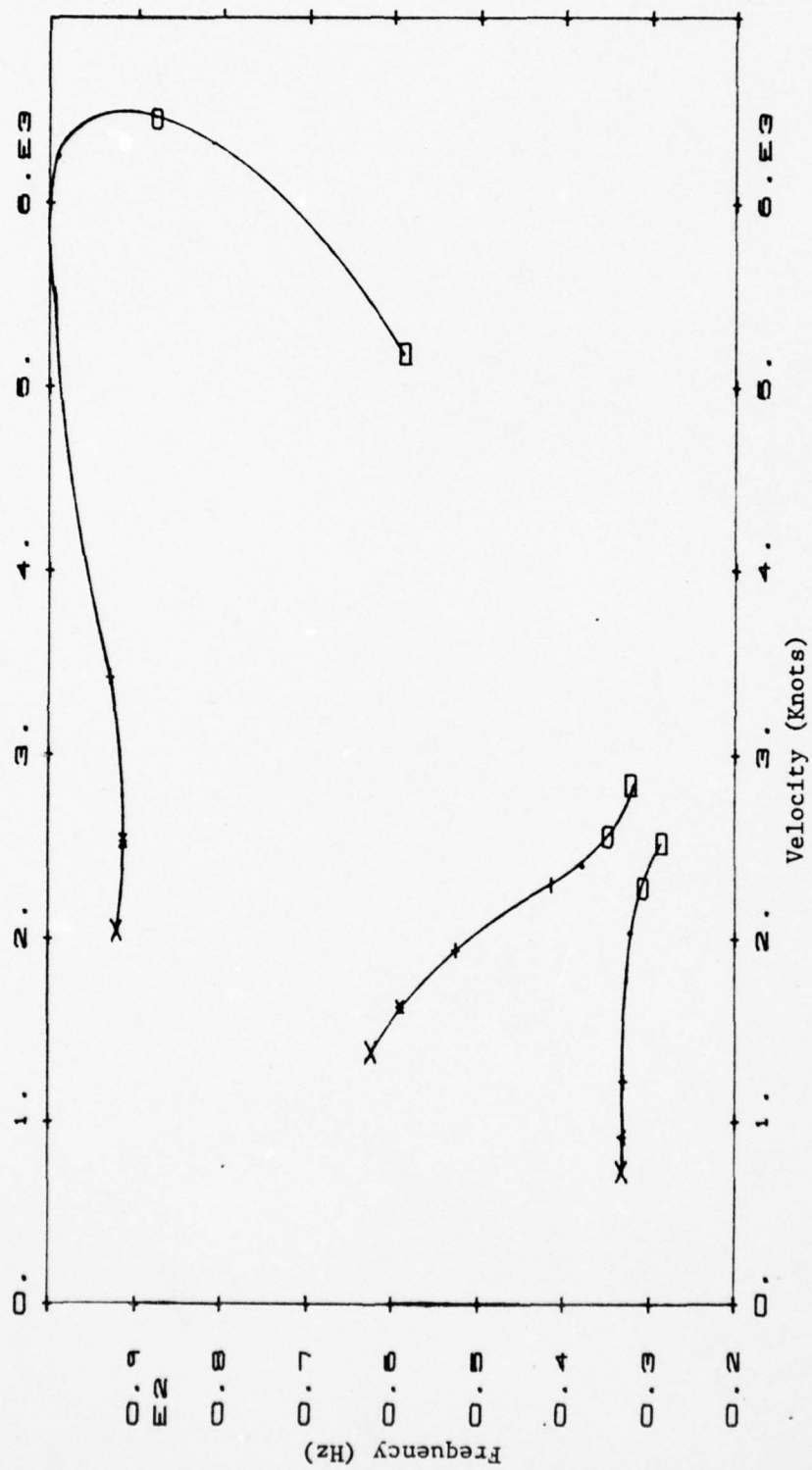


Fig. 29-B. Flutter Frequency Solution with 200 lb at Node 38

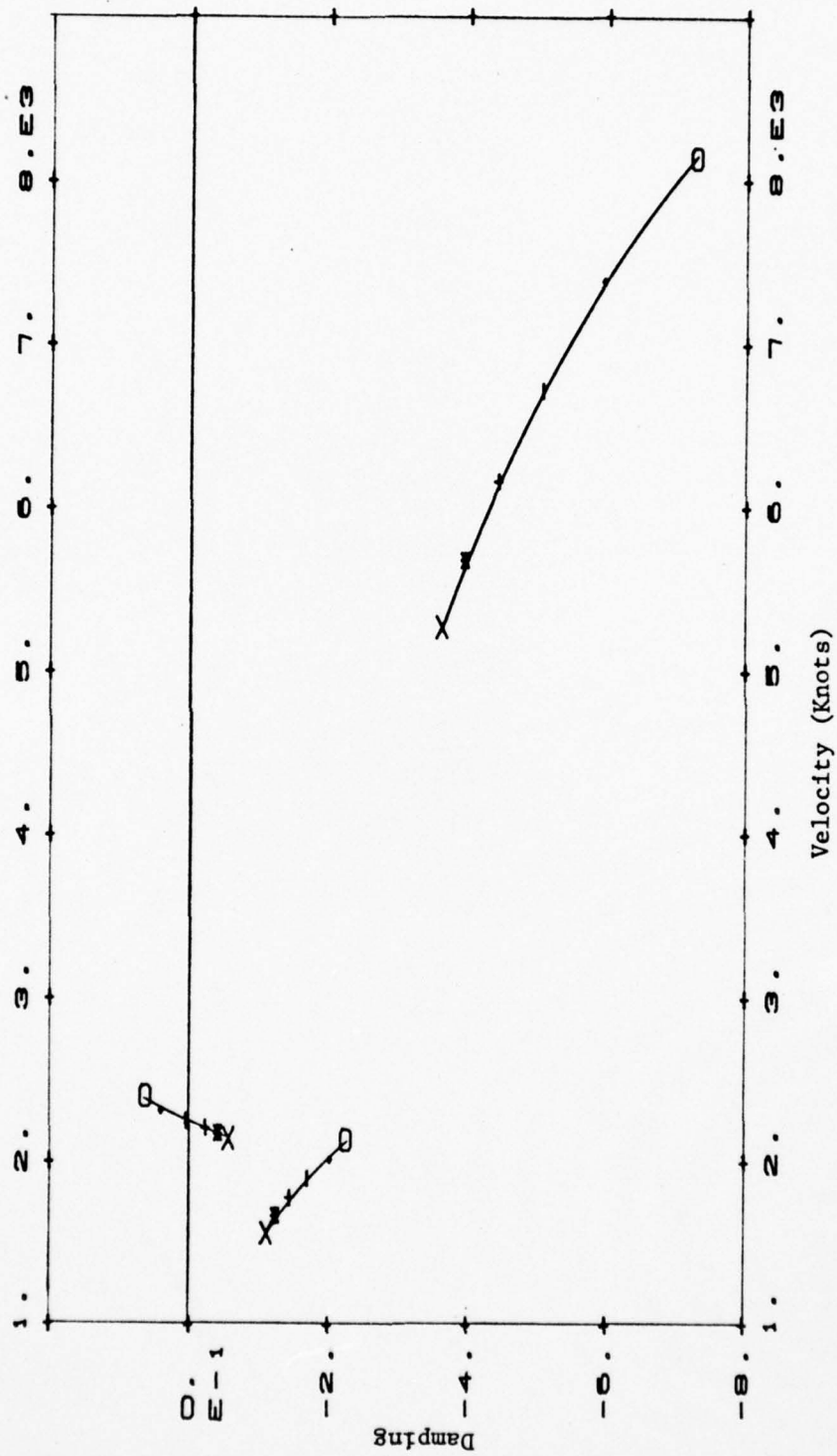


Fig. 30-A. Flutter Speed Solution with 200 lb at Node 48

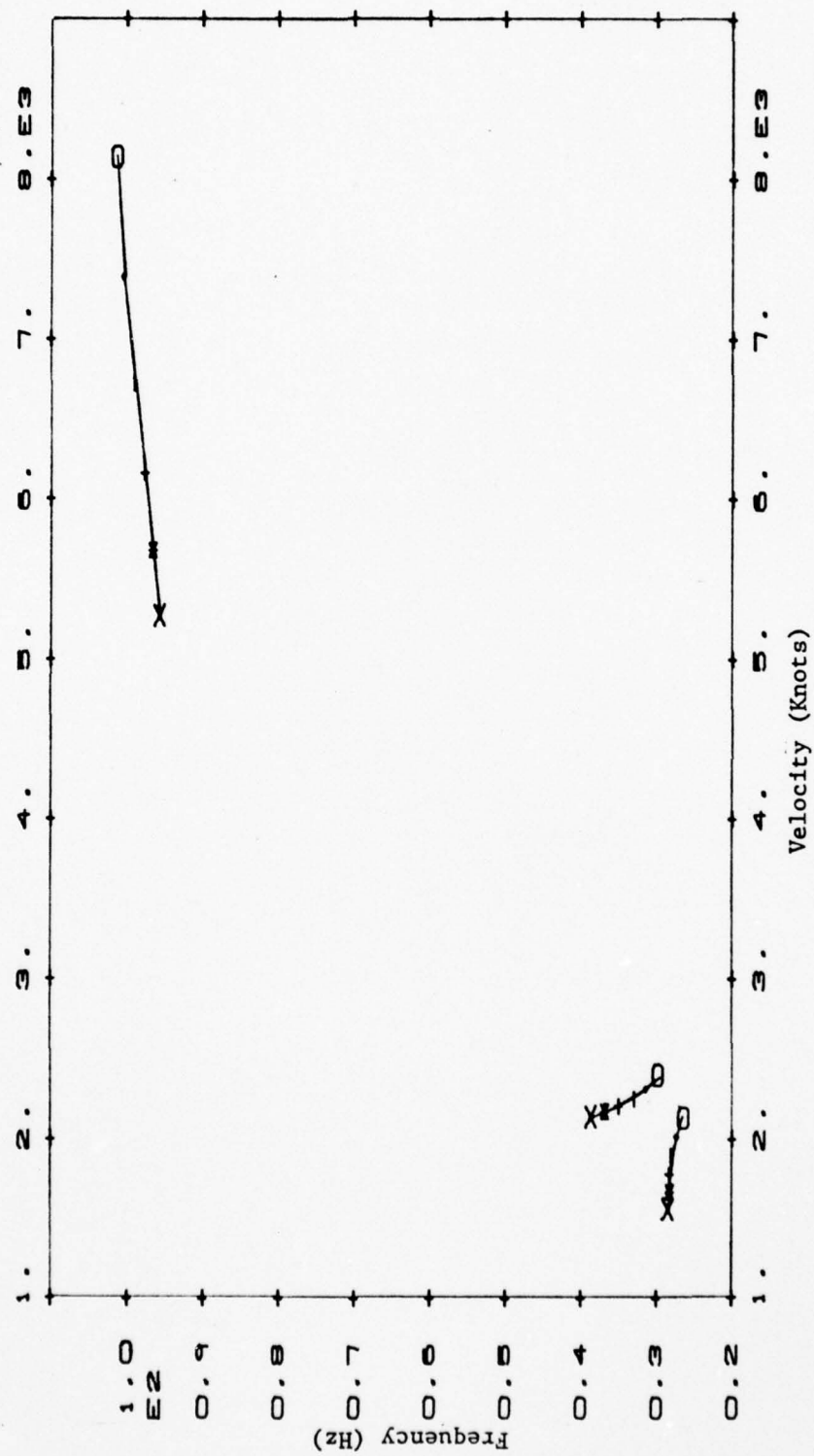


Fig. 30-B. Flutter Frequency Solution with 200 lb at Node 48

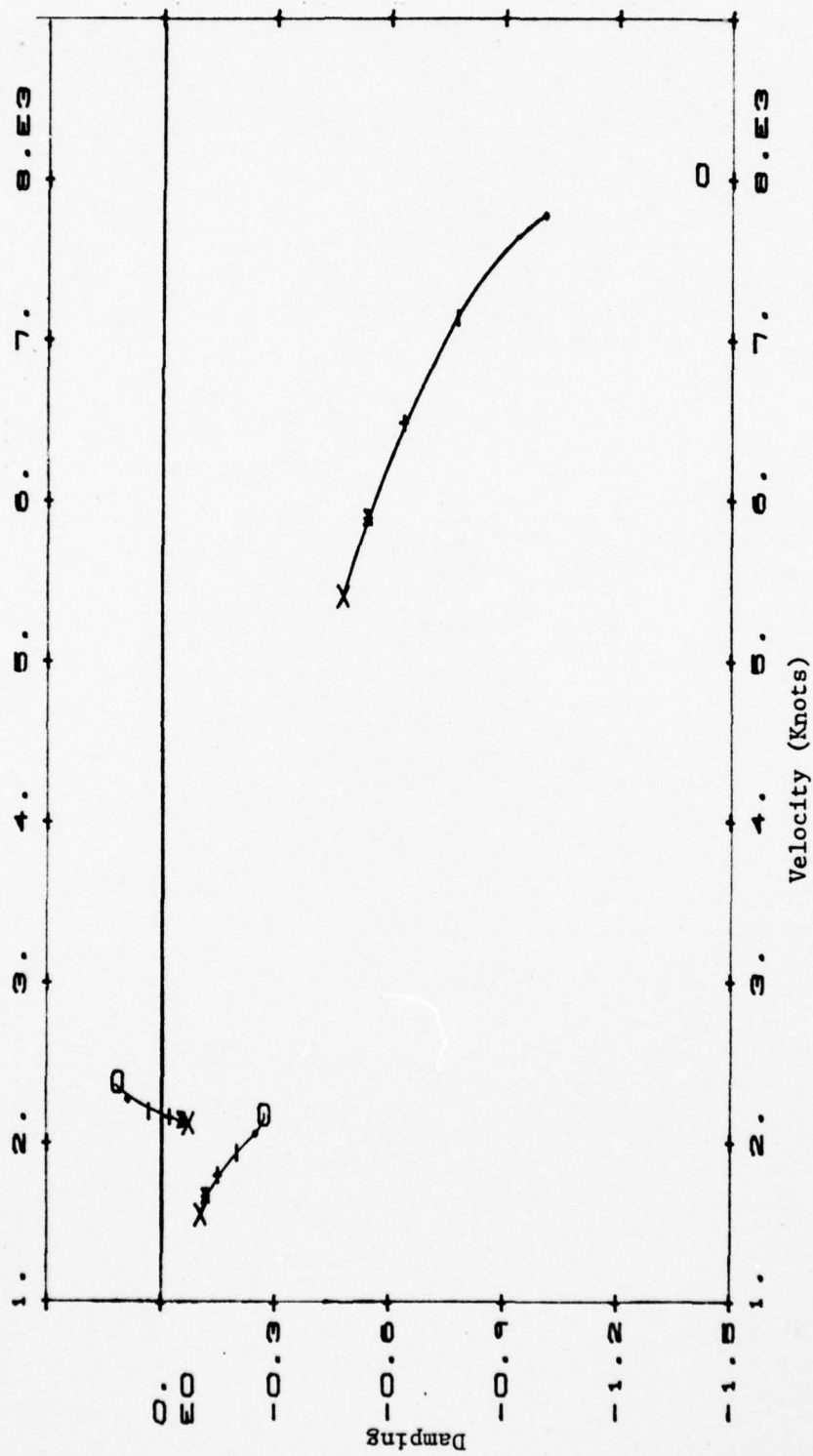


Fig. 31-A. Flutter Speed Solution with 200 lb at Node 58

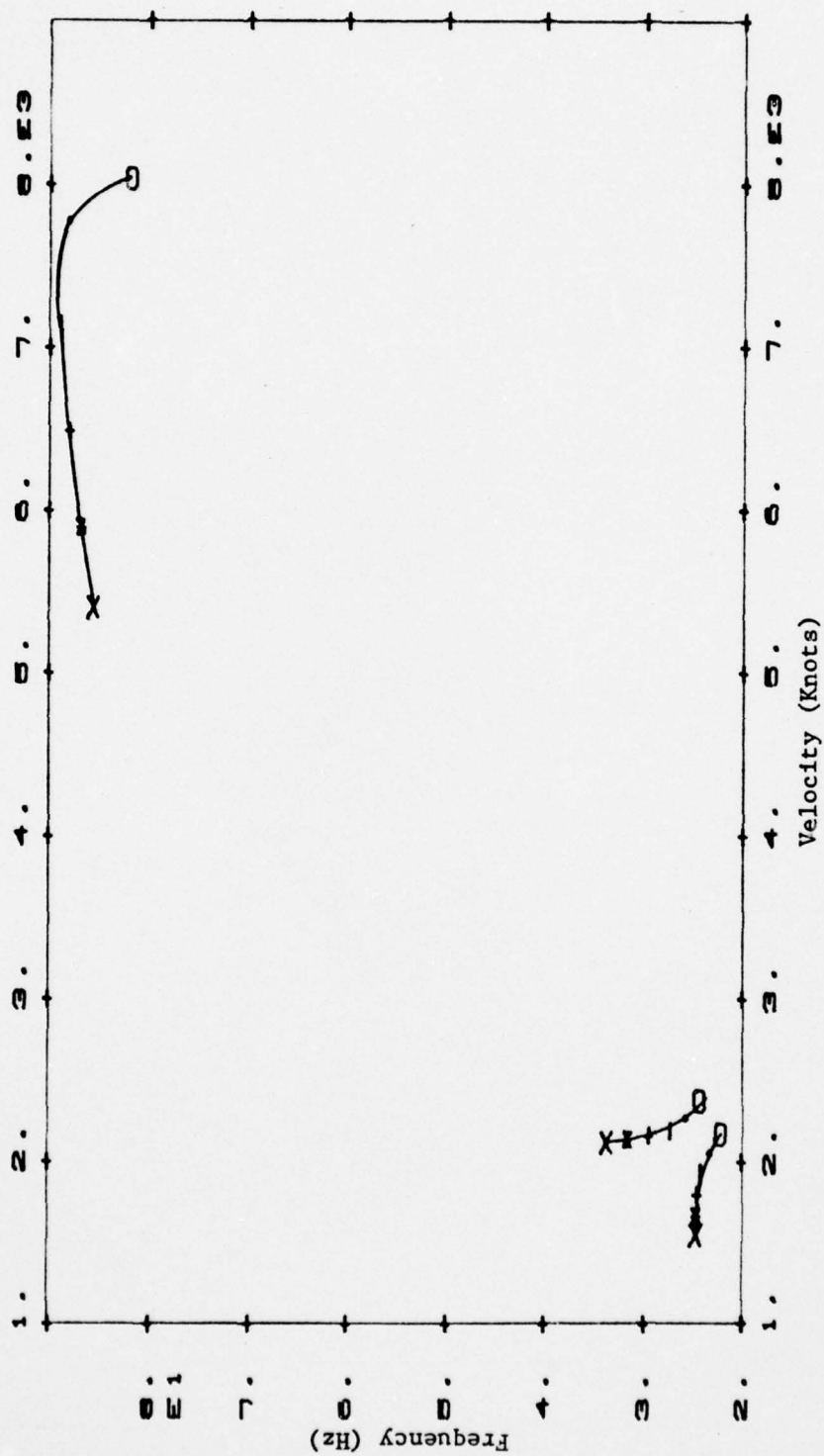


Fig. 31-B. Flutter Frequency Solution with 200 lb at Node 58

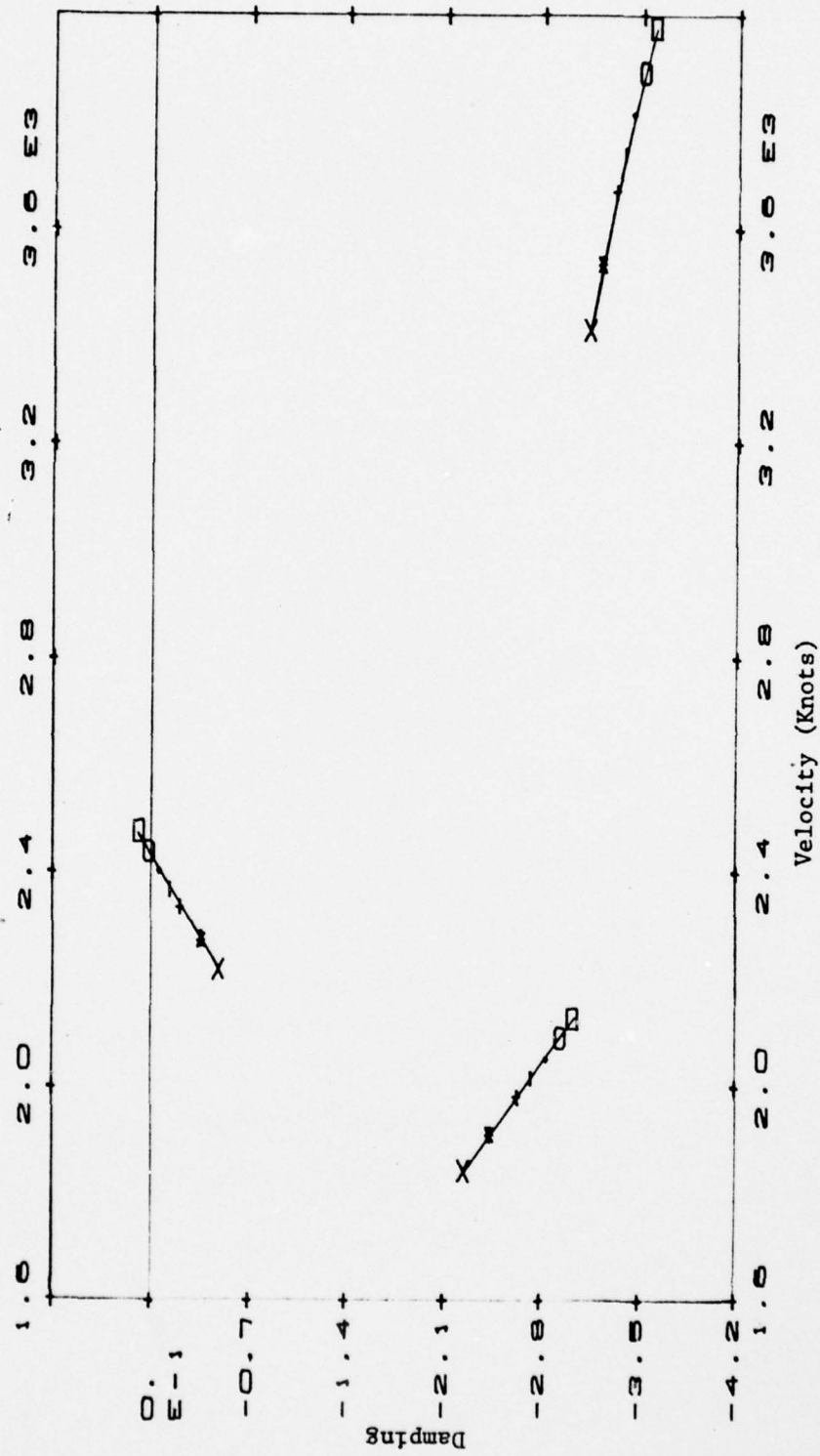


Fig. 32-A. Flutter Speed Solution with 100 lb at Node 26 and 100 lb at Node 30

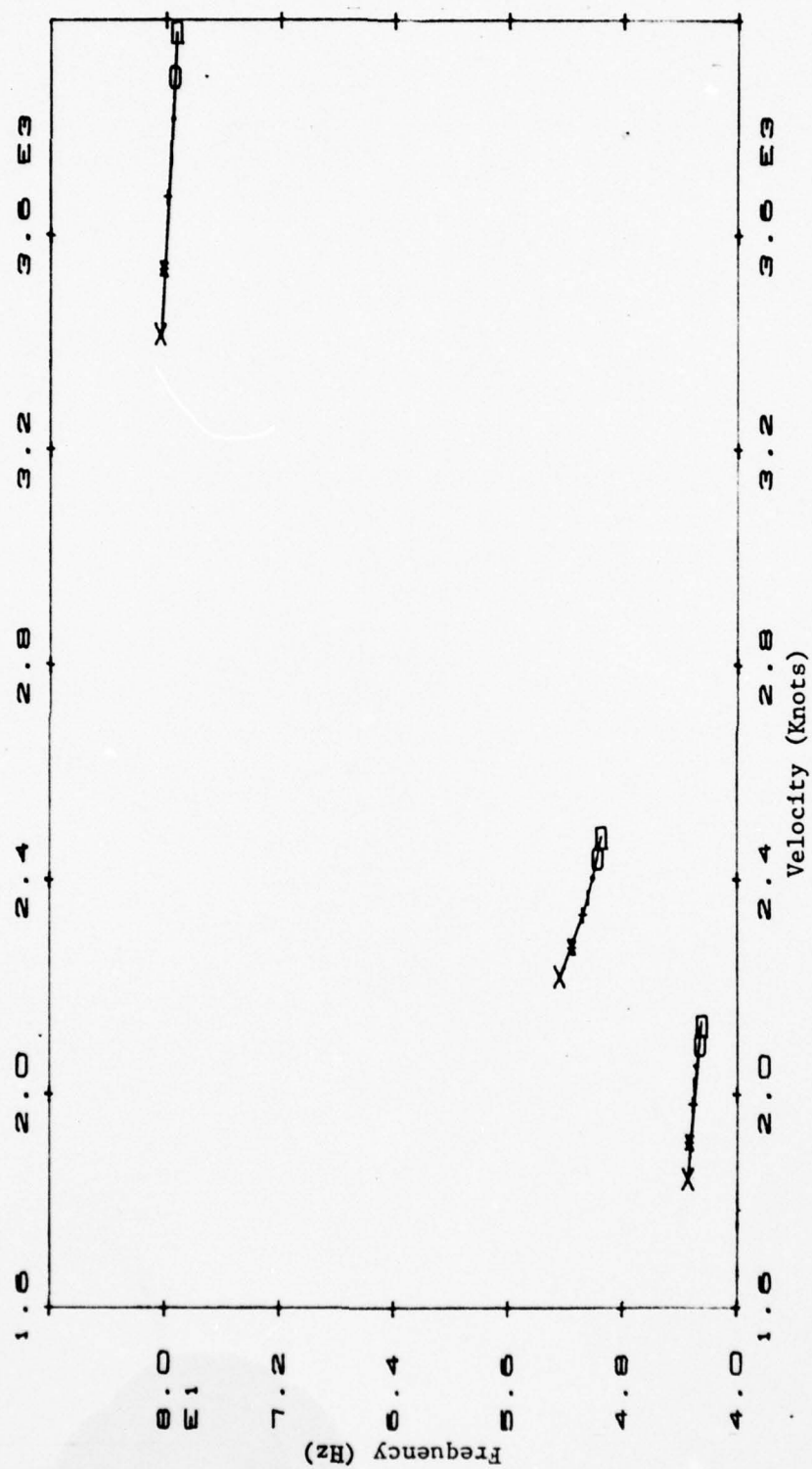


Fig. 32-B. Flutter Frequency Solution with 100 lb at Node 26 and 100 lb at Node 30

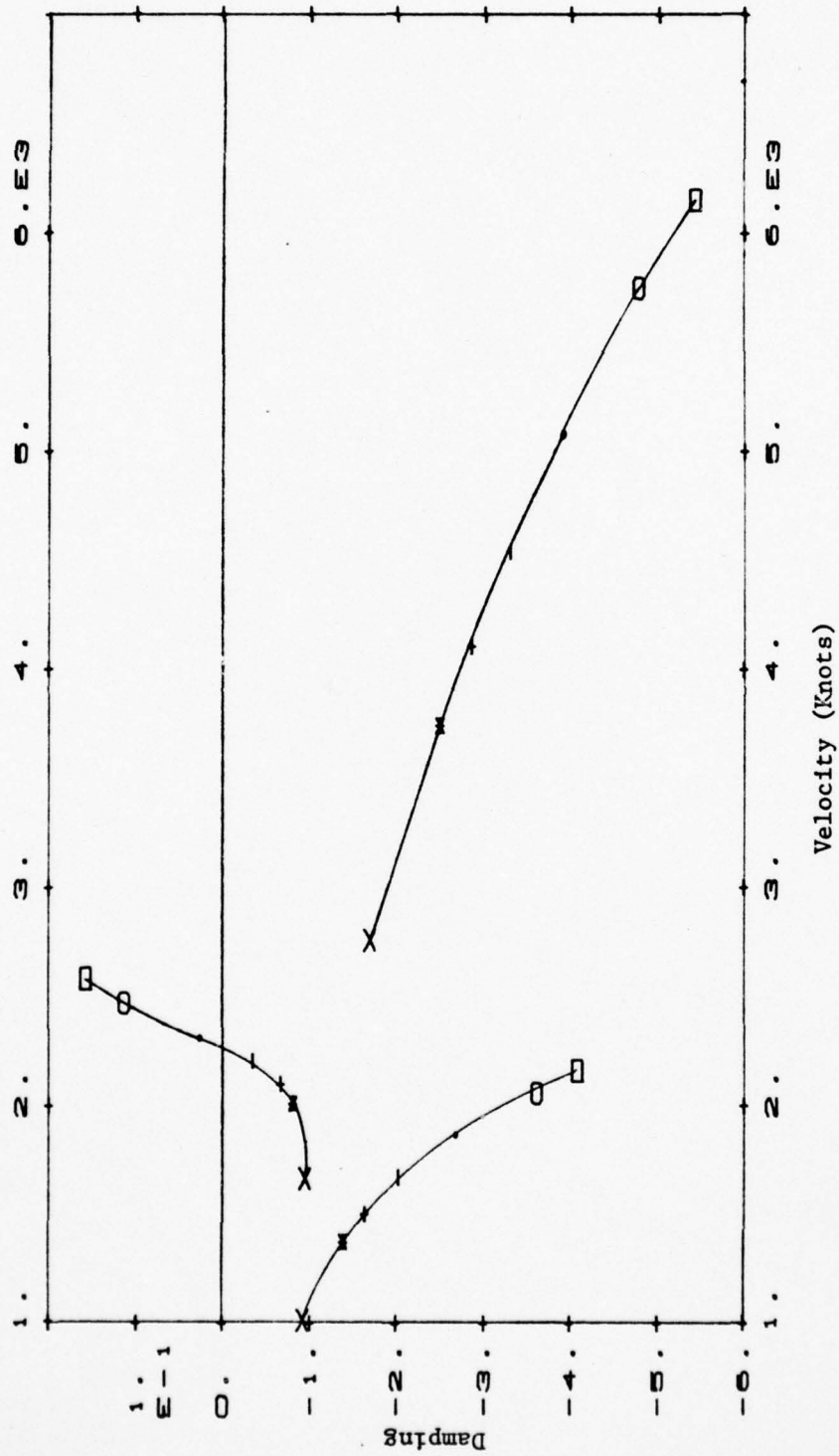


Fig. 33-A. Flutter Speed Solution with 100 lb at Node 36 and 100 lb at Node 40

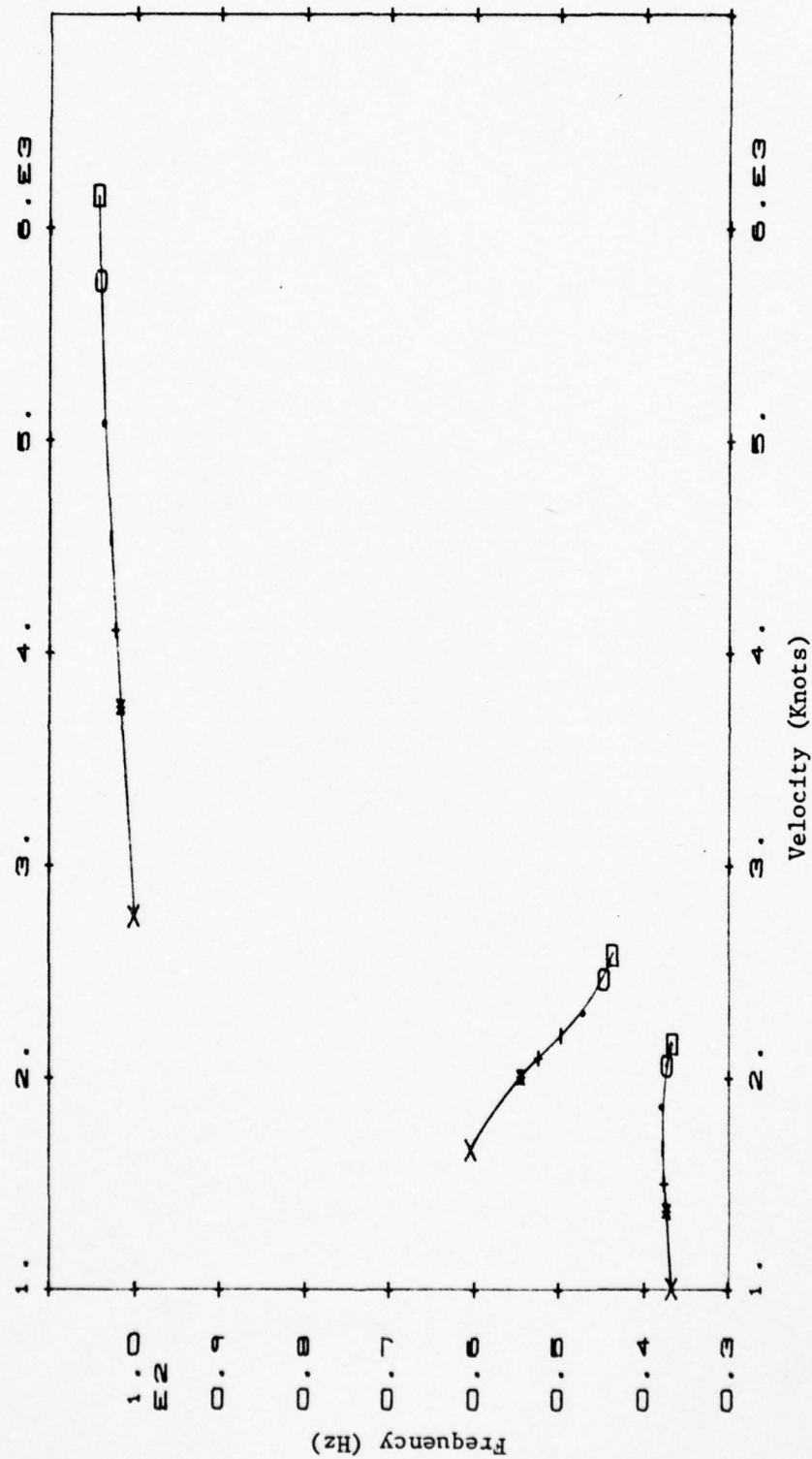


Fig. 33-B. Flutter Frequency Solution with 100 lb at Node 36 and 100 lb at Node 40

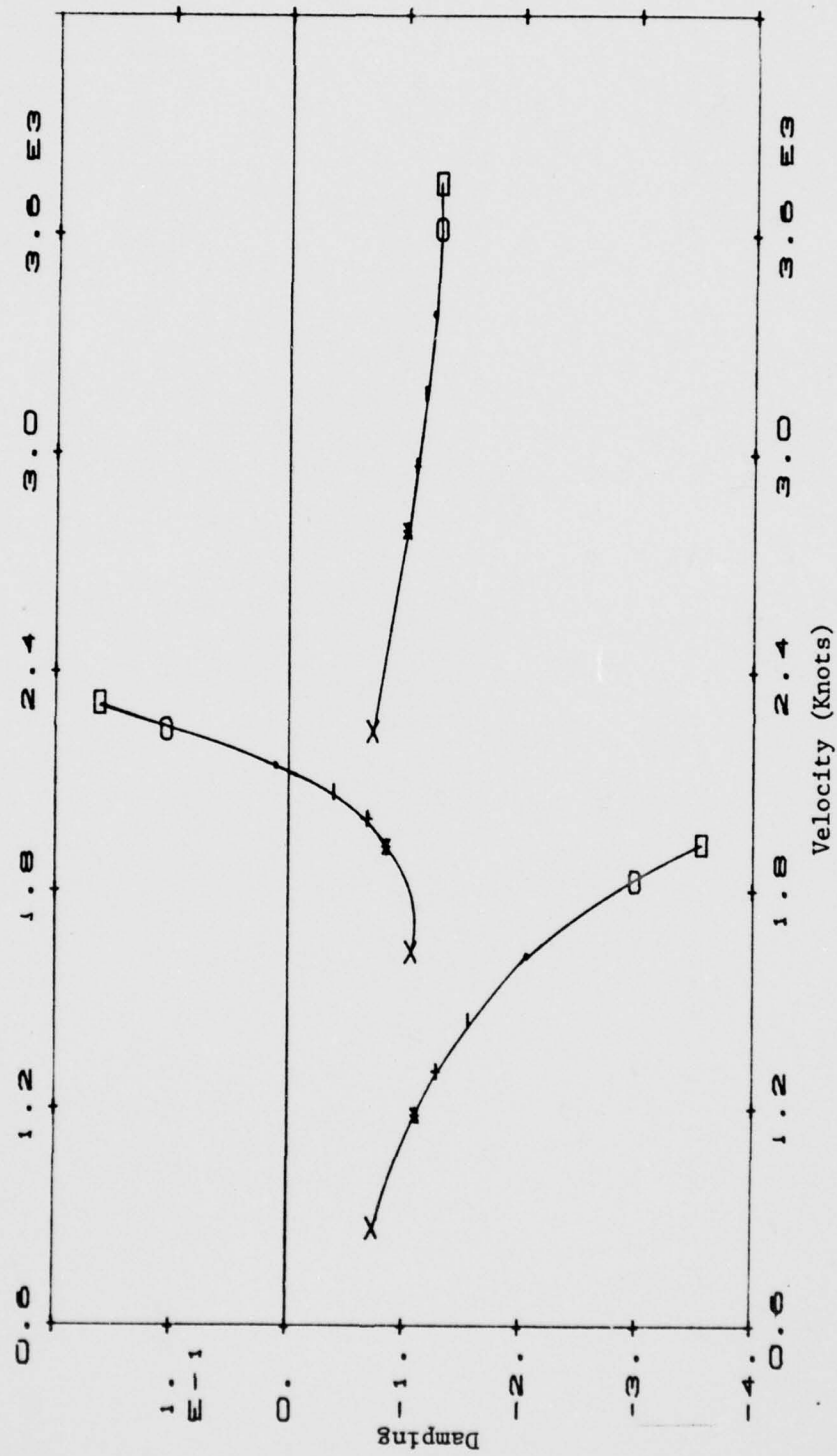


Fig. 34-A. Flutter Speed Solution with 100 lb at Node 46 and 100 lb at Node 50

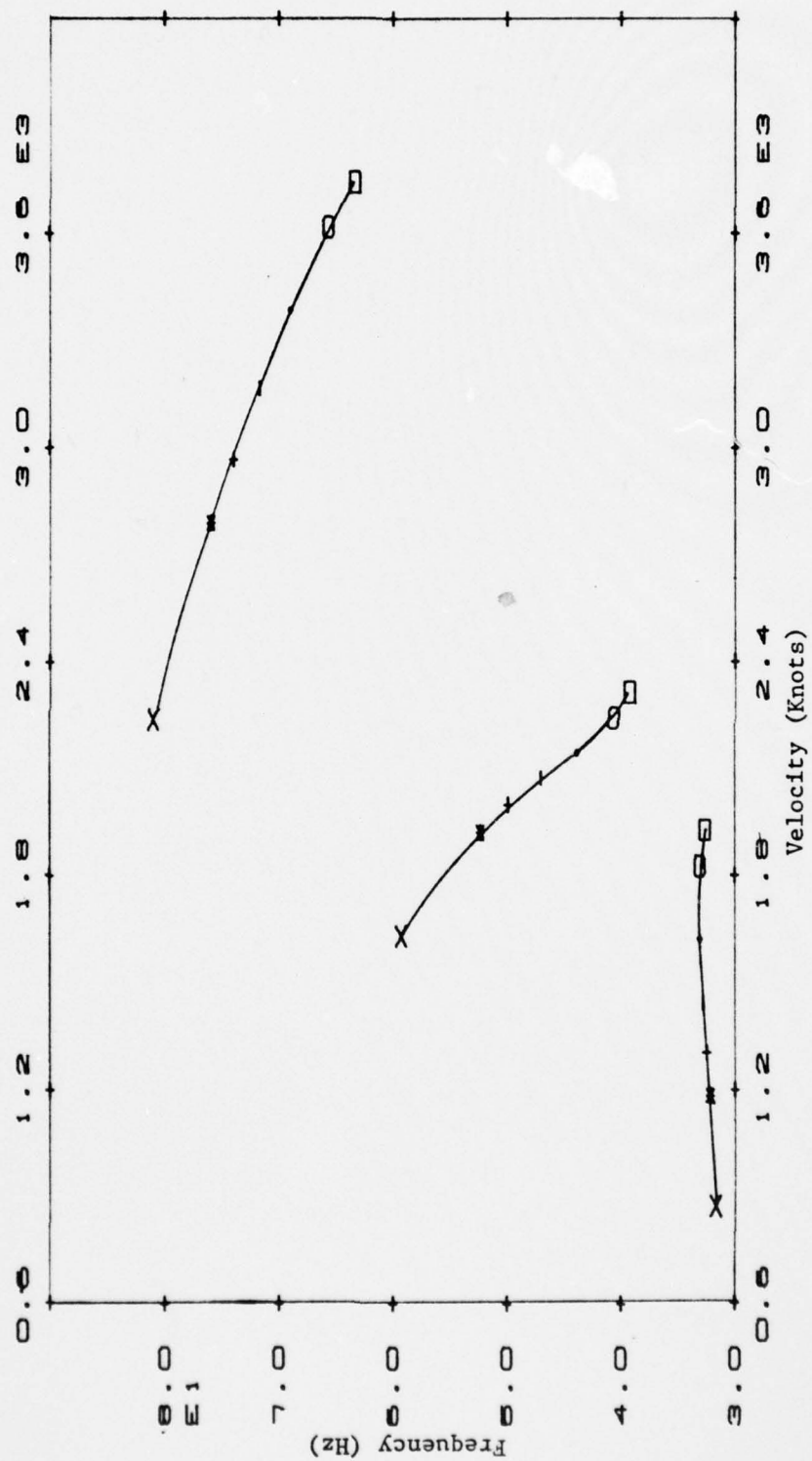


Fig. 34-B. Flutter Frequency Solution with 100 lb at Node 46
and 100 lb at Node 50

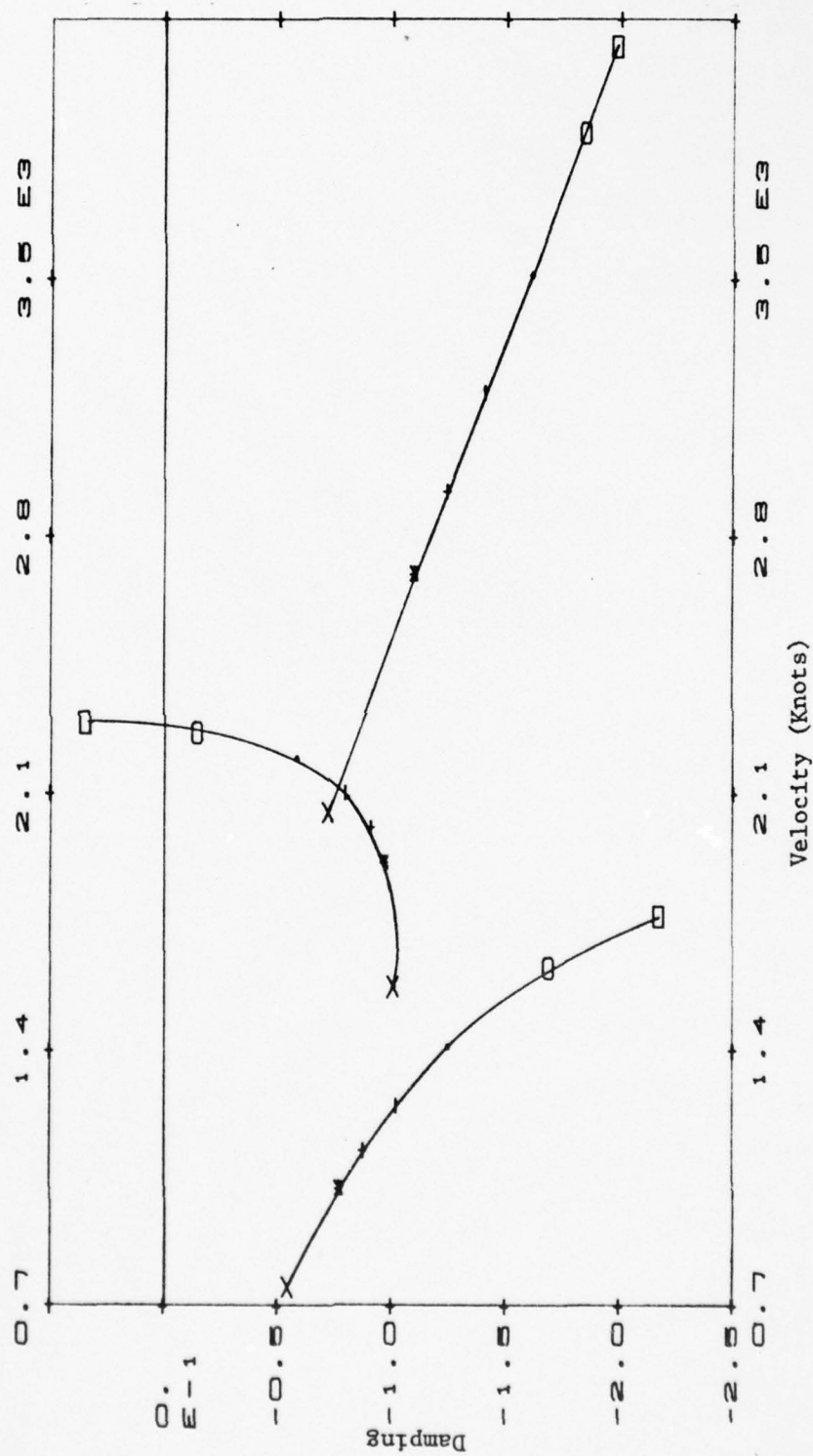


Fig. 35-A. Flutter Speed Solution with 100 lb at Node 56 and 100 lb at Node 60

AD-A048 360

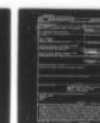
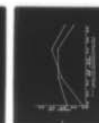
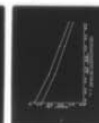
AIR FORCE INST OF TECH WRIGHT-PATTERSON AFB OHIO SCH--ETC F/G 20/4
THE EFFECTS OF EXTERNAL STORES ON THE FLUTTER OF A NON-UNIFORM --ETC(U)
DEC 77 V C SHERRER

UNCLASSIFIED

AFIT/GAE/AA/77D-13

NL

2 of 2
AD
A048360



END
DATE
FILMED

2-78
DDC

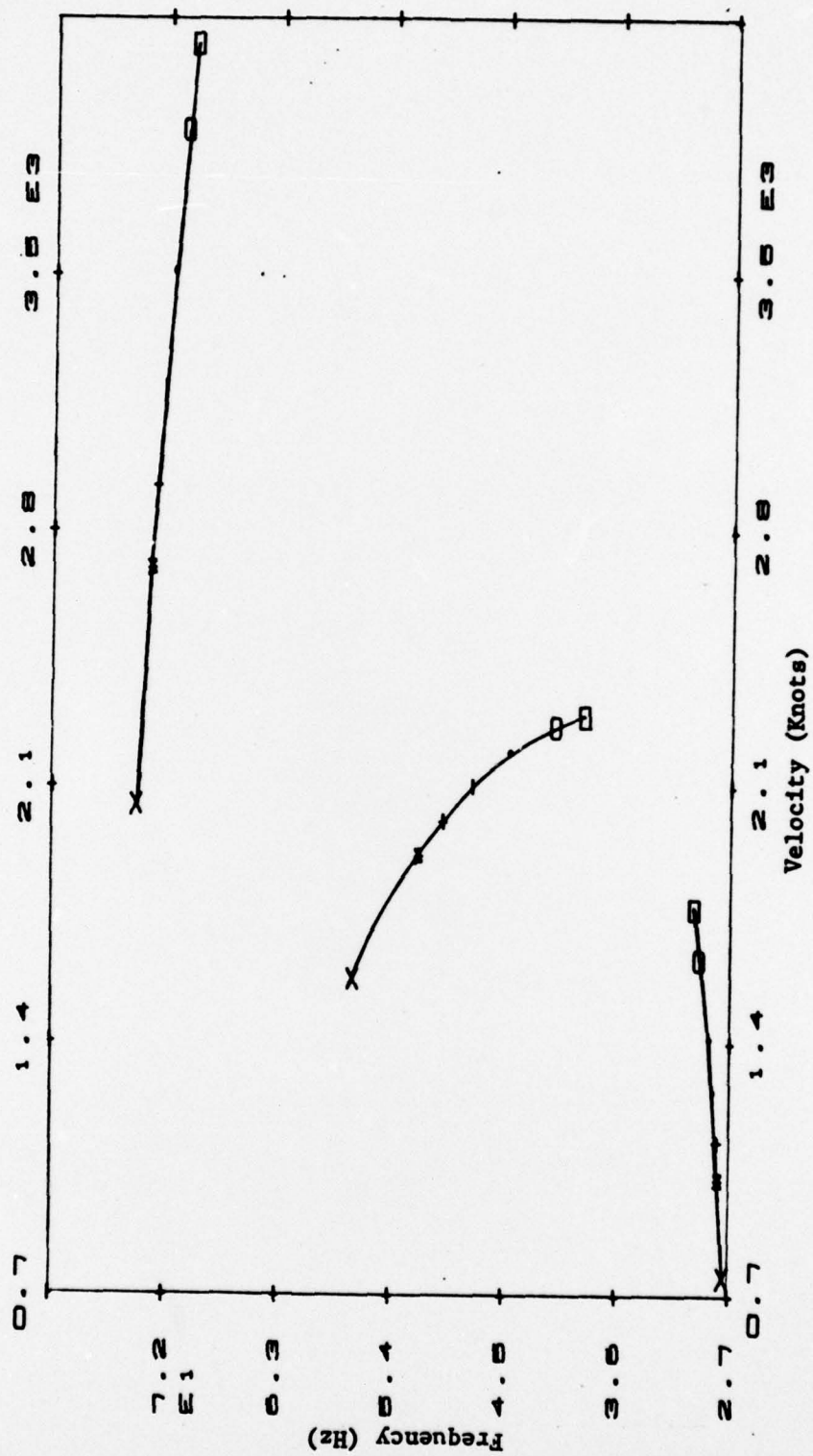


Fig. 35-B. Flutter Frequency Solution with 100 lb at Node 56 and 100 lb at Node 60

Appendix C

Table IV Free Vibration Frequencies (Hz)			
Node	Mode 1	Mode 2	Mode 3
No Mass Added			
	49.6	95.4	104.1
100 lb Concentrated at a Node			
38	40.5	75.8	98.9
48	36.4	77.7	103.0
58	32.6	70.9	99.8
100 lb Store (Two X 50 lb)			
36, 40	42.1	80.1	99.9
46, 50	38.1	80.4	102.2
56, 60	34.1	74.1	92.3
200 lb Concentrated at a Node			
28	39.4	61.1	96.6
38	33.4	69.0	98.6
48	28.9	72.7	102.7
58	25.1	67.8	99.7
200 lb Store (Two X 100 lb)			
26, 30	42.7	67.0	95.0
36, 40	36.2	70.2	98.5
46, 50	31.3	70.4	92.1
56, 60	27.0	64.5	77.2

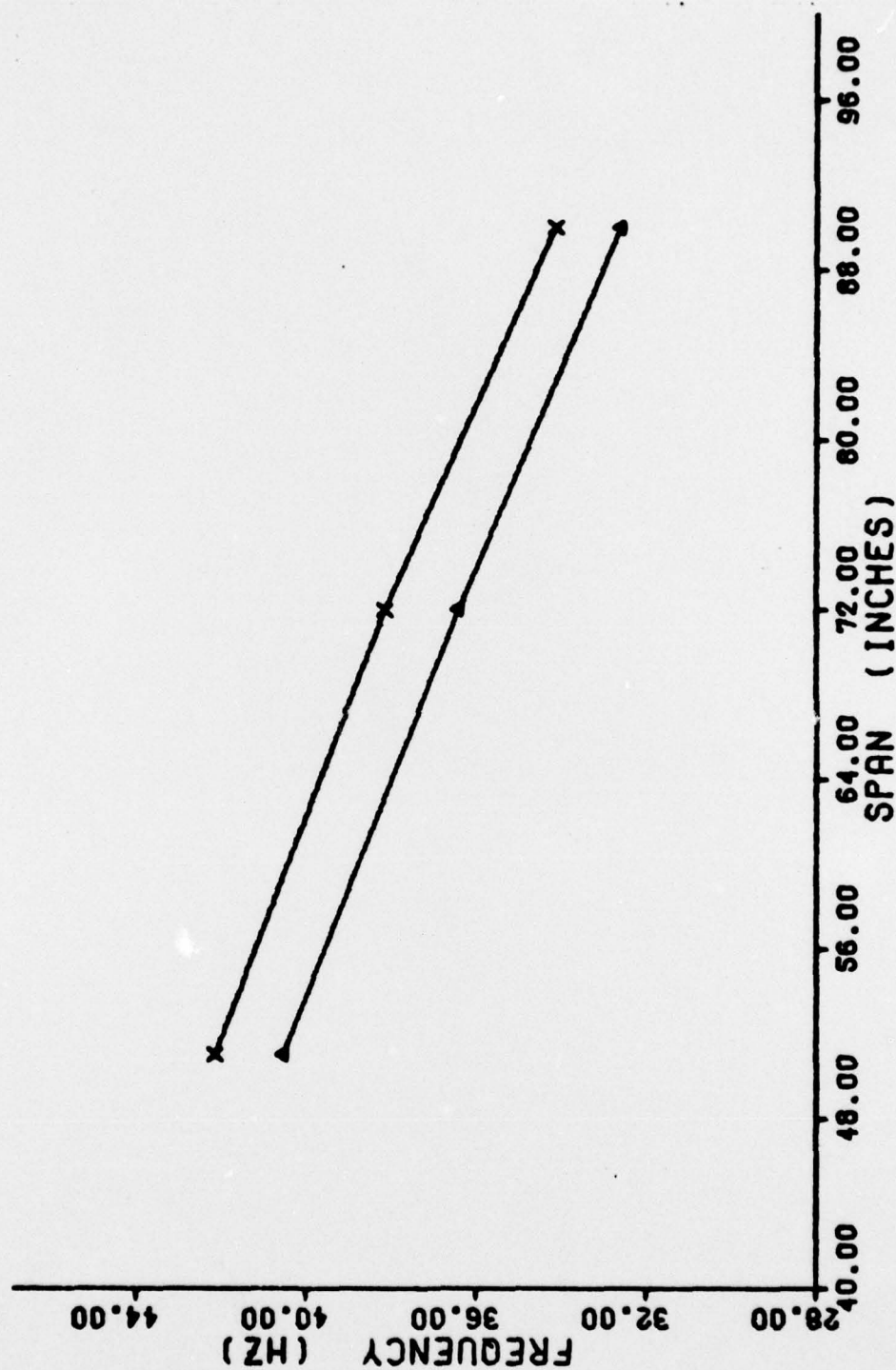


Fig. 36. Comparison of Mode 1 Free Vibration Frequencies of 100 lb Store Versus Single Concentrated Mass at 3/4 Chord Nodes

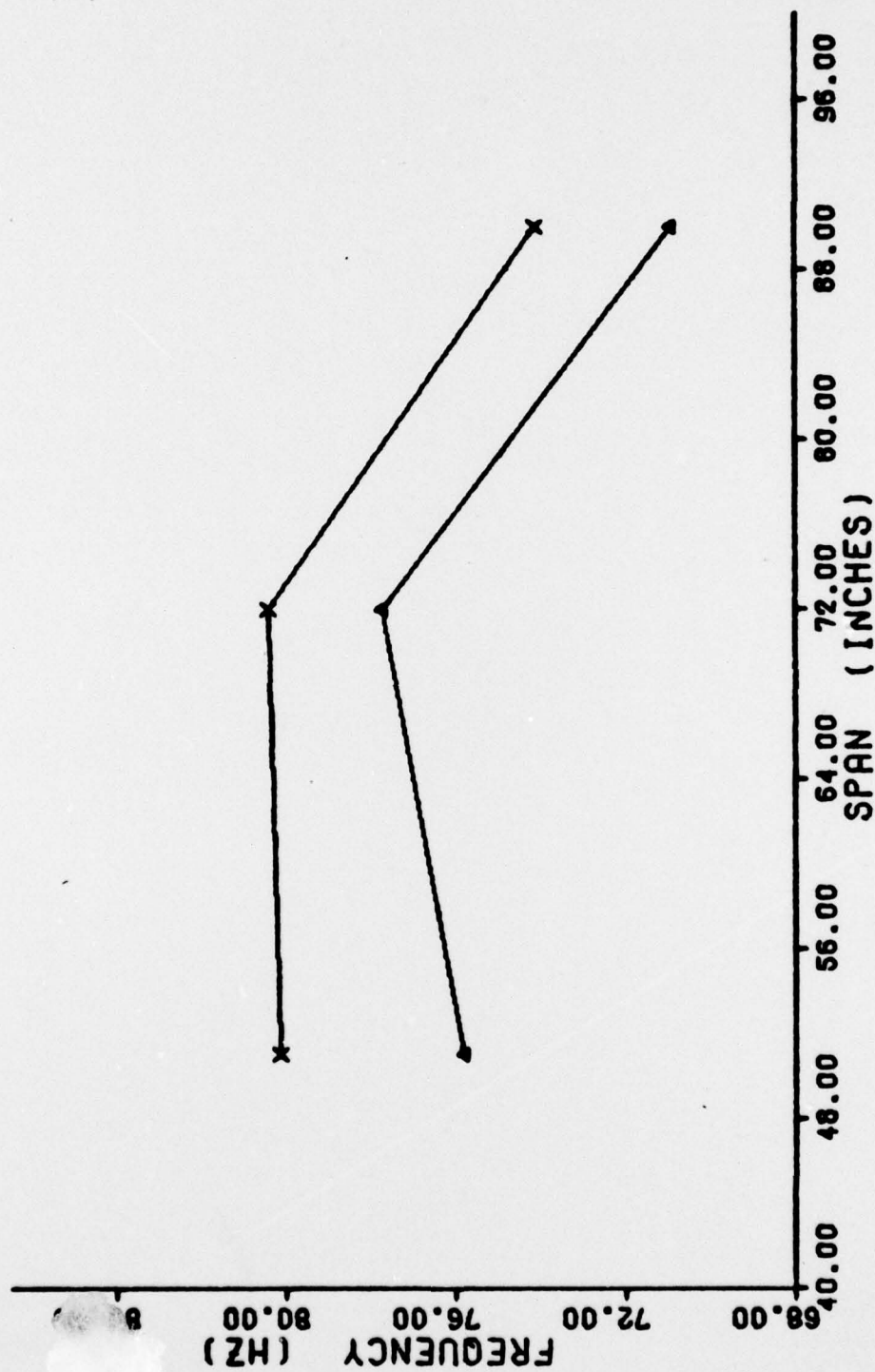


Fig. 37. Comparison of Mode 2 Free Vibration Frequencies of 100 lb Store Versus Single Concentrated Mass at 3/4 Chord Nodes

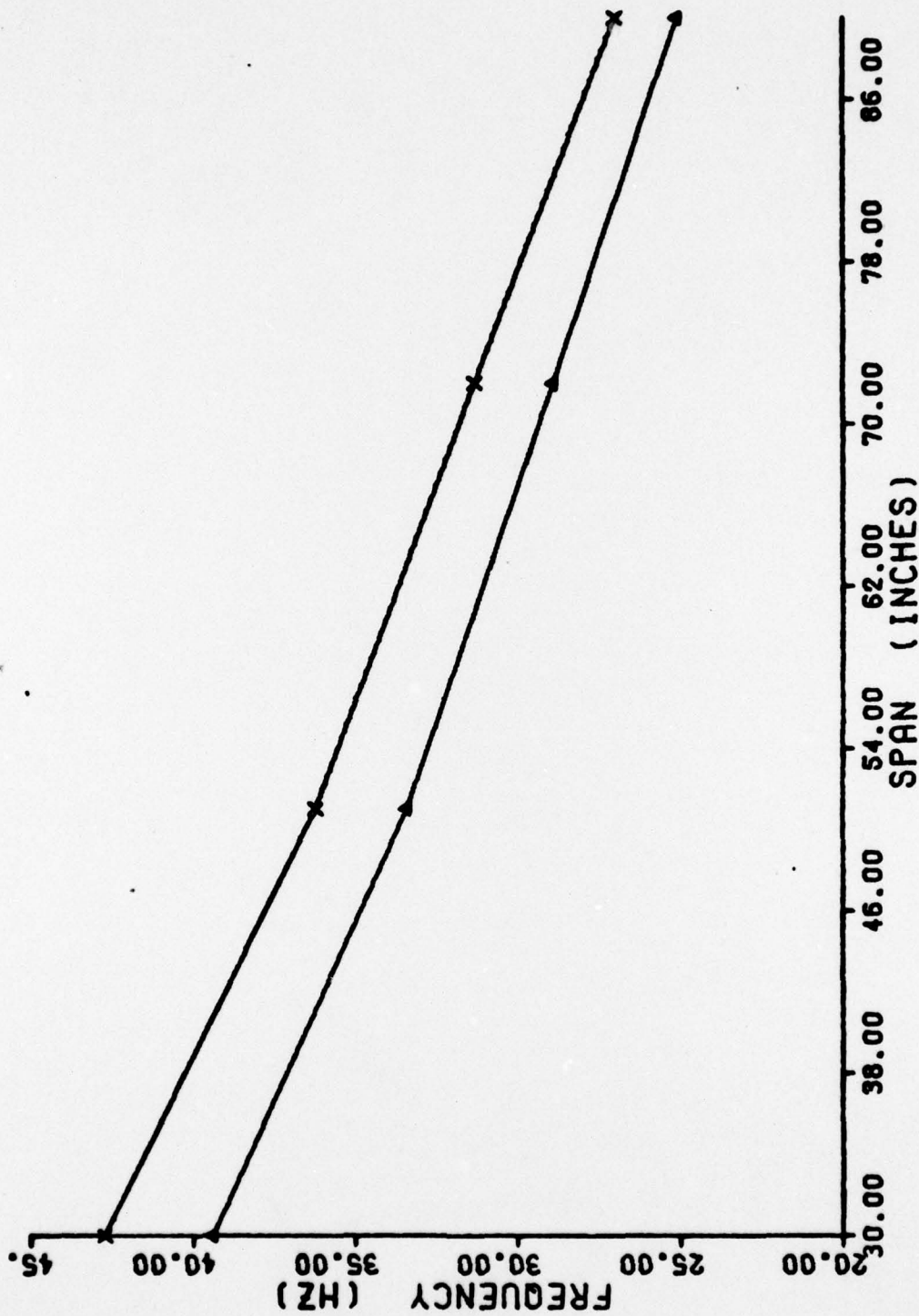


Fig. 38. Comparison of Mode 1 Free Vibration Frequencies of 200 lb Store Versus Single Concentrated Mass at 3/4 Chord Nodes

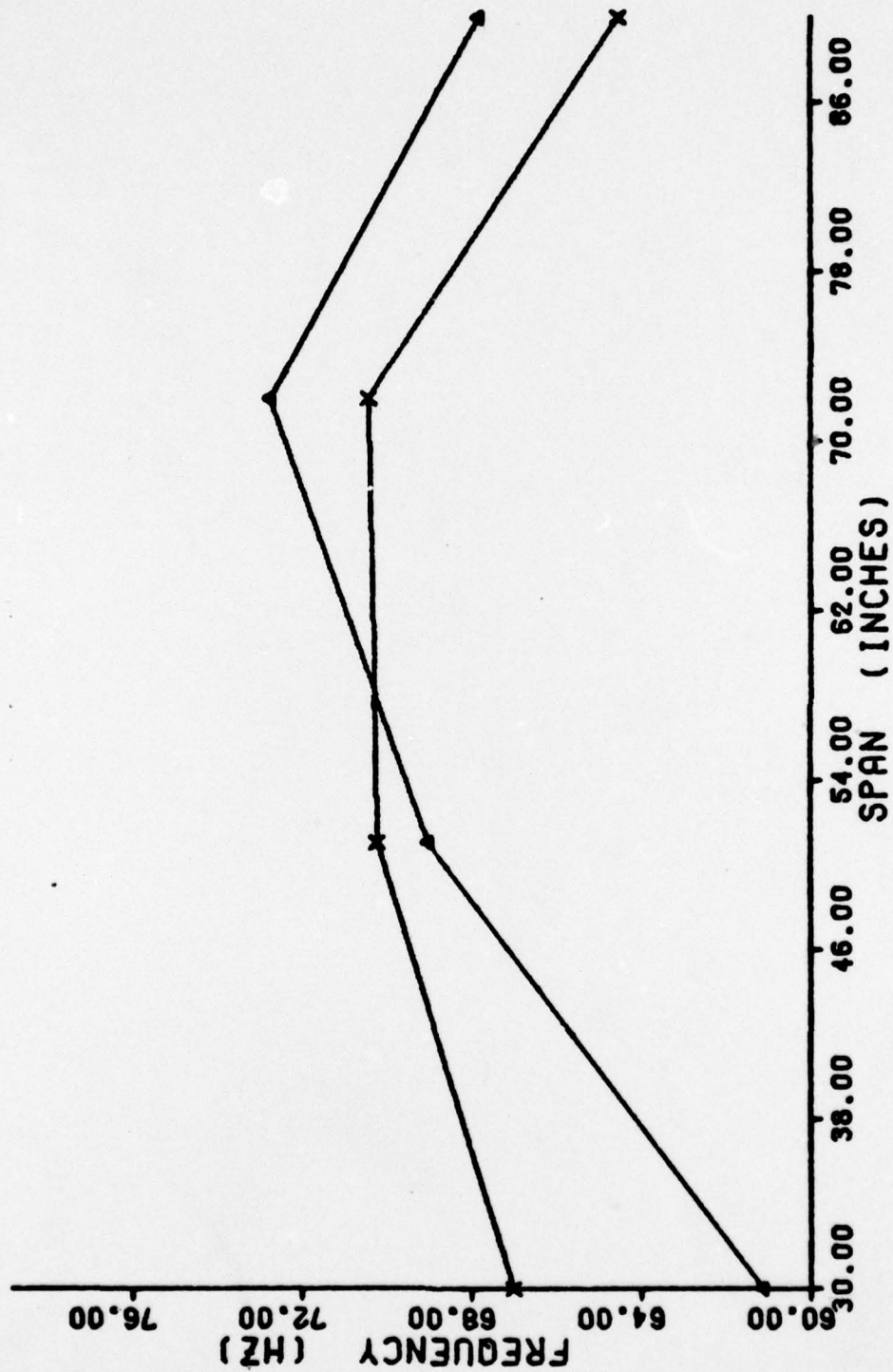


Fig. 39. Comparison of Mode 2 Free Vibration Frequencies of 200 lb Store Versus Single Concentrated Mass at 3/4 Chord Nodes

VITA

Van Craig Sherrer was born on 6 January 1947 in Bay City, Texas. He graduated from Bay City High School in 1965 and attended Wharton County Junior College from which he received an Associate in Arts degree. He then attended the University of Texas at Austin, receiving a Bachelor of Science in Aerospace Engineering in 1970. Upon graduation, he joined the USAF, received his commission through Officer Training School, and was then assigned to Laredo AFB, Texas, to attend pilot training. He received his wings in April 1971. He was assigned to Altus AFB, Oklahoma, to the 11th AREFS and flew the KC-135 as co-pilot and then as aircraft commander. While at Altus, he married Cheryl, an AF nurse, in February 1976. He entered the School of Engineering, Air Force Institute of Technology in June 1976.

Permanent Address:

908-8th Street
Bay City, Texas 77414

UNCLASSIFIED

SECURITY CLASSIFICATION OF THIS PAGE (When Data Entered)

14 REPORT DOCUMENTATION PAGE		READ INSTRUCTIONS BEFORE COMPLETING FORM
1. REPORT NUMBER AFIT/GAE/AA/77D-13	2. GOVT ACCESSION NO.	3. RECIPIENT'S CATALOG NUMBER
4. TITLE (and Subtitle) THE EFFECTS OF EXTERNAL STORES ON THE FLUTTER OF A NON-UNIFORM CANTILEVER WING.		5. TYPE OF REPORT & PERIOD COVERED Master's thesis, MS Thesis
7. AUTHOR(s) Van C. Sherrer Capt USAF		6. PERFORMING ORG. REPORT NUMBER
9. PERFORMING ORGANIZATION NAME AND ADDRESS Air Force Institute of Technology (AFIT-EN) Wright-Patterson AFB, Ohio 45433		8. CONTRACT OR GRANT NUMBER(s)
11. CONTROLLING OFFICE NAME AND ADDRESS Air Force Flight Dynamics Laboratory (FBR) Wright-Patterson AFB, Ohio 45433		10. PROGRAM ELEMENT, PROJECT, TASK AREA & WORK UNIT NUMBERS
14. MONITORING AGENCY NAME & ADDRESS (if different from Controlling Office)		12. REPORT DATE Dec 1977
		13. NUMBER OF PAGES 89
		15. SECURITY CLASS. (of this report) Unclassified
16. DISTRIBUTION STATEMENT (of this Report) Approved for public release; distribution unlimited		
17. DISTRIBUTION STATEMENT (of the abstract entered in Block 20, if different from Report)		
18. SUPPLEMENTARY NOTES Approved for public release; IAW AFR 190-17 JERRAL F. GUESS, Captain, USAF Director of Information		
19. KEY WORDS (Continue on reverse side if necessary and identify by block number) EXTERNAL STORES FLUTTER WING		
20. ABSTRACT (Continue on reverse side if necessary and identify by block number) A computer study of the effects of external stores simulated by lumped masses was conducted with a finite element, cantilever, non-uniform wing model. The NASTRAN (Level 16.0) computer program flutter format was used to obtain flutter speeds and frequencies. Mass balancing with a single concentrated mass caused a reduction in flutter speed as the mass was moved chordwise toward the trailing edge and spanwise toward the wing tip. Flutter speeds and frequencies of a 100 lb and a 200 lb store, simulated by two equal masses, were compared to an equivalent concentrated mass at the store center of gravity. The stores		

DD FORM 1 JAN 73 1473

EDITION OF 1 NOV 65 IS OBSOLETE

UNCLASSIFIED

SECURITY CLASSIFICATION OF THIS PAGE (When Data Entered)

[Faint handwritten notes]

consistently raised the flutter frequency over that of the single mass, but flutter speed results were not conclusive.

U. S. A. M. I. A.

ALL INFORMATION CONTAINED HEREIN IS UNCLASSIFIED
DATE 08-11-2010 BY 60322 UCBAW/SJS/STP

For C. I. Hunter
1907

[illegible]

721 500000

[illegible]

1933, 29

Approved: For release reference: 00-000000-000000

THE UNIVERSITY OF CHICAGO
CHICAGO, ILLINOIS 60637
DEPARTMENT OF POLITICAL SCIENCE

[illegible]

(U) (S)

SECURITY CLASSIFICATION OF THIS PAGE(When Data Entered)